let. - vol. 46 (2000) št. - no. 6

STROJNIŠKI VESTNIK 6

JOURNAL OF MECHANICAL ENGINEERING

strani - pages 329 - 396

ISSN 0039-2480 . Stroj V . STJVAX

cena 800 SIT

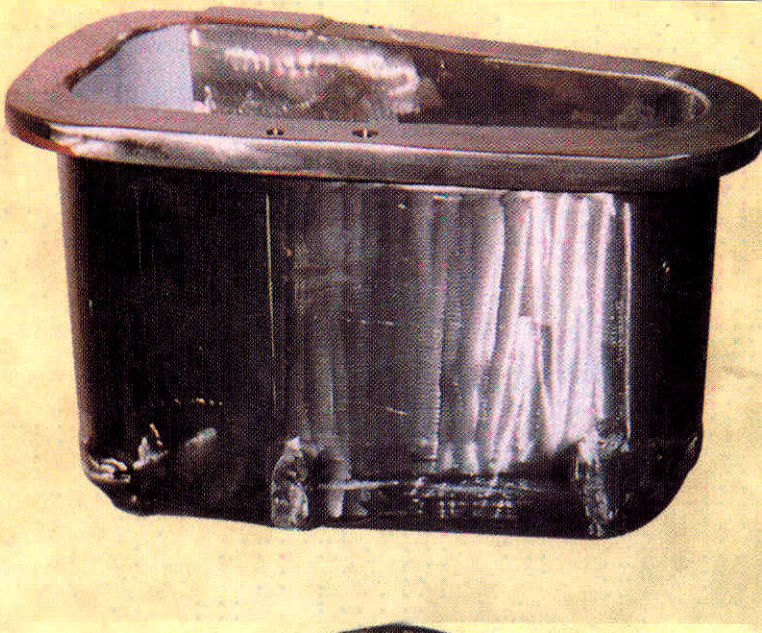

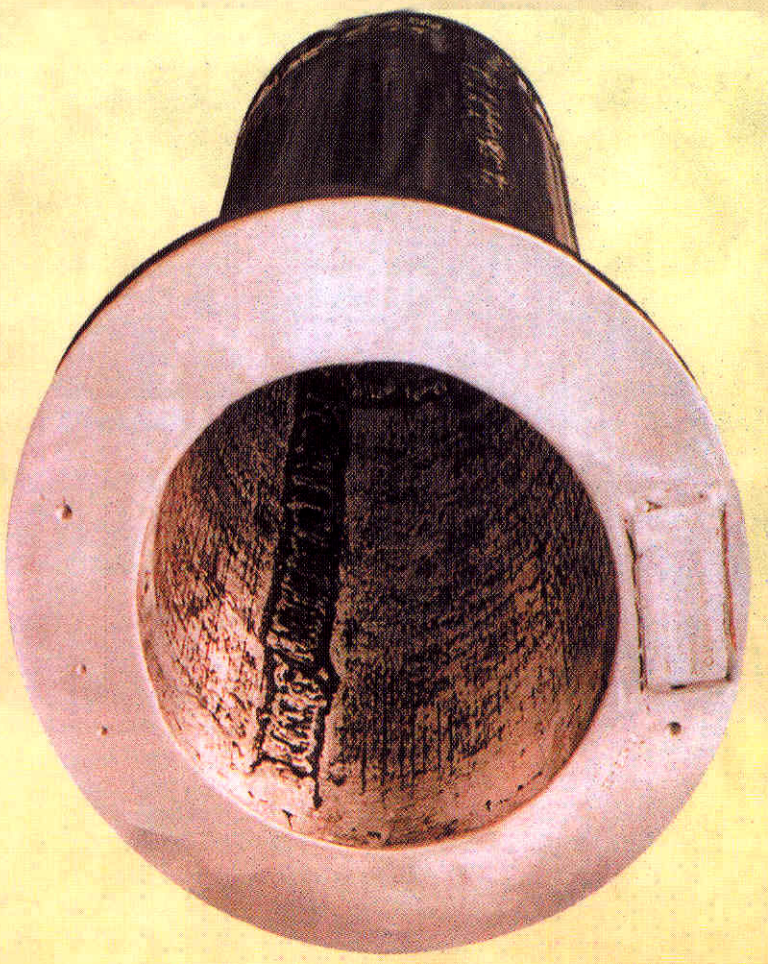

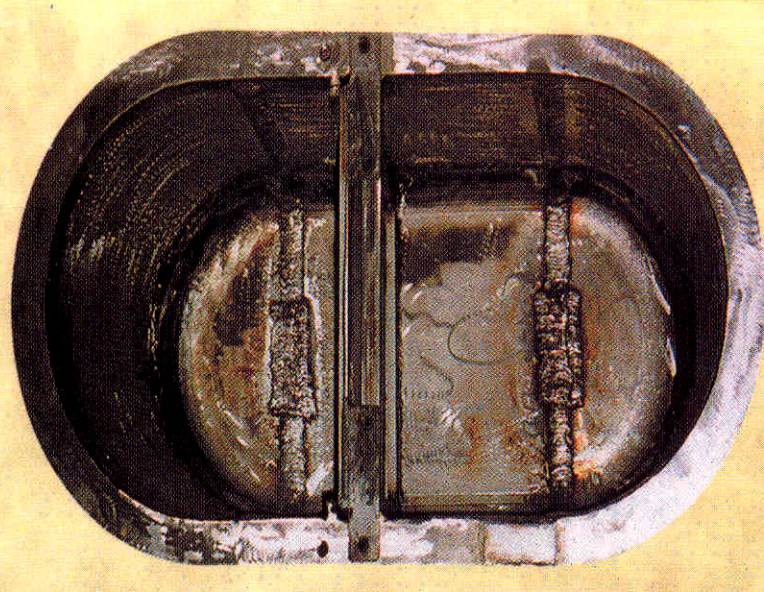

9 770039 248001

© Strojniški vestnik 46(2000)6,329
Mesečnik
ISSN 0039-2480

© Journal of Mechanical Engineering 46(2000)6,329
Published monthly
ISSN 0039-2480

Vsebina
Contents

Strojniški vestnik - Journal of Mechanical Engineering
letnik - volume 46, (2000), številka - number 6

© Strojniški vestnik 46(2000)6,330-341
ISSN 0039-2480
UDK 532.5:530.16
Izvirni znanstveni članek (1.01)

© Journal of Mechanical Engineering 46(2000)6,330-341
ISSN 0039-2480
UDC 532.5:530.16
Original scientific paper (1.01)

Analiza kinematike toka za utripajočim profilom spremenljive geometrijske oblike z uporabo računalniške vizualizacije

Analysis of the Flow Kinematics Behind a Pulsating Adaptive Airfoil Using Computer-Aided Visualisation

Brane Širok - Erik Potočar - Matej Novak

V polnorazvitem zračnem toku podzvočnega vetrovnika je bila z uporabo računalniške vizualizacije ter metode digitalnega procesiranja serije posnetkov izvedena analiza kinematike toka vzdolž deformljivega profila (NACA 4416) spremenljive oblike pri hitrostnih razmerah Re =1000.

V prvem delu raziskave je bila izvedena študija preoblikovanja strukture toka ob profilu pri ustaljenih spremembah oblike profila, v drugem delu pa smo se osredotočili na opazovanje sprememb struktur toka pri periodično utripajoči obliki profila. Obliko poprej geometrično umerjenega profila smo spreminjali s periodičnimi tlačnimi utripi zraka, uvajanega v notranjost profila. Osnovna frekvenca vrtinčne sledi za profilom se pod vplivom utripov oblike profila opazno spremeni. Na zaporednih posnetkih tokovnih struktur vrtinčne sledi za utripajočim profilom, posnetih z video kamero, je bila izvedena količinska analiza časovnih vrst s simultano digitalizacijo nivojev sivine v izbranih področjih (oknih) sekvenc posnetkov. Za tokovno polje vzdolž profila so značilne različne vrednosti spektralnih gostot nivojev sivine in pripadajočih standardnih odmikov. Z metodo računalniške vizualizacije so bile raziskane strukturne tokovne spremembe v vrtinčni sledi v odvisnosti od frekvence vzbujanja geometrijske oblike profila. Rezultati kažejo, da periodične spremembe oblike profila vplivajo na tokovno strukturo vzdolž profila oziroma na njeno frekvenco in amplitudo ter na položaj točke odlepljanja na opazovanem profilu. Pojavlja se možnost prilagodljivega spreminjanja tokovne kinematike vzdolž profila.

(Ključne besede: kinematika toka, analize tokov, strukture tokov, vizualizacija računalniška)

In the fully developed airflow of a non-return subsonic wind tunnel using flow visualization and a digital image-processing method, an experimental study of the flow kinematics along and behind a hollow NACA 4416 adaptive airfoil at Reynolds number Re = 1000 was performed.

The study was performed in two parts: first the observation of flow transformation at temporal stationary changes of the airfoil shape was performed, and the second part of the analysis focused on the transformation of the flow at periodic time-pulsating airfoil deformations. The shape of a previously geometrically calibrated airfoil was modified with periodic pressure changes inside the airfoil. The basic frequency of the vortex street behind the airfoil is changed under the influence of the pulsating frequency of the airfoil. A CCD camera was used to capture smoke visualization images of the turbulent airflow wake, illuminated by the light sheet. A quantitative analysis was made on time series, obtained by simultaneous digitization of the grey level in several small areas (windows) of the overall image. The flow field along and behind the airfoil exhibited various frequency spectra and standard deviations. With the help of the computer-aided visualization method, structural flow changes were investigated, i.e. variations of the wake frequency response and respective amplitudes depending on the airfoil pulsation frequency. Results show that periodic changes of the airfoil shape have an affect on the flow structure along and behind the airfoil, i.e. the amplitude and frequency of the wake, and the location of a separation point. There may exist possibilities for adaptive flow kinematics variation along and behind the airfoil.

(Keywords: flow kinematics, flow analysis, flow structure, computer aided visualization)

0 UVOD

Zaradi dolgoletnih prizadevanj za vse boljšimi aerodinamičnimi lastnostmi profilov in zato večjim izkoristkom strojev so ustaljene oblike profilov

0 INTRODUCTION

As a result of the continuous drive for better aerodynamic profile quality, and as a consequence, more efficient machinery, the im-

dandanes v sklepni fazi razvoja. V zadnjih tridesetih letih je prišlo do napredka na področju raziskav pretočnih razmer vzdolž profilov, ne samo zaradi uvedbe novih materialov in vključevanja novih eksperimentalnih metod analize toka, ampak tudi spričo hitrega razvoja računalniško podprtih numeričnih modelov toka ob profilih. Pretežni del študij je bil usmerjen v analizo aerohidrodinamičnih karakteristik časovno nespremenljivih oblik profilov v polno razvitem turbulentnem toku. Iz literature je znano, da so se analize tokovnih karakteristik vzdolž nihajočih profilov osredotočale bodisi na interakcijo vrtinec/profil [1] ali na razvoj samega vrtinca pri sunkovito pospešenem krilu [2]. Omenjeni problem je bil raziskan tako numerično kakor tudi eksperimentalno [3]. Vendar pa rezultati raziskav spremembe geometrijske oblike profila, o katerih poroča razpoložljiva literatura, niso zelo obsežni. Tako so v preteklosti na profilih izvajali statično preoblikovanje obrisa profila [4] ter pri nekaterih tipih letal uporabljali kombinacijo dveh različnih geometrijskih oblik profila [5].

Če spreminjamo obliko profila, se tokovna sestava za njim značilno spremeni. S časovnimi spremembami oblike profila krila se lahko tako ustvarja povsem različna tokovna sestava, ki jo je, kakor kaže tudi pričujoča študija, mogoče nadzirati z različnimi načini preoblikovanja profila. Na tokovno sestavo za profilom je mogoče vplivati bodisi s spremembami oblike celotnega profila ali le posameznih delov profila.

1 NARAVA TOKA OKOLI PROFILA V STVARNI TEKOČINI

V stvarni tekočini prihaja do pojava cirkulacije toka zaradi viskoznih sil. Pri študiji tokovnega polja okoli profila je najprej treba preučiti razmere, v katerih nastajajo vrtinci v opazovanem toku tekočine. Vrtinci nastajajo na obrisih telesa v toku tekočine celo pri telesih brez ostrih robov zaradi naraščanja tlaka v smeri toka in velikih hitrostnih gradientov ob površinah trdnih teles. Pri obtekajočih telesih, kakor je profil krila v tokovnem polju, nastajajo vrtinci v področju prehoda mejne plasti v polno razviti tok tekočine. Razvoj vrtincev je tako odvisen od časovnih in krajevnih sprememb hitrostnega polja ob profilu, od širine vrtinčne sledi in hrapavosti površine.

Na stični površini neoviranega in vrtinčnega toka ob telesu profila deluje trenje. Pri tem nastale hidrodinamične sile težijo k trganju vrtincev in njihovemu prenosu vzdolž toka. V trenutku, ko se gradient tlaka, ki zadržuje opazovani vrtinec v vrtinčni coni zmanjša, se vrtinec odtrga iz mejne plasti in potuje s tokom v področje vrtinčnega toka na izstopnem robu profila. Tako imenovani začetni vrtinec na mestu izstopnega roba profila se razvija navidez periodično. Energijo za svoj obstoj, rast in dinamiko črpa iz razvitih vrtincev vzdolž toka ob profilu. Glede na vpadni kot α neoviranega toka na profil se lega in oblika

provement of the airfoil form has been taken almost to the limit. Over the past thirty years, progress has been made not only in the discovery of new materials, but also in connection with use of computer techniques and other relevant methods. The analyses of flow characteristics around the airfoil have focused on the flow structure over an oscillating airfoil during vortex/airfoil interaction [1]. The study of vortex evolution on an impulsively started airfoil has also been discussed [2]. This problem has been treated in a mathematical and experimental way [3], however, the results of research into airfoil-shape modification are, according to our knowledge, not very extensive. Investigations report on the static shape control of an adaptive airfoil [4], and the use of two different airfoils for a plane glider [5].

When the airfoil profile is modified, the flow structure behind the airfoil is completely changed. With the dynamic airfoil profile changes, it can create a completely different flow structure behind the airfoil, a structure which we can control with different methods of dynamic modification to the airfoil shape. It is possible to alter the shape of the entire airfoil, or only the shape of a certain airfoil section.

1 DEVELOPMENT OF CIRCULATION AROUND THE AIRFOIL IN A REAL FLUID

In a real fluid the circulation develops because of the viscous forces. When considering a flow field around an airfoil, it is primarily the conditions under which the vortices are formed in the actual fluid flow that have to be studied. Vortices are formed on the edges of bodies in the fluid flow. Even for bodies that are round and do not have sharp edges, the vortices appear due to a pressure rise in the flow direction and because of large velocity gradients along the profile structure. At bluff bodies, e.g. at the profile in the flow field, vortices are generated in the regions of transfer of the boundary layer into the fully developed fluid flow. The development of vortices depends on time and space changes of the velocity field along the profile, and on the width of the boundary layer and roughness of the surface.

On the contact surface of free and vortex flows along the profile structure friction occurs. The hydrodynamic forces generate vortex separation and vortex transport along the flow. When the pressure gradient, which holds the observed vortex in the vortex zone, decreases, the vortex is separated from the boundary layer and transported by the flow into the vortex street. The so-called initial vortex that appears near the trailing edge develops quasi-periodically. The energy for its existence, growth, and dynamics is generated from vortices along the profile. According to the value of the incidence angle α of the free flow

začetnega vrtinca spreminjata. Zaradi tega se tudi zajemanje razvitih vrtincev vzdolž telesa profila spremeni in vpliva na asimetrično naravo toka ob profilu. Trganje začetnega vrtinca na izstopnem robu profila in gibanje tega vzdolž toka v vrtinčni sledi za profilom je podobno kakor pri vrtincih na mikro skali, odvisno od razmerij hidrodinamičnih sil na vrtincu. Nastanek tako imenovanih svobodnih vrtincev ob telesu in na izstopnem robu ima za posledico raztros kinetične energije in pripelje do uporov v tokovnem polju. Izhajajoč iz tega lahko pričakujemo, da oblika vrtinčnega polja okoli profila in v vrtinčni sledi neposredno vpliva na hidrodinamične karakteristike profila, vključno z raztrosnimi karakteristikami.

2 PRESKUS

Preskusi so bili izvedeni v podzvočnem vetrovniku odprtega tipa. Hitrost toka v vetrovniku se spreminja s spreminjanjem frekvence vrtenja ventilatorja z uporabo frekvenčnega regulatorja, ki omogoča spreminjanje frekvence od 0 do 50 Hz v korakih po 0,01 Hz. Preskusni del iz poliakrilnega stekla je kvadratnega prereza s stranico 300 mm in dolžino 1000 mm. Koeficient zožitve vetrovnika znaša 16,5 : 1. Nivo turbulentnosti vetrovnika pri preizkusnih hitrostnih razmerah znaša 2,8%. Profil (NACA 4415) dolžine vzdolž toka 89 mm in višine 14 mm je bil pritrjen v preskusni del vetrovnika po njegovi celotni širini. Profil je izdelan iz vzmetne pločevine CK 60, ki je bila ustrezno termično obdelana. Na konceh profila je bil le ta zaprt s silikonskima čepoma. S tem je omogočena ob napihovanju profila njegova enakomerna sprememba oblike po celotni širini ob ustrezni tesnosti. Profil je bil, tako kakor tudi zadnja stena vetrovnika, prebarvan s črno barvo, kar zagotavlja kar največje zmanjšanje odboja svetlobe pri vizualizaciji tokovnega polja ob profilu. Natočni kot zraka na profil med preskusi je znašal 12^0.

onto the profile, the position and shape of the initial vortex changes. Consequently, the capturing of oncoming vortices along the profile structure is changed, and this influences the non-symmetric flow nature along the profile. The separation of the initial vortex that appears on the profile trailing edge and its movement along the flow in the vortex street is similar to phenomena on a micro scale, and depends on the relationship between the hydrodynamic vortex forces. Generation of the so-called “free vortices” along the profile structure and at the trailing edge causes the dissipation of kinetic energy and consequently generates the resistance in the flow field. Therefore it can be expected that the vortex field shape around the profile and in the vortex street directly influences the hydrodynamic and dissipation characteristics of the profile.

2 EXPERIMENTAL FACILITY

The tests were performed in a non-return subsonic wind tunnel. The wind tunnel fan speed is controlled by a frequency regulator with a range from 0 to 50 Hz in steps of 0.01 Hz. The test section has a square cross-section, made of plexi-glass, with a width of 300 mm and a length of 1000 mm. The wind-tunnel contraction ratio is 16.5:1. The turbulence level is 2.8%. The NACA 4415 airfoil was mounted so that it spanned the tunnel working section. The airfoil has an 89 mm stream-wise length and a thickness of 14 mm. It was mounted so that it spanned the tunnel working section. It was made from spring-tin plate CK 60, which had undergone a sufficient thermal treatment. The tips were filled with silicone, which enabled the airfoil to change its form symmetrically throughout its length. The airfoil was painted black, as was the back tunnel wall, to reduce the reflection of light during visualisation of the flow field around the profile. The angle of attack of the airfoil during the experiments in the wind tunnel was 12^0.

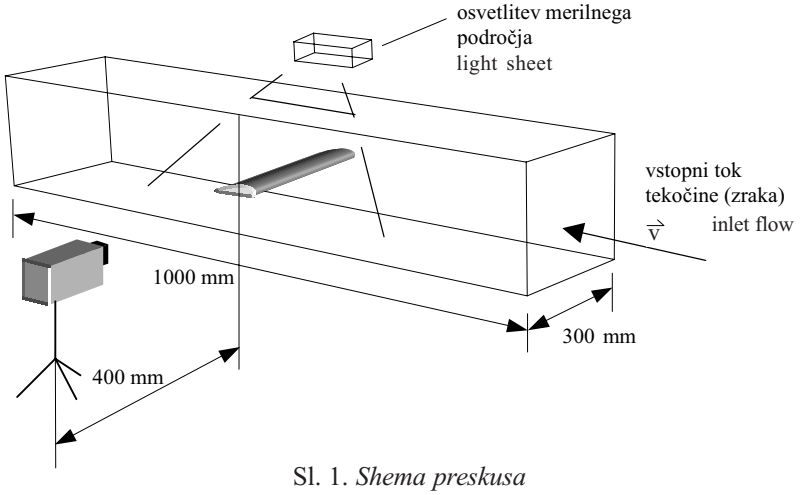

Sl. 1. *Shema preskusa*
Fig. 1. *The experimental configuration*

Vrtinčna sled vzdolž profila je bila vizualizirana z uporabo polutanta - dima parafinskega olja, ki smo ga uvajali v vetrovnik na oddaljenosti 20 mm pred profilom skozi cevko notranjega premera 1,5 mm.

Vrtinčna sled je bila osvetljevana od zgoraj s halogensko lučjo z močjo 1000 W. Širina svetlobnega snopa je znašala približno 2 mm. Zaporedni posnetki vrtinčne sledi so bili posneti z video kamero s frekvenco 25 posnetkov v sekundi, ki je bila usmerjena pravokotno na smer toka v osi profila (sl. 1). Resolucija vsakega posnetka je bila 736 x 560 točk, pri čemer je bila velikost točke pri danem eksperimentu 0,4 mm. Nivo sivine v času in prostoru ustvarja skalarne vzorce, ki jih z uporabo računalniške vizualizacije lahko opazujemo. Z zaporedno digitalizacijo gradientov sivine v opazovanih območjih (oknih) dobimo simultane skalarne časovne vrste.

Za določitev količinskih lastnosti tokovnih vzorcev za opazovanim profilom vpeljemo celoštevilčno spremenljivko $A(k, t)$ [6]:

$$A(k,t) = \sum_{l=1}^{L}\sum_{m=1}^{M} E(l,m) \qquad E(l,m) = \{0,1,2,3.....255\} \tag{1}.$$

S skalarno spremenljivko $A(k, t)$ je podana prostorsko povprečena intenzivnost sivine v opazovanem oknu k v času t. Opisani model povezuje intenzivnost svetlobe z navzočnostjo delca v opazovanem oknu. Časovni interval je definiran s frekvenco zajema slik na kameri in s številom zaporednih slik poljubno izbranega časovnega intervala.

Intenzivnost svetlobe $E(l, m)$, zaznavamo v 256 nivojih sivine, od popolnoma črne pri 0 do popolnoma bele pri 255. Časovne vrste lokalno krajevno povprečenega nivoja sivine so bile dobljene za vsakega od opazovanih oken.

Standardni eksperimentalni odmik lokalnega nivoja intenzivnosti sivine v posameznem oknu je bil izračunan po naslednji enačbi:

$$\sigma = \sqrt{\frac{1}{n}\sum_{k=1}^{n}\left\langle \left(A(k,t) - \left\langle A(k,t) \right\rangle \right)^2 \right\rangle} \tag{2},$$

kjer $\left\langle A(k,t) \right\rangle$ pomeni časovno povprečeno vrednost krajevno povprečene intenzivnost sivine $A(k, t)$:

$$\left\langle A(k,t) \right\rangle = \frac{\sum_{k=1}^{n} A(k,t)}{n} \tag{3},$$

kjer je $A(k, t)$ trenutna prostorsko povprečena intenzivnost sivine.

Za podrobno analizo fluktuacij intenzivnosti sivine $A(k, t)$ uporabimo 1024 zaporednih digitaliziranih posnetkov za vsakega od analiziranih oken. Spektre moči izračunamo iz osnovnih časovnih vrst s standardno Fourierjevo transformacijo osnovnih časovnih vrst:

In order to visualise the vortex street behind the airfoil, paraffin oil smoke was injected into the wind tunnel in front of the airfoil through a specially modified hose with a 1.5 mm internal diameter. The hose was 20 mm away from the airfoil and directed onto the half thickness of the airfoil.

The visualised streak lines were illuminated from above by continuous lighting supplied by a 1000 W halogen lamp. The light-sheet was approximately 2 mm wide. The successive images of the visualised vortex street were captured by a CCD camera, aimed along the spanwise axis of the airfoil, with 25 frames/s (Fig. 1). The resolution of each of the frames was 736 x 560 pixels. The spatial resolution of a pixel is about 0.4 mm for this experiment. The grey level in time and space generates scalar patterns, which can be observed with the help of a computer-aided visualization. Quantitative analysis was made on a time series, obtained by simultaneous digitization of the grey level in several small areas (windows) of the overall image.

For the assessment of the quantitative behaviour of the patterns of the flow behind the airfoil, an integer-type scalar's variable $A(k, t)$ was introduced [6]:

$A(k, t)$ is the space averaged light intensity (grey level) of an observed window k at time t, and corresponds to the instantaneous smoke concentration in the observed window. This is obtained by summing each individual pixel brightness $E(l, m)$ over the entire window. The time interval of the observation is defined by the camera speed and by the number of sequentially taken pictures in an optional time interval.

The light intensity can vary from complete blackness with a zero value, to complete whiteness with a value of 255. The time series of local space-averaged grey intensity level at our disposal were obtained for each observed window.

The standard deviation of the local grey intensity level in the window is defined as:

where $\left\langle A(k,t) \right\rangle$ is the time-averaged value of the space averaged light intensity $A(k, t)$:

and $A(k, t)$ is the instantaneous space-averaged light intensity.

For detailed studies of the fluctuations in the light intensity $A(k, t)$, 1024 successive frames were digitised for each window analysed. The power spectra of the time series may be obtained using the Fourier transform:

$$A(k,\omega) = \frac{1}{2\pi}\sum_{t} A(k,t)e^{-i\omega t} \quad (4).$$

Obliko profila, ki je bila poprej geometrično umerjena, smo spreminjali s periodičnimi tlačnimi utripi z zrakom, ki smo ga uvajali v notranjost profila. Meritve fluktuacij toka so bile izvedene v dveh sklopih. Najprej pri različnih tlakih v notranjosti profila, ki so imeli za posledico različno časovno ustaljeno obliko profila in nato pri periodičnih časovnih utripih geometrijske oblike profila. Tlak v profilu smo nadzirali s tlačnim ventilom, povezanim prek kartice z računalnikom. Merilna veriga z računalniškim nadzorom vzbujanja (sl. 2) je bila sestavljena iz utripnega generatorja, merilnika sunkov in izpisa časovnega stanja krmilnega ventila. Na drugem računalniku pa je bilo mogoče prebrati tlačne spremembe na opazovanem profilu s tlačnim pretvornikom KISTLER Kristal tip 4285A5 v frekvenčnem področju do 1 kHz.

The airfoil shape was modified with periodic pressure changes inside the airfoil. For the geometrically calibrated airfoil, measurements of airflow kinematics were performed at stationary integral parameters, and at periodic time-pulsating airfoil deformations. The pressure in the airfoil was controlled with the aid of a pressure valve. The valve was controlled by a computer with a Visual Designer data-acquisition board. The measurement chain for pressure-valve control in the Visual Designer program is composed of pulse generator, impulse meter, and of a pulsation function display. Pressure changes were displayed on a second computer, measured by a KISTLER type 4285A5 pressure probe with a frequency range up to 1 kHz. A schematic of the pressure-control measuring set-up is shown in Fig. 2.

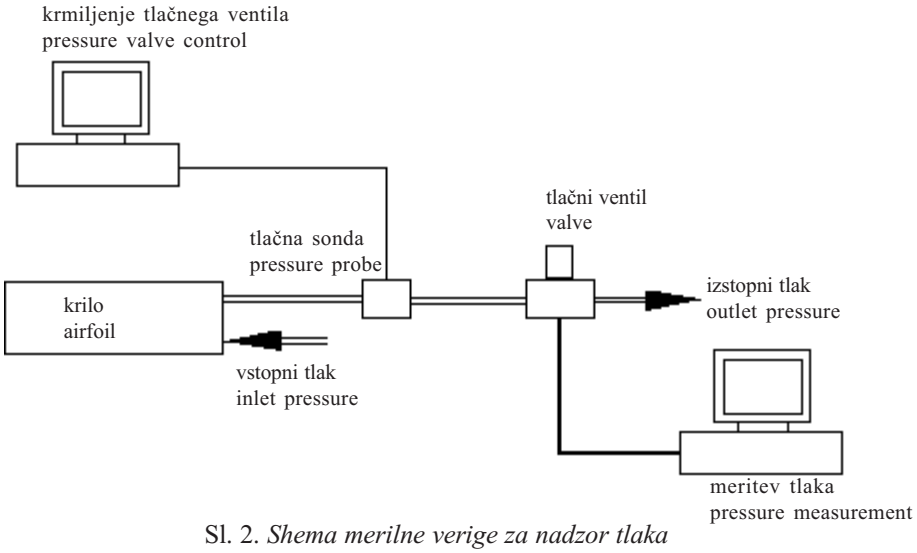

Sl. 2. *Shema merilne verige za nadzor tlaka*
Fig. 2. *Schematic of the pressure control measuring set-up*

Tlačna sprememba v profilu spremeni obliko profila v profil z bistveno drugačnimi aerodinamičnimi karakteristikami. Nenapihnjeni profil je imel obliko profila NACA 4416. Ko se je tlak znotraj profila zvišal na največjo vrednost 2,4 bar, se je višina profila povečala za 4,19 mm, tako da se je oblika tlačno deformiranega profila približala obliki profila tipa NACA 4421.

A pressure change in the airfoil modifies its shape to an airfoil with completely different aerodynamic characteristics. The non-deformed airfoil has the shape of the NACA 4416 airfoil. When the pressure inside the airfoil was increased up to a maximum of 2.4 bar, and as a result the airfoil thickness increased by 4.19 mm, the shape was modified to that of the airfoil NACA 4421.

3 PREDSTAVITEV REZULTATOV

3.1 Kinematika vrtinčne sledi pri ustaljenih parametrih

V vetrovniku je bila najprej izvedena analiza kinematike vrtinčne sledi pri ustaljenih integralnih parametrih oblike profila za nedeformiranim in deformiranim profilom. Območje opazovanja, prikazano

3 RESULTS AND DISCUSSION

3.1 Vortex street kinematics at stationary integral parameters

The first analysis in the wind tunnel was of the vortex street kinematics at stationary integral parameters behind a non-deformed and deformed airfoil. The observation area, shown in

na sliki 3, je bilo izbrano tako, da omogoča analizo toka okoli zadnjega roba profila ter vrtinčne sledi za profilom. Predpostavljamo namreč, da so spremembe dinamike toka v omenjenem območju najintenzivnejše. Velikost opazovanega območja je znašala 350 x 100 točk (1 točka znaša 0,4 mm za obravnavani preskus). Opazovano območje je bilo razdeljeno v 350 oken velikosti 10 x 10 točk. Reynoldsovo število za osnovni profil je znašalo v času trajanja eksperimenta Re = 1016. Na slikah 4 in 5 sta predstavljeni topološki sestavi standardnega eksperimentalnega odmika lokalnega nivoja intenzivnosti sivine $\sigma(x,y)$ v tokovnem polju za osnovnim in deformiranim profilom.

Fig. 3, was chosen in a manner that enables observation of the rear end of the airfoil and of the vortex street. We assumed that the changes are the most significant in the chosen area. The size of the observation area was 350 x 100 pixels (1 pixel was about 0.4 mm), and was divided into 350 windows, 10 x 10 pixels in size. The Reynolds number, based on a profile during the experiments, was Re = 1016. In Figs. 4 and 5 the topological standard deviation maps of the average grey intensity $\sigma(x,y)$ in the flow field behind a non-deformed and deformed airfoil are presented.

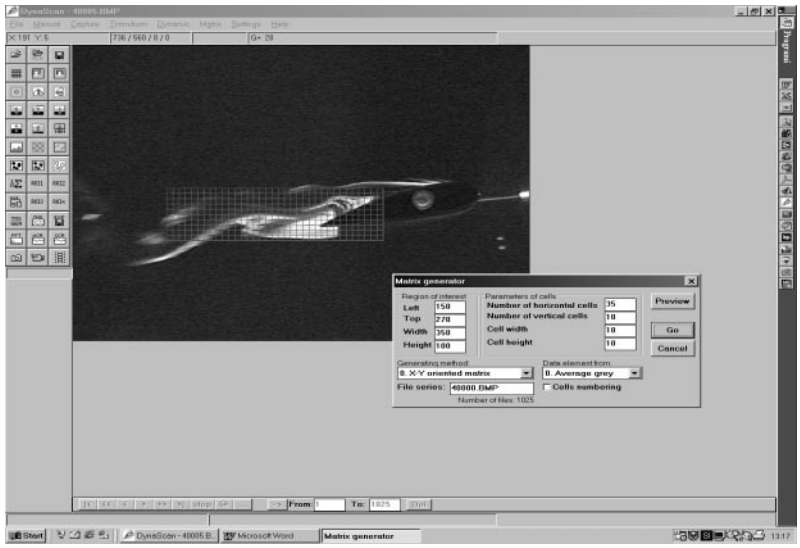

Sl. 3. *Opazovano območje za profilom*
Fig. 3. *Location of the observation area behind the airfoil*

V diagramu standardnega eksperimentalnega odmika nivoja sivine nedeformiranega - osnovnega profila NACA 4416 (sl. 4) lahko opazimo, da je vrednost standardnega eksperimentalnega odmika večja (nad 50) v območju, kjer se polutant dalj časa zadržuje, kar kaže na pojav vrtinčenja. To območje je po abscisni osi pri vrednosti $x = 200$ točk in po ordinatni okoli $y = 40$ točk in je podolgovate oblike. Na zgornjem delu zadnjega roba profila se vidi področje z višjo vrednostjo spremenljivke σ (nad 25), kar je povezano s povratnim tokom ob lopatici.

In the diagram of the standard deviation of the average grey intensity of a non-deformed basic airfoil NACA 4416 (Fig. 4), one can see that the value of the standard deviation is larger (over 50) in the region where smoke particles persist and denote whirling. The maximum value of the area is around the value of 200 on the x-axis, and around 40 on the y-axis, and has an oblong shape. On the upper part of the airfoil edge, where the flow is recurrent, an area with a larger standard deviation value σ (over 25) can be sensed.

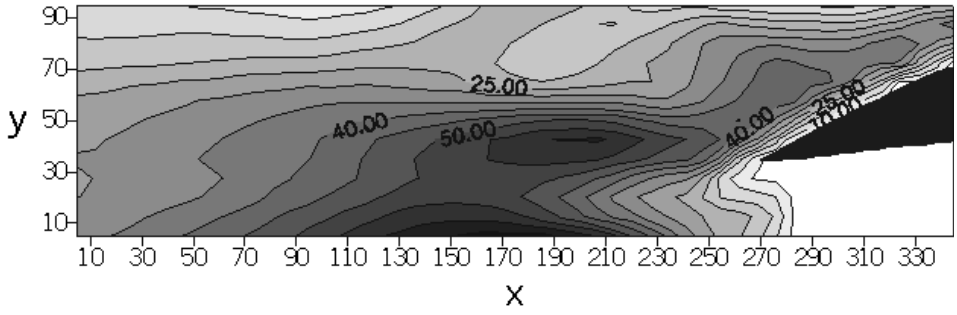

Sl. 4. *Standardni odmik nivoja sivine za nenapihnjeno lopatico (NACA 4416)*
Fig. 4. *Standard deviation of the average grey intensity of a non-deformed airfoil (NACA 4416)*

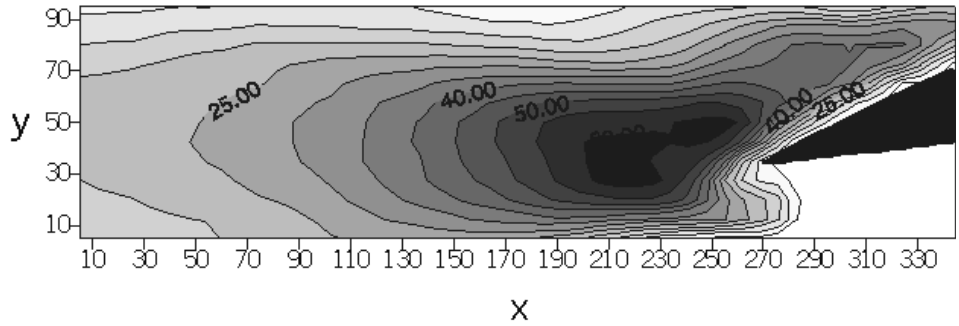

Sl. 5. *Standardni odmik nivoja sivine za napihnjeno lopatico (NACA 4421)*
Fig. 5. *Standard deviation of the average grey intensity of a deformed (blown) airfoil (NACA 4421)*

V diagramu standardnega odmika povprečnega nivoja sivine deformiranega profila NACA 4421 (sl. 5), lahko opazimo, da se je območje za lopatico, ki predstavlja začetni vrtinec, pomaknilo bliže zadnjemu robu profila (x = 220 točk, y = 45 točk), kar je pri debelejšem profilu pričakovano. Pri tem se je nivo standardnega odmika povečal in razširil proti zgornjemu delu krila (povratni tok ob krilu se pomika nazaj proti toku). Pri deformiranem profilu se tokovnice slabše prilagajajo obrisu profila. Iz primerjave obeh primerov vidimo, da s spremembo oblike profila dobimo različne tokovne sestave ob krilu in v vrtinčni sledi.

3.2 Kinematika vrtinčne sledi pri periodičnem utripnem spreminjanju geometrijske oblike profila

V drugem delu je bila izvedena analiza kinematike vrtinčne sledi za profilom, kateremu smo z uporabo tlačnih utripov periodično spreminjali obliko. Na sliki 6 je predstavljen del sekvence zaporednih posnetkov vrtinčne sledi profila pri Re = 1016.

Iz zaporednih posnetkov Karmanove vrtinčne sledi, dobljene pri frekvenci tlačnih utripov 0,25 Hz lahko opazimo, da se na zgornji površini profila razmeroma hitro odtrga mejna plast in ustvari sled, ki se neposredno za profilom združi s sledjo s spodnje površine profila. Tu nato prihaja do nastanka polno razvite vrtinčne sledi za profilom. Spodnja in zgornja slednica se izmenoma združujeta ena v drugo in delata Karmanovo vrtinčno sled. V njej se oblikujejo v enakem časovnem zaporedju, manjši vrtinci, ki se pomikajo s tokom. Ti vrtinci se pojavljajo v enakem zaporedju izmenoma na zgornji in spodnji strani. Razdalja med njimi se vzdolž toka povečuje. Pri slikah k in l (sl. 6) lahko vidimo značilen pojav nenadne porušitve v vrtinčni sledi, ki je posledica tlačnega vzbujanja profila in nelinearne interakcije med vrtinci. Pri tem prihaja do naključne aperiodične vzpostavitve popolnoma nove navidez periodične vrtinčne sledi. Za količinsko analizo toka pri utripajočem profilu je bilo v vrtinčno sled nameščenih 12 oken opazovanja, katerih položaj je prikazan na sliki 7. V nadaljevanju bodo predstavljeni rezultati analize časovnih vrst nivoja sivine v 11. oknu.

In the diagram of the standard deviation of the average grey intensity of a deformed, i.e. blown airfoil NACA 4421 (Fig. 5), one can observe that the area of the maximum vorticity behind the airfoil is moved closer to the trailing edge (with the centre at x = 220, y = 45) as was expected for the thicker airfoil. Moreover, the magnitude of the area has increased and moved towards the upper airfoil surface, i.e. the recirculated flow above the airfoil has lifted. The qualitative inspection of both non-deformed and deformed airfoil image sequences showed that the streamlines above the upper surface of the airfoil for the deformed airfoil are straighter. Therefore, the difference between both respective airfoil shapes can be seen and as a consequence, they have various influences on the vortex street.

3.2 Vortex street kinematics at periodic time-pulsating airfoil deformations

The next stage was to analyse the vortex street kinematics for periodic time-pulsating airfoil deformations. In Fig. 6 a part of the successive image sequence is shown for the airfoil vortex street obtained at Re = 1016.

In the successive images the Karman vortex street can be observed, obtained at an airfoil pulsation frequency of 0.25 Hz. The flow is separated at the upper airfoil surface and generates a streamline which is behind the airfoil amalgamated with the lower streamline. The connected streamline oscillates, and vortices are shed alternately from each side of the airfoil and persist for some distance downstream, forming a double row, typical of a Karman vortex street. In images k and l of Fig. 6 a sudden brake of the vortex street shape occurs, caused by the airfoil pulsation. Consequently, a new type of the vortex street is formed. For the quantitative analysis of the flow behind the pulsating airflow the 12 observation windows were located in the vortex street behind the airfoil (Fig. 7). In continuation the results of the grey level intensity time series analysis for the 11th window are presented.

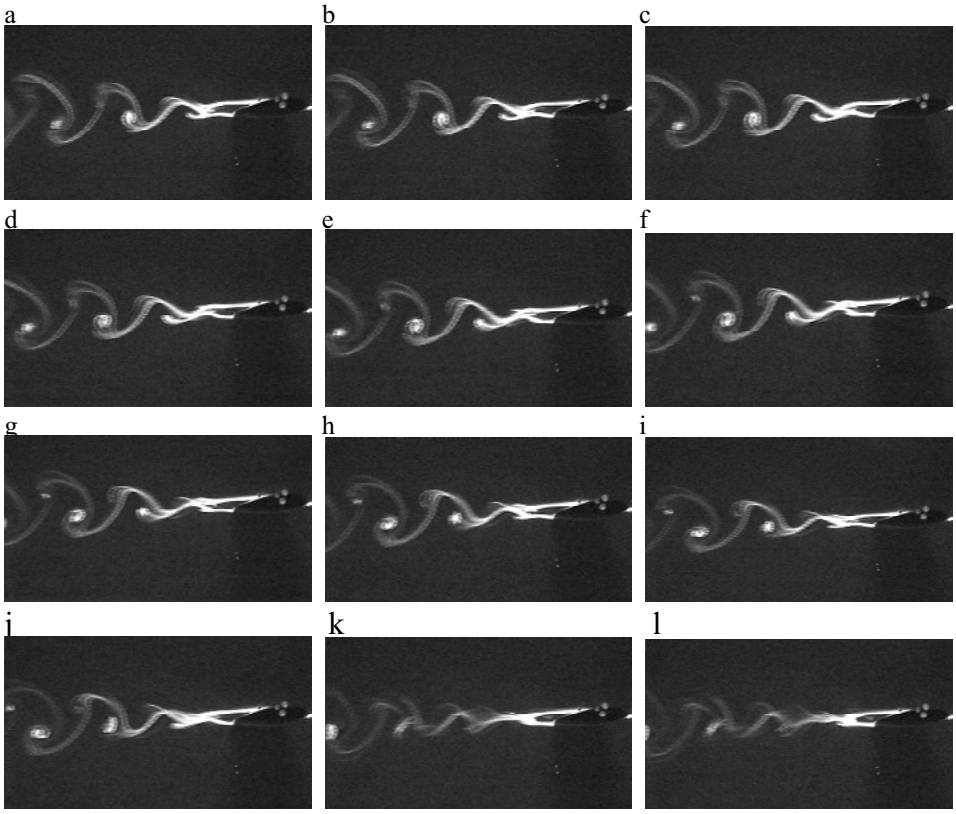

Sl. 6. *Zaporedje posnetkov vrtinčne sledi za utripajočim profilom*
Fig. 6. *Image sequence of the pulsating airfoil vortex street*

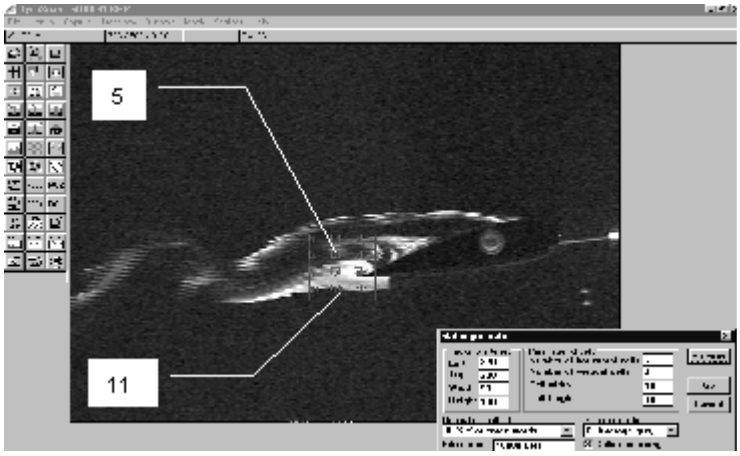

Sl. 7. *Lega posameznih območij opazovanja*
Fig. 7. *Position of the observed windows in the pulsating airfoil vortex street*

Opravili smo analizo časovnih vrst krajevno povprečenega nivoja sivine v izbranem oknu ter pripadajočih spektrov moči pri različnih frekvencah utripanja profila v razponu od 0,25 do 10 Hz. Na slikah 8 in 9 lahko vidimo, da se pri povečevanju frekvence utripanja profila vrednost osnovne frekvence vrtinčne sledi in pripadajočega višjega harmonika spreminja. Pri tem lahko glede na stopnjo naraščanja celotno območje utripnih frekvenc pri nespremenjenem Re številu razdelimo na dve ločeni področji, prvo do frekvence utripanja profila 2,5 Hz in drugo nad njim.

The grey level intensity time series and their spectra were observed at different airfoil pulsation frequencies, varying between 0.25 and 10 Hz. From Figs. 8 and 9 one is able to recognise that when increasing the pulsation frequency, the characteristic frequency of the vortex street along with its higher harmonics changes. There are basically two regions of the gradient of increase, the first below the airfoil pulsation frequency of 2.5 Hz, and the second above it. In the first part, the dynamic reply of a vortex street is significant. In the area of pulsating frequencies

V prvem področju je odgovor dinamike vrtinčne sledi na vzbujanje vpliven. V frekvenčnem področju od 0 do 0,5 Hz, je gradient spreminjanja frekvence vrtinčne sledi največji. V drugem območju s frekvenco utripanja profila nad 2,5 Hz pa je dinamični odziv vrtinčne sledi majhen.

Iz navedenega lahko povzamemo, da vsiljeno utripanje profila povzroča nastajanje vedno večjega števila vrtincev v vrtinčni sledi, kar pripelje do povečanja frekvence vrtinčne sledi. Pri frekvenci utripov, ki je blizu karakteristični frekvenci vrtinčne sledi nenapihnjenega profila, vrednost karakteristične frekvence vrtinčne sledi vzbujanega profila doseže svoj vrh. Ko je omenjeno frekvenčno območje preseženo, povečevanje frekvence utripov ne vpliva bistveno na osnovno frekvenco vrtinčne sledi.

between 0 and 0.5 Hz, the gradient of the vortex street frequency change is the highest. In the second region, with pulsation frequencies above 2.5 Hz, the dynamic reply of a vortex street, however, is minimal.

From the above mentioned it can be concluded that the growth of the pulsation frequency generates more vortices in the vortex street, which consequently leads to the growth of the vortex street frequency. At the frequency of pulsation close to the characteristic frequency of the vortex street for the non-blown profile, a vortex street frequency behind the pulsating airfoil reaches its maximum. After that point, the increase in pulsation frequency does not influence significantly the basic frequency of the vortex street any more.

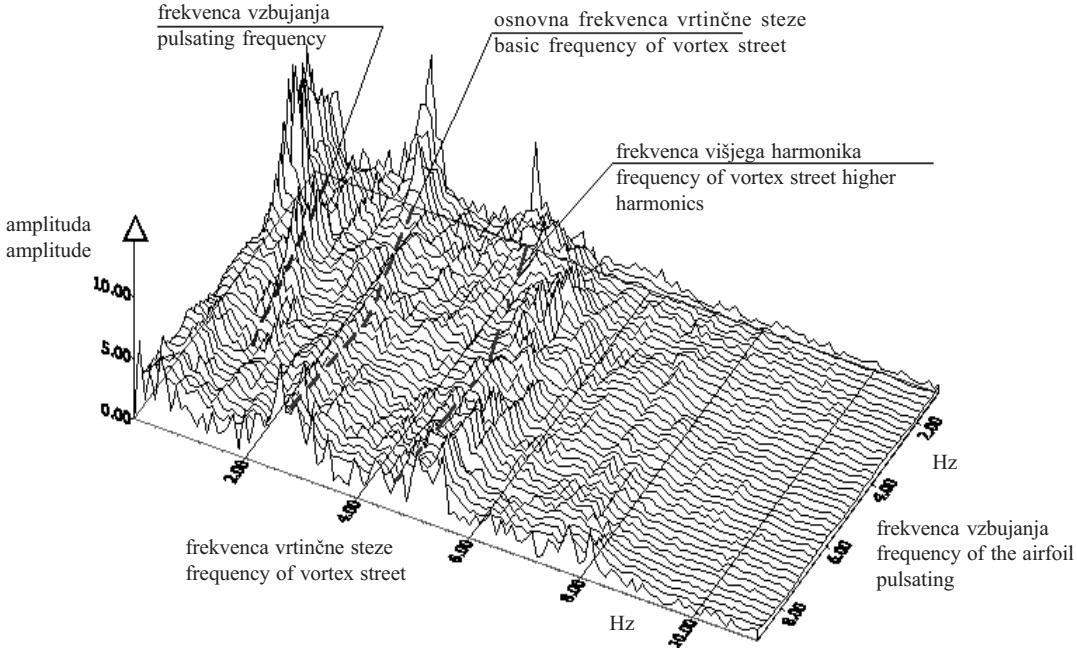

Sl. 8. *Diagram frekvenčnih spektrov vrtinčne sledi za 11. okno za vse frekvence vzbujanja profila*
Fig. 8. *3D diagram of a frequency spectra of different pulsation frequencies of the 11th window*

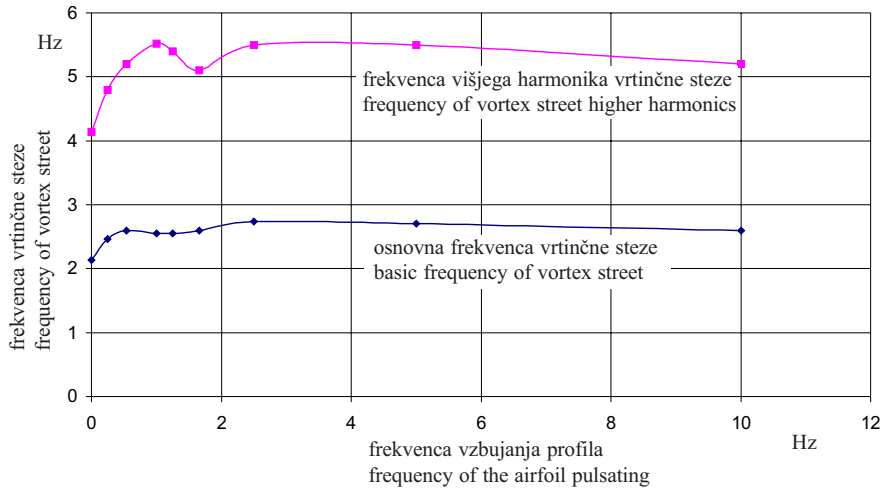

Sl. 9. *Osnovna frekvenca in višji harmonik vrtinčne sledi v odvisnosti od frekvence vzbujanja profila*
Fig. 9. *Basic vortex street frequency and higher harmonics vs. the airfoil pulsation frequency*

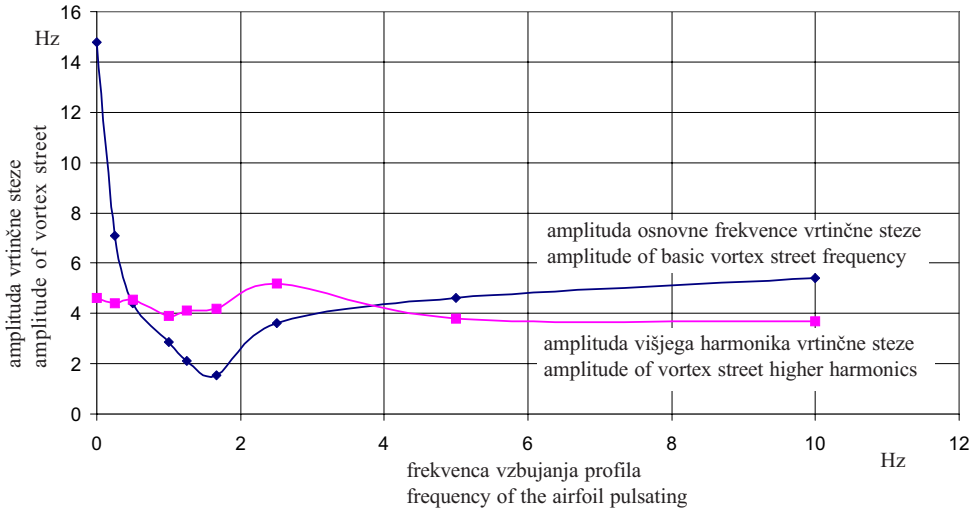

Sl. 10. *Amplitudi osnovne frekvence in višjega harmonika vrtinčne sledi v odvisnosti od frekvence vzbujanja profila*
Fig. 10. *Amplitude of basic vortex street frequency and higher harmonics versus the airfoil position frequency*

Amplituda osnovne frekvence vrtinčne sledi (sl. 10) se pri povečevanju frekvence nihanj znatno zmanjšuje do frekvence vzbujanja 1,7 Hz in se zatem začne ponovno povečevati. Amplitude v območju frekvence višjega harmonika pa se pri različnih frekvencah vzbujanja ne spreminjajo značilno in se stabilizirajo v področju nad lastno frekvenco vrtinčne sledi, podobno kakor amplituda osnovne frekvence.

Bistveno pri periodičnem spreminjanju oblike profila je, da utripi znatno vplivajo na frekvenco in obliko fluktuacij toka v vrtinčni sledi in je mogoče s pulzacijami oblike profila frekvenco vrtinčne sledi ter njeno amplitudo spreminjati. Ta vpliv je močan v področju vzbujanja pri frekvenci vzbujanja, nižji od lastne frekvence sprememb v vrtinčni sledi opazovanega profila.

4 SKLEP

Namen pričujočega prispevka je bila analiza sprememb v vrtinčni sledi okoli utripajočega profila v vetrovniku. Spremembe v vrtinčni sledi smo opazovali z uporabo računalniško podprte vizualizacije. Želeli smo odgovoriti na vprašanje, ali se tokovne razmere spremenijo in v kakšni meri, če s periodičnimi utripi spreminjamo obliko profila. Pri analizi smo opazovali povezavo med dinamiko spreminjanja oblike profila in sestavo toka za in okoli profila.

Rezultati so razdeljeni v dve osnovni skupini: v prvem delu so predstavljeni rezultati razlik v toku pri dveh različnih oblikah profilov brez dinamičnega vzbujanja. Skladno s pričakovanji se velikost vrtincev pri debelejšem profilu poveča in vrtinčni tok se pomakne bliže k zadnjemu robu profila.

V drugem delu raziskave je bila izvedena analiza tokov za periodično vzbujanim profilom v

The amplitude of the basic frequency of the vortex street, when increasing the pulsating frequency, decreases to a pulsating frequency of 1.7 Hz and then slowly begins to increase again (Fig. 10). The amplitude of the higher harmonic however does not change significantly with the pulsating frequency. It stabilises in the region above the basic frequency of the vortex street, like it does for the amplitude of the basic frequency.

The most distinctive phenomenon of the periodic changes of profile shape is the significant influence of pulsation on the frequency and shape of vortex street fluctuations. With aid of profile shape pulsation, the frequency and amplitude of the vortex street can be altered. The influence is significant mainly in the pulsating frequency region lower than the basic frequency of the vortex street of the non-deformed profile.

4 CONCLUSION

The purpose of this study was the observation of changes in the vortex street behind and around the pulsating adaptive airfoil in a wind tunnel. Modifications in the vortex street were observed with the help of a computer-aided visualisation. We tried to answer the question, whether the flow conditions behind the airfoil can be changed, and to what extent, by the shape-altering pulsation of the airfoil. We focused as well on the connections between the dynamics of the airfoil shape and the flow structure behind and around the airfoil.

The results are divided into two parts: in the first part, the results from the observation of flow transformation at temporal stationary changes of the airfoil's shape are presented. In accordance with expectations, the size of the vortices is enlarged when the airfoil is thicker and the flow moves closer to the rear edge of the airfoil.

In the second part, the analysis was focused on the transformation of the flow at the pulsating air-

določenem razponu tlačnih utripov. Opazimo lahko, da je s periodičnim preoblikovanjem profila mogoče spreminjati obliko tokovne sestave za profilom in da je le ta različna od oblike pri časovno ustaljenih razmerah. Osnovna frekvenca vrtinčne sledi se pod vplivom utripov profila spremeni. Pri zviševanju vrednosti frekvence utripov se vrednost osnovne frekvence vrtinčne sledi povečuje, vrednost amplitude v področju osnovne frekvence pa zmanjšuje. Pri frekvenčnih vrednostih utripov, ki so blizu osnovni frekvenci vrtinčne sledi nenapihnjenega profila, je amplituda osnovne frekvence vrtinčne sledi za profilom najnižja in frekvenca največja. Z nadaljnjim povečevanjem frekvence pulzacij profila se učinek utripne frekvence na vrtinčno sled naglo zmanjšuje.

Bistveno pri utripanju oblike profila je, da utripanje znatno vpliva na frekvenco vrtinčne sledi in je mogoče z utripanji oblike profila frekvenco vrtinčne sledi ter njeno amplitudo spreminjati. Na ta način je mogoče spreminjati sestavo toka za profilom, kar odpira nove možnosti uporabe oziroma uporabe aerodinamičnih lastnosti profila. Prav tako pa je z omenjeno metodo mogoče povečati uporabno območje posameznega profila, kar navaja na možnost prilagodljivega krmiljenja tokovnih razmer na različnih tehničnih uporabah.

foil. The flow structure behind the airfoil can be altered by periodic pulsation of the airfoil's shape and it differs from the stationary one. The basic frequency of the vortex street behind the airfoil is changed under the influence of the pulsating frequency of the airfoil. As the pulsating frequency is increased, the value of the basic vortex street frequency rises, and its amplitude in the region of the basic frequency decreases. At pulsating frequencies close to the basic frequency of the stationary non-deformed airfoil shape, the amplitude of the basic frequency of the vortex street behind the pulsating airfoil is the lowest, and the frequency is a maximum. However, with the continual growth of the pulsating frequency, the effect of the pulsating frequency on the vortex street rapidly decreases.

The most notable change when pulsating the airfoil shape is that the pulsation influences the basic frequency of the vortex street to a great extent, and that the frequency of the vortex street and its amplitude can be altered. In this way the structure of the flow behind the airfoil can be significantly modified. This opens up new possibilities for the exploitation of aerodynamic properties of the airfoil. It can also increase the operational range for which the airfoil is adequate and opens up new possibilities for future adaptive control of flow conditions in various technical applications.

5 SIMBOLI
5 NOMENCLATURE

celoštevilčna skalarna spremenljivka – nivo sivine	$A(k, t)$	integer-type scalar variable – level of greyness
amplituda	$A(k, \omega)$	amplitude
intenzivnost svetlobe	$E(l, m)$	light intensity
opazovano okno	k	observed window
celo število	L	integer number
število vrstic	l	number of rows
celo število	M	integer number
število stolpcev	m	number of columns
število vzorcev	N	number of samples
Reynoldsovo število	Re	Reynolds number
čas	t	time
vodoravna lega v točkah	x	horizontal position in pixels
navpična lega v točkah	y	vertical position in pixels
standardni eksperimentalni odmik lokalnega nivoja intenzivnosti sivine	σ	standard deviation of the local grey level intensity

6 LITERATURA
6 REFERENCES

[1] Cheng – Hsiung Kuo, J.K.Hsieh (1998) Flow structure over an oscillating airfoil during vortex/airfoil interaction, 8Th Internationnal symposium on flow visualization.
[2] P. Ghosh Choudhuri, D.D. Knight (1994) Two-dimensional unsteady leading – edge separation on a pitching airfoil, AIAA Journal.
[3] Isogai, K. and Y. Shinmoto (1999) Numerical simulation and visualization of unsteady viscous flow around an oscillating tandem airfoil in hovering mode, Proceedings of PSFVIP-2.
[4] Austin, F., Michael J. Rossi (1994) William Van Nostrad and Gareth Knowles, Static shape control for adaptive wing, AIAA Journal, vol.32, No.9.
[5] Streather, R.A. (1982) Variable geometry aerofoils as applied to the Beatty B-5 and B-6 sailplanes.
[6] Novak, M., Širok, B., Hočevar, M., Philpott, D.R., P. R. Bullen (1999) Analysis of turbulent mixing flow of a bluff body wake using a computed vision system, 3rd ASME/JSME JointFluid Engineering Conference July 18 – 22, San Francisco, California.

Naslovi avtorjev: doc.dr. Brane Širok
Fakulteta za strojništvo
Univerze v Ljubljani
Aškerčeva 6
1000 Ljubljana

Erik Potočar
Ministrstvo za znanost in tehnologijo
1000 Ljubljana

Matej Novak
Turboinštitut
1000 Ljubljana

Authors' Addresses: Doc.Dr. Brane Širok
Faculty of Mechanical Eng.
University of Ljubljana
Aškerčeva 6
1000 Ljubljana, Slovenia

Erik Potočar
Ministry of Science and Tech.
1000 Ljubljana, Slovenia

Matej Novak
Turboinstitute
1000 Ljubljana, Slovenia

Prejeto: 20.4.2000
Received:

Sprejeto: 2.6.2000
Accepted:

© Strojniški vestnik 46(2000)6,342-346
ISSN 0039-2480
UDK 697.97:628.85
Izvirni znanstveni članek (1.01)

© Journal of Mechanical Engineering 46(2000)6,342-346
ISSN 0039-2480
UDC 697.97:628.85
Original scientific paper (1.01)

Dinamični model nadzora temperature prostora s stropnim hlajenjem

A Dynamic Model for the Control of a Room's Temperature by Means of Ceiling Cooling

Tonko Ćurko - Ivan Galaso

V prispevku je predstavljen model dinamičnega simuliranja toplotnih razmer v prostoru v poletnem času. Analizirali smo dva različna sistema nadzora temperature prostora: stropno hlajenje in dovod hladnega zraka. Predstavljene so primerjave obeh sistemov: primerjava parametrov vpliva in vpliv na spremembo temperature prostora.

(Ključne besede: modeli dinamični, temperature sobne, regulacija temperature, hlajenje stropov)

This paper presents a dynamic-simulation model of a room's thermal behavior during summer conditions. Two different systems for the room's temperature control, i.e. ceiling cooling and cold air supply, were analyzed. A comparison of the influencing parameters and the influence on the operating room temperature variation applying both systems are reported.

(Keywords: dynamic models, room temperature control, ceiling cooling)

0 UVOD

Hladilno obremenitev lahko definiramo kot količino energije, ki jo vnašamo v prostor in hkrati odvzemamo klimatizacijski napravi, da ohranjamo stalno temperaturo v prostoru. To količino energije lahko odvzamemo z vpihovanjem ohlajenega zraka v prostor ali z ohlajanjem katere izmed površin v prostoru, npr. stropno hlajenje. V tem primeru se izmenjava energije večinoma izvaja s prenosom toplote s sevanjem med notranjimi površinami v prostoru. Različna načina ohranjanja sobne temperature v teh dveh primerih predstavljata prav tako različne parametre toplotnega ugodja.

Hladilna obremenitev prostora je toplota, ki jo je treba prenesti iz prostora (s hlajenjem), da ohranimo stalno temperaturo zraka – povprečno sobno temperaturo. Hlajenje izvajamo z zrakom, ki ga hladimo z različnimi sistemi (OPKH – ogrevanje, prezračevanje, klimatizacija, hlajenje - HVAC). Eden izmed načinov nadzora temperature prostora je stropno hlajenje. Pri tem postopku se večina toplote znotraj prostora prenaša s sevanjem med hladnejšim stropom in preostalimi, toplejšimi površinami v prostoru. Različni sistemi za OPKH, ki jih uporabljamo za nadzor temperature v prostoru,

0 INTRODUCTION

The cooling load may be defined as the amount of energy that is transferred to the room air and simultaneously removed by conditioning equipment, to keep a constant temperature in the room. This amount of energy can be removed either by blowing cooled air in to the room or by cooling one of the interior surfaces of the room, for example, ceiling cooling. In this case, the exchange of energy takes place mostly as heat transfer due to radiation between interior surfaces of the room. The different characters of room temperature maintenance in these two cases also mean different thermal comfort parameters.

The room-cooling load is the heat to be transferred out of the room (by cooling) in order to keep a constant air temperature – the mean room temperature. Cooling is carried out by the air, which is cooled in various HVAC (Heating, Ventilation, Airconditioning, Cooling) systems. One of the methods for room temperature control is ceiling cooling. In this procedure, the majority of the heat transferred within the room is a result of radiation between the colder room ceiling and other room surfaces, which are warmer. A different HVAC system used for control of the room's temperature causes a different varia-

povzročajo različne oblike parametrov, ki določajo posameznikovo ugodje v prostoru. Da bi lahko raziskali medsebojni vpliv parametrov, smo razvili modeliranje in simuliranje toplotnih sprememb določenega prostora. V analiziranem modelu je bila zahtevana temperatura zraka v prostoru ϑ_p = 24°C za obdobje 24 ur. Določili smo hladilno obremenitev prostora in temperature vseh površin za oba obravnavana primera.

1 RAČUNSKA METODA

Izračun stropne hladilne obremenitve je mogoč, ko določimo enačbe toplotnega ravnotežja za vse stične površine prostora [1]. Enačbe, ki določajo stopnjo prenosa toplote na katerikoli notranji površini *j* v določenem času *t*, so:

$$q_{j,t} = \alpha_{j,t}\left(\vartheta_p - \vartheta_{j,t}\right) + \sum_{k=1}^{B} G_{j,k}\left(\vartheta_{k,t} - \vartheta_{j,t}\right) + RA_{j,t} \tag{1}$$

kjer je $G_{j,k}$:

$$G_{j,k} = 4\,\varepsilon_j\,\varepsilon_k\,\sigma\;T_p^{3}\,F_{j,k} \tag{2}$$

Toplotni tok na notranjo površino, ki se izvaja s konvekcijo in sevanjem, je enak toplotnemu toku prenesenemu na površino s prevodom.

$$q_{j,t} = \sum_{i=0}^{Nj} X_{j,i}\vartheta_{j,t-i} - \sum_{i=0}^{Nj} Y_{j,i}\vartheta_{j,t-i} + R_j q_{j,t-i} \tag{3}$$

Vstopni parametri, ki določajo toplotno obremenitev, so spremembe temperature na zunanji površini zidu *j*, ki hkrati vplivajo na spremembe temperature na notranji površini zidu *j* in nasprotno. Zato je treba določiti enačbe toplotnega ravnotežja na znanji površini *j*. Zunanje površine mejijo na okolico ali na sosednje prostore. Ko določimo vse enačbe toplotnega ravnotežja, oz. toplotne tokove za vse zidove na notranjih in zunanjih površinah, dobimo sistem *n* enačb z *n* neznanimi temperaturami notranjih površin zidov. Izračun hladilne obremenitve prostora je sedaj mogoč s povprečenjem enačbe za toplotno ravnotežje zraka v prostoru.

$$\Phi_{p,t} = \rho c_p V_{Kl,t}\left(\vartheta_p - \vartheta_{Kl,t}\right) = \sum_{j=1}^{B} A_j\alpha_{j,t}\left(\vartheta_{j,t} - \vartheta_p\right) + \rho c_p V_{In,t}\left(\vartheta_{v,t} - \vartheta_p\right) + RK_{p,t} \tag{4}$$

Sistem enačb, ki določajo temperature notranjih površin in hladilno obremenitev, je v primeru stropnega hlajenja enak. V prvem koraku izračuna določimo temperaturo površine stropa in nato v časovnih korakih vsako uro, ko je hladilna obremenitev enaka nič. Tako lahko nadziramo notranjo temperaturo prostora z nadzorom stropne temperature.

Na temelju opisanega modela, smo razvili lasten računalniški program. Program omogoča simuliranje toplotnega obnašanja določenega prostora.

tion of the parameters, which determine personal comfort. In order to examine this interaction, modeling and simulation of the thermal behavior specific of the room has been carried out. In the analyzed model, the required air temperature of the room during the 24 hour period was ϑ_p = 24 °C. The cooling load of the room and the temperatures of all the surfaces were determined in both the treated models.

1 CALCULATION METHOD

Calculation of the room-cooling load is possible when the equations for thermal equilibrium for all bordering surfaces of the room and for the room air are established [1]. The equations determining the heat transfer rate at any interior surface *j* at a specific time *t* are:

where $G_{j,k}$ is:

The heat flux on the inner surface, which is realized through convection and radiation, equals the heat flux transferred to the surface by conduction.

Input parameters, which determine the heat load, are the temperature changes on the exterior wall surface *j,* which at the same time influence temperature changes on the interior wall surface *j,* and vice versa. It is necessary therefore, to establish the equations of thermal equilibrium on the exterior surface *j*. The exterior surfaces are adjacent either to the environment or to the neighboring rooms. When all the thermal-balance equations, i.e. the heat fluxes for all the walls on the interior and exterior surfaces are established, a system of *n* equations with *n* unknown temperatures for the interior wall surface is obtained. Calculation of the room-cooling load is now possible by means of the equation for thermal equilibrium of the interior air.

The system of the equations which determine the interior-surface temperatures and the cooling load is identical to the case of ceiling cooling. The temperature of the ceiling surface is set for the first step of the calculation, and is subsequently determined in hour-by-hour steps for the ceiling temperature at which the cooling load equals zero. In this way, control of the interior temperature is possible by controlling the ceiling temperature.

Based on the described model, an authorized computer program was developed. The program enables simulation of the thermal behavior of one specific room.

2 OPIS MODELA IN REZULTATI

Izmere izbranega prostora so 4 × 5 × 3 m z eno zunanjo steno (1) in enim oknom (7), velikosti 3,2 × 1,25 m. Vmesni zidovi (2,3,4), tla (5) in strop (6) mejijo na prostore z enakimi toplotnimi razmerami, kakršne ima analiziran prostor. Prostor je usmerjen na jug in postavljen v zagrebški regiji, z vsemi potrebnimi podatki za značilen poletni dan, 21. julij. Notranji viri toplote so tri osebe in naprave z močjo 100 W. Temperatura v prostoru je ϑ_p = 24°C.

Analize rezultatov so prikazane v diagramih, Sl. 1-4.

2 MODEL DESCRIPTION AND RESULTS

The dimensions of the chosen room are 4 × 5 × 3 m with one external wall (1) having one window (7) of size 3.2 × 1.25 m. Partitioning walls (2,3,4), floor (5) and ceiling (6) are adjacent to the rooms having thermal conditions identical to the conditions in the analyzed room. The room orientation is south, the location is the Zagreb region, with all relevant data characteristic for a summer's day i.e. July 21. The internal heat sources are three persons and equipment of 100 W power. The room temperature is ϑ_p = 24 °C.

Analysis of the results are shown in diagrams, Fig.1 - 4.

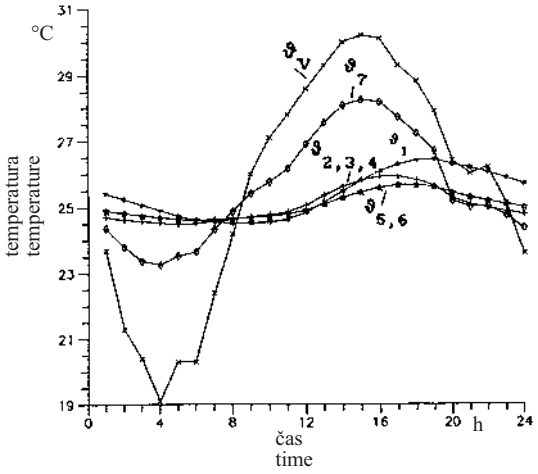

Sl.1. *Potek zunanje temperature in notranjih temperatur površin v prostoru*

Fig. 1. *Variation of enviroment temperature and room surface interior temperature*

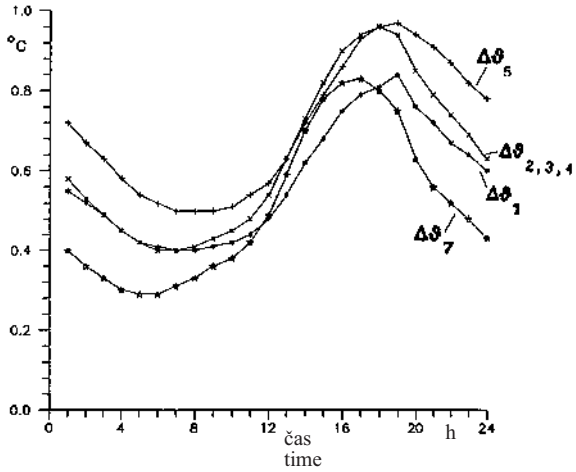

Sl.2. *Razlika med temperaturami površin v prostoru z upoštevanjem in brez upoštevanja hladilne obremenitve*

Fig. 2. *Difference between room-surface temperatures with and without applied ceiling cooling load*

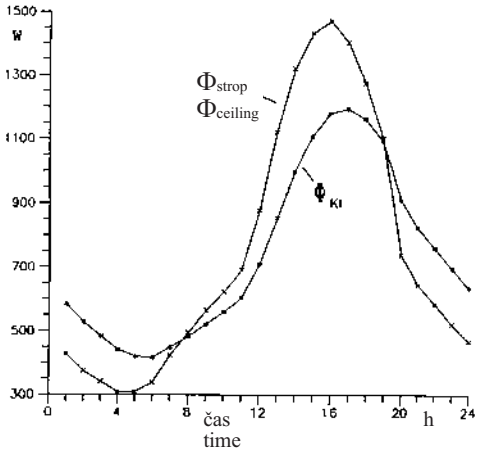

Sl.3. *Pretok stropne hladilne obremenitve*

Fig. 3. *Ceiling cooling load flow*

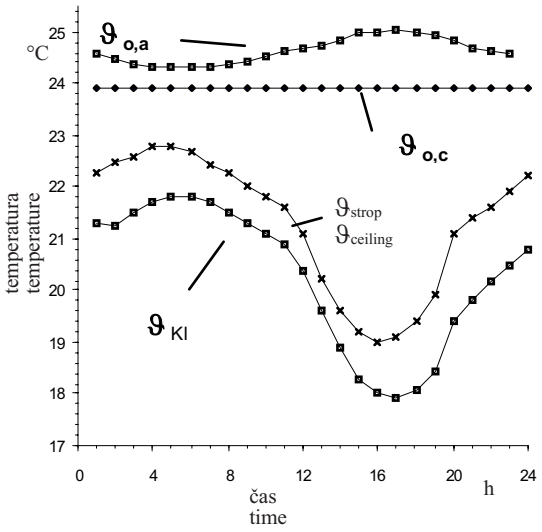

Sl.4. *Sprememba temperature stropa in občutene temperature z upoštevanjem hladilne obremenitve na sliki 3*

Fig. 4. *Variation of ceiling temperature and operating temperature with applied cooling load in figure 3*

Sprememba zunanje temperature ϑ_v in ustreznih temperatur vseh notranjih površin prostora so prikazane na sliki 1. Ustrezna hladilna obremenitev Φ_{Kl} je prikazana na sliki 3. Na temelju največje hladilne obremenitve smo izračunali pretok zraka, ki je potreben za pokritje potreb hladilne obremenitve, V_{kl} = 600 m^3/h. Izračunali smo tudi ustrezno temperaturo zraka ϑ_{Kl}, ki je prikazana na sliki 4. Diagram na sliki 2 prikazuje razliko med temperaturami na površinah v prostoru v skladu s sliko 1 in temperaturami istih površin ob upoštevanju stropnega hlajenja. Sprememba hladilne obremenitve za ta primer je prikazana na sliki 3, ustrezna temperatura stropa, ϑ_{strop}, pa na sliki 4. Ustrezni občuteni temperaturi prostora $\vartheta_{0,a}$ in $\vartheta_{0,c}$ sta prav tako prikazani na sliki 4.

Na temelju izračuna temperatur notranjih površin smo za oba analizirana modela določili srednjo sevalno temperaturo in občuteno temperaturo [4]. V primeru, ko vzdržujemo temperaturo prostora s "pokrivanjem" hladilne obremenitve s cirkulacijo hladnega zraka, se srednja temperatura sevanja spreminja od 24,3°C (ob 5h) do 25,9°C (ob 17h) in občutena temperatura prostora od 24,3°C do 25°C. Sprememba teh parametrov ustreza spremembi hladilne obremenitve prostora. Kadar uporabljamo stropno hlajenje, sta srednja temperatura sevanja in občutena temperatura prostora stabilni in sta enaki 23,8°C oziroma 23,9°C.

3 SKLEP

Krmiljenje temperature prostora z uporabo zračnega sistema je v primerjavi s stropnim hlajenjem pokazal zmanjšanje časovne zakasnitve in povečanje amplitude največje hladilne obremenitve. Z upoštevanjem kriterija posameznikovega ugodja v določenem prostoru, to je z upoštevanjem srednje sevalne temperature in dejanske temperature v prostoru, stropno hlajenje zagotovi izjemno stabilnost teh temperatur. Hkrati pa je njihova vrednost zelo blizu temperaturi zraka v prostoru, kar ustreza sobni temperaturi.

The variation of the environment temperature, ϑ_v, and the corresponding temperatures of all the room's interior surfaces are shown in Fig. 1. The adequate cooling load, Φ_{Kl}, is shown in Fig. 3. Based on the maximal cooling load, the air volume needed to cover the cooling load is calculated, it is V_{kl} = 600 m^3/h. The corresponding air temperature, ϑ_{Kl}, is also calculated and is shown in Fig. 4. The diagram in Fig. 2 shows the difference between the room-surface temperatures according to Fig. 1 and the temperatures of the same surfaces when ceiling cooling is applied. The cooling-load variation in this case is shown in Fig.3 and the corresponding ceiling temperature, $\vartheta_{ceiling}$, is shown in Fig. 4. The corresponding operating room temperatures $\vartheta_{0,a}$ and $\vartheta_{0,c}$ are also shown in Fig. 4.

Based on the calculation of interior-surface temperatures in the room, in both analyzed models the mean temperature of radiation and the operating room temperature are determined [4]. In the case when the room temperature is maintained by covering of the cooling load by means of cold air circulation, the mean temperature of radiation varies from 24.5 °C (5 A.M.) to 25.9 °C (5 P.M.), and the operating room temperature varies from 24.3 °C to 25 °C. The variation in these parameters corresponds with the variation in the room-cooling load. When ceiling cooling is used, the mean temperature of radiation and operating room temperature are stable, i.e. 23.8 °C and 23.9 °C, respectively.

3 CONCLUSION

Control of the temperature of the room by means of the air system shows a decrease in the time delay and an increase of the amplitude of the maximum cooling load, in comparison with ceiling cooling. When considering the criteria for personal comfort in a specific room, i.e. the mean radiation temperature and the actual room temperature, ceiling cooling provides remarkable stability of these temperatures. At the same time, their value is very close to the temperature of the room air, which corresponds to the room temperature.

4 OZNAČBE
4 NOMENCLATURE

količina toplote prenešena z notranje površine j v času t, W/m^2	$q_{j,t}$	rate of heat conducted out of interior surface j at time t, W/m^2
koeficient prestopa toplote notranje površine j v času t, W/m^{2}K	$\alpha_{j,t}$	convective heat transfer coefficient at the interior surface j at time t, W/m^{2}K
temperatura notranjega zraka, °C	ϑ_p	inside-air temperature, °C
povprečna temperatura notranje površine j v času t, °C	$\vartheta_{j,t}$	uniform temperature of interior surface j at time t, °C
število površin (j = 1, 2,.... B, k = 1,2,.... B)	B	number of surfaces (j = 1, 2,.... B, k = 1,2,.... B)
emisijski faktor površin j in k	ε_j, ε_k	emission factor of the j and k surface
Boltzmannova sevalna konstanta, 5,67·10^{-8} W/(m^2 K^4)	σ	Boltzmann radiation constant, 5.67·10^{-8} W/(m^2 K^4)

faktor oblike sevanja med notranjima površinama *j* in *k*	$F_{j,k}$	radiation shape factor between interior surfaces *j* and *k*
povprečna temperatura notranje površine *k* v času *t*, °C	$\vartheta_{k,t}$	uniform temperature of interior surface *k* at time *t,* °C
količina sončnega sevanja in sevalne toplote opreme, razsvetljave in ljudi v prostoru, ki jo absorbira notranja površina *j* v času *t,* W/m^2	$RA_{j,t}$	rate of solar heat and rate of heat radiated from equipment, lights and occupants absorbed by interior surface *j* at time *t,* W/m^2
funkciji prevoda, [2], [3]	$X_{j,i}, Y_{j,i}, (R_j)$	conduction transfer functions, [2], [3]
število členov funkcije prevoda ($i = 0,1,.....Nj$)	Nj	number of conduction transfer function terms ($i = 0,1,.....Nj$)
povprečna temperatura notranje površine *j* v času *t*-1, *t*-2, ..., *t*-*Nj* (ure) pred časom *t,* °C	$\vartheta_{j,t-i}$	uniform temperature of interior surface *j* at time *t*-1, *t*-2, ..., *t*-*Nj* (hours) before time *t,* °C
hladilna obremenitev prostora v času *t*, W	$\Phi_{p,t}$	room-cooling load at time *t*, W
gostota zraka, kg/m^3	ρ	air density, kg/m^3
specifična toplota zraka, J/kgK	c_p	air specific heat capacity, J/kgK
masni pretok ventilacijskega zraka v času *t*, kg/s	$V_{Kl,t}$	mass flow rate of conditioning air at time *t,* kg/s
temperatura ventilacijskega zraka v času *t*, °C	$\vartheta_{Kl,t}$	conditioning air temperature at time *t,* °C
masni pretok zunanjega zraka, ki prehaja v prostor v času *t*, kg/s	$V_{In,t}$	mass flow rate of outdoor air infiltrating into room at time *t,* kg/s
temperatura zunanjega zraka v času *t*, °C	$\vartheta_{v,t}$	outdoor air temperature at time *t,* °C
količina toplote,ki jo oddajajo oprema, ljudje v prostoru in zrak, ki prehaja v prostor v času *t*, W	$RK_{p,t}$	rate of heat obtained from equipment, occupants and convected into room air at time *t,* W
občutena temperatura v prostoru, ko je hlajenje zraka upoštevano, °C	$\vartheta_{0,a}$	operating room temperature when air cooling is applied, °C
občutena temperatura v prostoru, ko je stropno hlajenje upoštevano, °C	$\vartheta_{0,c}$	operating room temperature when ceiling cooling is applied, °C

5 LITERATURA
5 REFERENCES

[1] Procedure for determining heating and cooling loads for computerizing energy calculations, Algorithms for building heat transfer subroutines (1976) *ASHRAE, Atlanta.*

[2] Stephenson, D.G., G.P. Mitalas (1967) Cooling load calculation by thermal response factor method; Room thermal response factors. *ASHRAE Transactions*, Vol. 73/1, III.11-III.1.7, III.2.1-III.2.10.

[3] Kusuda, T. (1969) Thermal response factors for multi-layer structures of various heat conduction systems. *ASHRAE Transactions*, Vol. 75/1, 246-271.

[4] ASHRAE Handbook, (1999) HVAC Applications, Comfort Applications, *ASHRAE, Atlanta,GA*.

Naslov avtorjev: prof. dr. Tonko Ćurko
prof. dr. Ivan Galaso
Univerza v Zagrebu
Fakulteta za strojništvo in pomorstvo
Ivana Lučića 5
10 000 Zagreb, Hrvaška

Authors' Address: Prof.Dr. Tonko Ćurko
Prof.Dr. Ivan Galaso
University of Zagreb
Faculty of Mechanical Engineering and Naval Architecture
Ivana Lučića 5
10 000 Zagreb, Croatia

Prejeto: Received: 23.12.1999

Sprejeto: Accepted: 2.6.2000

© Strojniški vestnik 46(2000)6,347-358
ISSN 0039-2480
UDK 551.506:536.2:697.9(569.1)
Izvirni znanstveni članek (1.01)

© Journal of Mechanical Engineering 46(2000)6,347-358
ISSN 0039-2480
UDC 551.506:536.2:697.9(569.1)
Original scientific paper (1.01)

Sistemizacija, organizacija, razvoj in uporaba podatkovne baze urnih postavk meteorološkega leta za območje Damaska

Sistematization, Organization, Development and Utilization of an Hourly Reference Meteorological Year Database for Damascus Zone

Kamal Skeiker

Vremenske podatke za območje Damaska je od leta 1970 do 1993 spremljala meteorološka postaja, ki jih je nato pregledala in uredila. Z uporabo teh podatkov je bila organizirana in razvita podatkovna baza za referenčno meteorološko leto "RMY", glede na naslednje modele: 1-urno mesečno povprečje, 2-urno povprečje, 3-dnevno količino sonca, merjeno v urah.

Računalniški program LOS-A0 za dinamične analize prenosa toplote v stavbah je bil prilagojen za uporabo glede na delovne razmere in letne čase v Siriji in je bil pripravljen na podlagi urnega mesečnega povprečja. Z novo verzijo CLIMA, ki je bila zasnovana na podlagi urnega povprečja, so lahko dobili optimalno obdobje skozi vse leto. Po natančnih primerjavah in analizah dobljenih rezultatov obeh omenjenih različic, so se odločili za CLIMA program.

(Ključne besede: podatki meteorološki, baze podatkov, programi računalniški, analize dinamične)

The weather data for the Damascus zone for the years 1970 through 1993 as measured by the Department of Meteorology were obtained, examined and reconditioned. Using these measured data, a Reference Meteorological Year "RMY" Database was organized and developed according to the following patterns: 1- monthly average of hourly weather data,2- hourly weather data,3- daily sunshine hours.

The LOS-A0 computer program for the dynamic analysis of heat transfer in buildings was modified for use according to the working conditions and weather seasons in Syria. It was provided with an hourly weather database of the first pattern. This last version was developed, and a new version CLIMA, in which the calculation is carried out for an optional period during the year, was obtained. The computer program CLIMA was provided with an hourly database of the second pattern. These two versions were used to study an enclosure as an example. After detailed analysis of the calculated results obtained by each of the two mentioned versions, the computer program CLIMA was chosen.

(Keywords: meteorologic data, data bases, computer programs, dynamic analysis)

0 UVOD

Zaradi naslednjih dejavnikov, je bila zadnji dve desetletji povečana pozornost racionalizaciji porabe energije in iskanju novih energijskih virov:

- povečane letne porabe energije, ki izhaja iz naraščanja števila prebivalstva in ekonomskega razvoja;
- okoljevarstvenih učinkov, ki izhajajo iz porabe energije.

Zaradi tega je racionalizacija porabe energije in uporaba novih energijskih virov postala nuja. V mnogih državah so vlade zaprosile znanstvenike in raziskovalce za izvedbo raziskav in projektov, da bi razrešili potencialni problem

0 INTRODUCTION

During the last two decades, increased attention has been paid to the rationalization of energy consumption and the search for new energy resources, as a consequence of the following factors:

- The increased rate of energy consumption per annum, as a result of an increasing population and economic growth.
- Environmental effects arising from the use of energy.

As a result, the rationalization of energy consumption and the use of new energy resources has become an urgent matter. Governments in many countries have been motivated to request academics and researchers to carry out research and experimental

tako imenovane energijske krize. Ti so natančno proučili racionalizacijo energijske porabe in zmanjšanje stroškov za energijo v različnih področjih.

Raziskave poslopij so se nanašale na: razvoj matematičnih modelov za izračun in simuliranje toplotnih sistemov, organizacijo in avtomatizacijo notranjih hladilnih sistemov, oblikovanje pasivnih in aktivnih toplotnih solarnih sistemov, uporabo izolacije na zunanjih površinah in dvojno zasteklitev oken.

Poraba energije različnih panog v Siriji: 42% za zgradbe in kmetijstvo, 41% za transport in 17% za industrijo. Glede na to, da se največji del energije porabi v poslopjih so raziskave usmerjene predvsem v to smer.

V okviru razvoja matematičnih modelov za izračun in simuliranje sistemov, smo poskušali izpeljati naslednje:

- Razviti podatkovno bazo "RMY", da bi jo uporabili skupaj s sedanjimi računalniškimi programi za dinamične analize prenosa toplote v poslopjih "model LOS-A0". Razvoj takšne podatkovne baze je temeljil na razpoložljivih urnih podatkih o vremenu za območje Damaska, ki jih je merila meteorološka postaja oddelka za meteorologijo. To podatkovno bazo štejejo za prvo takšne vrste na tem področju, katera vključuje urne vrednosti za naslednje vremenske parametre:
  1- temperaturo suhega zraka,
  2- temperaturo vlažnega zraka,
  3- temperaturo rosišča,
  4- relativno vlago,
  5- atmosferski tlak,
  6- hitrost vetra in smer,
  7- celotno stopnjo sončnosti in tip oblačnosti,
  8- intenzivnost globalnega sončnega sevanja.
  Upoštevana je tudi dnevna količina sonca merjena v urah.
- Prilagoditi računalniški program LOS-A0 okoliščinam in letnim časom v Siriji.
- Reorganizirati računalniški program LOS-A0 in ga prilagoditi za računanje obdobja v letu izbranega po prosti presoji.

1 PRIDOBITEV, NADZOR IN OBDELAVA VREMENSKIH PODATKOV ZA OBMOČJE DAMASKA

Da bi organizirali in razvili podatkovno bazo RMY, so potrebni urni podatki, ki so omenjeni v uvodu. Podatki so bili dobljeni na mednarodnem letališču v Damasku in v Kharabu. Mednarodno letališče Damask se nahaja na 32°36´ vzhodne zemljepisne dolžine, 26°33´ severne zemljepisne širine in leži 608 m visoko nad morjem. Postaja v Kharabu je locirana na 36°32´ vzhodne zemljepisne dolžine,

projects with the aim of overcoming the potential problems of the so-called energy crisis. Academics and researchers looked closely at energy consumption rationalization and decreasing its costs in various fields.

Buildings research was directed towards: the development of mathematical models for thermal system calculations and simulations, organization and automation of internal air-conditioning systems, design of passive and active solar thermal systems, use of outer surfaces thermal insulation and double-glazed windows.

The energy consumption of various sectors in Syria is: 42% for building and agriculture, 41% for transportation and 17% for industry [1]. Since the greatest share of total energy consumption is in buildings, it is useful to carry out research in this field.

Within the framework of the Development of Mathematical Models for Calculation and Simulation of Engineering Systems, we therefore attempted to carry out the following:

- To develop a RMY Database, to be used with existing computer programs for dynamic analysis of heat transfer in the building "model LOS-A0" [2]. Development of such an RMY Database was based on the available hourly weather data for the Damascus zone, which were measured by the Department of Meteorology. This Database is considered as the first of its kind in this field that includes hourly values for the following weather parameters in the Damascus zone:
  1- air dry-bulb temperature,
  2- air wet-bulb temperature,
  3- air dew-point temperature,
  4- relative humidity,
  5- atmospheric pressure,
  6- wind velocity and direction,
  7- global cloudless degree and cloud type,
  8- global solar radiation intensity.
  Daily sunshine-hours values are included too.
- To modify the LOS-A0 computer program according to the working conditions and weather seasons in Syria.
- To re-organize the LOS-A0 computer program and adapt it to calculate for an optionally determined period in a year.

1 OBTAINMENT, SCRUTINY AND RECONDITION OF DAMASCUS ZONE WEATHER DATA

In order to organize and develop the RMY Database, the hourly weather data mentioned in the introduction are required. The Department of Meteorology agreed to provide the available data. They supplied us with hourly weather data from the meteorological stations in Damascus International Airport and in Kharabo. Damascus International Airport Station is located at 32° 36' east longitude, 26° 33' north latitude and at an elevation of 608 m above the sea level. Kharabo

30°33´ severne zemljepisne širine, nadmorska višina je 620 m.

Podatki od leta 1970 do 1993 so nam na voljo za parametre 1 do 7. Za osmi parameter so na voljo le od leta 1971 do 1974 in od 1984 do 1986. Imamo podatke tudi za dnevno količino sonca, merjeno v urah od leta 1978 do 1988. V primeru manjkajočih parametrov so bile kode 99, 999, 99.9, 999.9 in 9999.9, ki so nakazale pomemben stolpec.

Podatki so bili razdeljeni v podmape, ki so morale vsebovati toliko vrstic, kolikor je bilo merjenih ur oziroma dni v obdobju (to je 8760 oz. 365). Računalniški program ERRLINE.F OR je bil pripravljen za določitev ur ali dni v letu, ko ustreznih podatkov ni bilo na voljo.

Da bi dopolnili podatke, so bili manjkajoči in netipični podatki zamenjani z ocenjenimi vrednostmi. Te vrednosti so bile izračunane po postopku interpolacije in so temeljile na ustrezni vrednosti parametra na dan, ko je podatek manjkal.

2 ORGANIZIRANJE IN RAZVOJ PODATKOVNE BAZE RMY

Na tej stopnji se pri analizi podatkov pojavi vprašanje: "Kateri model naj bi uporabili za predstavitev niza podatkov?" Čeprav je na to vprašanje težko odgovoriti, poznamo nekaj tehnik, ki nam pri sprejemanju odločitve pomagajo z analiziranjem.

Po praktičnih izkušnjah je bilo ugotovljeno, da je uporaba normalne porazdelitve najprimernejša za označevanje mnogih fizikalnih meritev in ostalih vrst podatkov. Izbran je bil za predstavitev opazovanih podatkov za vsako uro v letu (ali za vsako sončno uro). Normalna porazdelitev, označena kot $N(\mu, \sigma^2)$, je opisana z gostoto verjetnosti:

$$f(x) = \frac{1}{\sigma\sqrt{2\pi}} \exp\left[-\frac{(x-\mu)^2}{2\sigma^2}\right], \qquad -\infty < x < \infty \tag{1}$$

μ pomeni porazdelitev, σ pa pomeni standardno odstopanje porazdelitve ([3] do [5]). Krivulja je simetrična na μ in ima obliko zvonca. Normalna porazdelitev prikazuje standardno odstopanje (σ), ki omogoča najboljši pregled razpršitve, tako kakor m omogoča najboljši pregled glavne tendence. Medtem ko je porazdelitev simetrična na μ, so povprečna vrednost, srednja vrednost in najpogostejša vrednost vse enake μ ([6] in [7]).

Za model preverjanja domnevne porazdelitve je bila uporabljena Kolmogorovova metoda ([3] in [8]). Postopek te metode je zelo preprost. Primerjati je treba kumulativno frekvenco podatkov s kumulativno frekvenco krivulje

station is located at 36° 32' east longitude, 30° 33' north latitude and at an elevation of 620 m above the sea level.

The data for the years 1970 through 1993 for each of the parameters 1 to 7 were provided. The data for the 8th parameter, were provided for the years 1971 through 1974 and for 1984 through 1986. Daily sunshine-hours data for the years 1978 through 1988 were also provided. For the case of a missing parameter the codes 99, 999, 99.9, 999.9 or 9999.9 were indicated in the relevant column.

The data were divided into sub-files, each of which included data values of the measured parameters for one year only. These sub-files had to contain a number of lines equal to the number of measuring hours or days per annum, (that is 8760 or 365). A computer program, ERRLINE.FOR, was prepared to determine the hours or days in a year, where the relevant data were not recorded. It also determines the lines with which the codes indicating missing data, for all the parameters included in the file, are recorded.

To complete the data, missing and atypical data were replaced by estimated values. These values were generated by an interpolation method, based on the corresponding parameter values for the day on which the missing data occurred.

2 ORGANIZING AND DEVELOPING AN RMY DATABASE

At this stage an important question, which normaly arises during the analysis of data; namely, "which model should be used to describe a given set of data"?, was raised. Although this is generally a difficult question to answer, there are several techniques available which can assist the analyst in making such a decision.

The normal distribution model is found from practical experience to be appropriate for many types of physical measurements and other types of data.. It was shosen for representing the observed data for each hour of the year (or each day for sunshine hour). The normal distribution, denoted by $N(\mu, \sigma^2)$ is described by the probability density function:

Where, μ is the mean of the distribution and σ is the standard deviation of the distribution ([3] to [5]). It has the well-known bell shape and the curve is symmetrical about μ. The normal distribution demonstrates the standard deviation (σ) may be looked upon as the best measure of dispersion, just as the mean (μ) may be seen as the best measure of central tendency. Since the distribution is symmetrical about μ, the mean, median and mode coincide, all being equal to μ ([6] and [7]).

We may be unsure as to whether a particular probability distribution is appropriate for our observations. The Kolmogorov method ([3] and [8]) was used to check whether an assumed distribution model is adequate to represent a set of data. The principle of the Kolmogorov approach is very simple. It involves

teoretične porazdelitve. Ko so hipotetične in eksperimentalne krivulje narisane, lahko preberemo največjo navpično razliko med njima in lahko primerjamo te vrednosti s tabeliranimi vrednostmi. Ta metoda uporablja vsak posamezni podatek in je tako enako učinkovita za manjšo in večjo količino podatkov.

V primeru normalne porazdelitve lahko izračunamo funkcijo teoretične kumulativne porazdelitve:

comparing the cumulative frequency of the data to be tested with the cumulative frequency curve of the hypothesized (theoretical) distribution. When the hypothetical and experimental curves have been drawn, the test statistics are obtained by finding the maximum vertical difference between them, and comparing this value with a set of tabulated values. This method uses each individual data point and so is equally effective for either small or large sets of data.

In the case of the normal distribution, the theoretical cumulative distribution function is given by:

$$F(z) = \int_{-\infty}^{z} \frac{1}{\sqrt{2\pi}} \exp\left(-\frac{z^2}{2}\right) dz \qquad (2)$$

To enačbo zasledimo v mnogih zbirkah statističnih preglednic za različne vrednosti z. Najprej moramo spremeniti začetne podatke v standardno spremenljivko z. To storimo z naslednjo enačbo:

which is well-tabulated and given in many collections of statistical tables for different values of z. So we must first transform the original data, which might have any values for their mean and standard deviation, into the standard normal variable, z. This is done using the equation:

$$z = (x - \mu) / \sigma \qquad (3)$$

Predpostavljamo, da si določeni podatki sledijo $x_1 \leq x_2 \leq x_3 \ldots\ldots \leq x_n$. Krivulja kumulativne frekvence množice je določena z:

Suppose that we observe an ordered set of data $x_1 \leq x_2 \leq x_3 \ldots\ldots\ldots\ldots\ldots \leq x_n$. The set cumulative frequency curve is defined by:

$$S_n(x_j) = j/n\,;\ j = 1,2,3\ldots..n \qquad (4)$$

$$S_n(x) = 0 \text{ za / for } x < x_1 \text{ in / and } S_n(x) = 1 \text{ za / for } x \geq x_n \qquad (5)$$

Preveritveni postopek je določen z naslednjimi koraki:
Korak 1.
H_0: x ima obliko krivulje kumulativne frekvence $F(z)$.
H_1: x nima oblike krivulje kumulativne frekvence $F(z)$.
Korak 2. Izberemo γ, stopnjo signifikantnosti preveritve.
Korak 3. Določitev odklonitvenega področja $R = \{D_{max} \mid D_{max} > D_n^{(\gamma)}\}$, kjer $D_n^{(\gamma)}$ dobimo iz ustrezne preglednice.
Korak 4. Izračunamo statistiko: $D_{max} = \max_i\{| F(z_i) - S_n(x_i) |, | F(z_i) - S_n(x_{i-1}) |\}$.
Korak 5. Če je $D_{max} > D_n^{(\gamma)}$, H_0 ni primeren, nakar sledi, da $F(z)$ ne popiše podatkov; drugače pa ob sprejemu H_0 izhaja, da $F(z)$ popiše podatke.

Z uporabo Kolmogorovove metode za testiranje pravilnosti porazdelitve je bilo ugotovljeno, da so razpoložljivi meteorološki podatki za vsako uro v letu (ali število ur sonca na dan) prikazani kot normalna porazdelitev. Značilno vrednost za vsak parameter so dobili s povprečnimi vrednostmi za vsako uro (ali za vsak dan v primeru sončnih ur). Njen razpon je določen s pogojem:

The test procedure is now defined as follows:
Step 1.
H_0: x has cumulative frequency curve $F(z)$.
H_1: x does not have cumulative frequency curve $F(z)$.
Step 2. Select γ, the level of significance of the test.
Step 3. Specify the rejection region $R = \{ D_{max} \mid D_{max} > D_n^{(\gamma)}\}$, where $D_n^{(\gamma)}$ is obtained from the relevant table.
Step 4. Calculate the statistic: $D_{max} = \max_i\{| F(z_i) - S_n(x_i) |, | F(z_i) - S_n(x_{i-1}) |\}$.
Step 5. If $D_{max} > D_n^{(\gamma)}$, reject H_0 and conclude that $F(z)$ does not describe the data; otherwise, accept H_0 and conclude that $F(z)$ describes the data.

Testing for normality of distribution, using the Kolmogorov method, it was found that the available sets of meteorological data for each hour of the year (or each day for sunshine hours) are drawn from a normal distribution. Thus for each parameter, the mean value of the overall available years was taken for each hour (or each day in the case of sunshine hours) of the year and defined as a representative value. Its range is defined by the condition:

$$\bar{x} - 1{,}96(\sigma/\sqrt{n}) < \mu < \bar{x} + 1{,}96(\sigma/\sqrt{n}) \qquad (6)$$

Izraz (6) podaja 95% zanesljivost povprečnega intervala v primerjavi z mejo zaupanja $1{,}96\,(\sigma/\sqrt{n})$.

Expression (6) gives the 95% confidence interval of the mean with the confidence limit $1{,}96\,(\sigma/\sqrt{n})$.

2.1 Ureditev podatkovne zbirke RMY

Cilj vnaprej pripravljenih vremenskih podatkov je bil določitev urnih stopenj za vsak vnaprej določen fizični parameter. V ta namen je računalniški program (MEANVAL.FOR) izračunal in dobil rezultate (REFERENC.YER) z 8769 vrsticami in 578160 bajti. Urni vremenski podatki za RMY so bili vneseni kakor prikazuje naslednji primer:

2.1 Organization of the RMY Database

On the basis of the previously prepared weather data, the aim was to quantify the hourly rates for each of the predetermined physical parameters. For this purpose, a computer program (MEANVAL.FOR) was prepared for the calculations and recording the results in a separate file (REFERENC.YER) with 8760 lines, and a size of 578160 bytes. The hourly weather data for a RMY were recorded in free format according to the arrangement shown in the following example:

DAN DAY	URA HOUR	DBT	WBT	DPT	RH	SP	WS	WD	TC	CTYP	MGO
-	-	°C	°C	°C	%	mbar	m/s	°	0-8	0-9	W/m^2
1	1	3	2,2	1	87	948,2	3	16	3	0	0
1	2	3	2,2	1	87	948,2	3	15	3	0	0
-	-	-	-	-	-	-	-	-	-	-	-
-	-	-	-	-	-	-	-	-	-	-	-
1	9	4,5	3,4	2	84	949,3	2	13	5	0	290

Z uporabo računalniškega programa MEANVAL.FOR je bilo mogoče tudi določiti dnevno stopnjo sonca. Ta nova različica se je imenovala MEANSUN.FOR, rezultati so bili zapisani v REFERENC.SUN s 365 vrsticami in velikosti 6205 bajtov. Naslednji primer prikazuje vnos podatkov za količino sonca na dan v urah.

The MEANVAL.FOR computer program was also modified to quantify the daily sunshine hour rate. This new version was named MEANSUN.FOR the results were recorded in the file REFERENC.SUN with 365 lines and a size of 6205 bytes. The daily sunshine hours for a RMY were recorded in free format according to the arrangement shown in the following example.

MESEC MONTH	DAN DAY	URA HOUR
1	1	4,4
1	2	5,2
1	3	3,8
1	4	4,8

2.2 Razvoj podatkovne baze RMY glede na zahteve prilagojene strukture ter prilagojenega in reorganiziranega računalniškega programa LOS-A0

Sedanji računalniški program LOS-A0 z nizom podatkov RMY določi mesečno povprečje za vsak vnaprej določen fizični parameter. Namen je bil razviti program za numerično simuliranje toplotnega sistema za izbrani časovni interval v letu.

Računalniški program REFERLOS.FOR je bil pripravljen za naslednje namene:

- Za branje vrednosti podatkovnega niza RMY iz dokumenta REFERENC.YER.
- Za določitev mesečnega povprečja z uporabo urnih vremenskih podatkov za vsak parameter iz dokumenta REFERENC.YER.
- Za zapisovanje povprečne mesečne vrednosti urnih vremenskih podatkov v ločen dokument.
- Za kopiranje vsebine dokumenta REFERENC.YER v drug dokument

2.2 Development of the RMY Data Base According to the Requirements of the Construction of Modified and Modified & Re-Organized LOS-AO Computer Programs

The existing LOS-A0 computer program requires an RMY Database, in which the monthly average of hourly weather data for each of the predetermined physical parameters are recorded in a specific sequence. The aim was to develop this program for use in numerical simulation of thermal systems for an optionally determined time interval within the year.

For this purpose, the computer program REFERLOS.FOR was prepared to serve as a means for executing the following:

- To read the values of the RMY Database from the file REFERENC.YER.
- To quantify the monthly average of hourly weather data for each of the included parameters in the file REFERENC.YER.
- To record the quantified monthly average of hourly weather data in a separate file.
- To re-record the contents of the file REFERENC.YER in a separate file.

3 PRILAGODITEV IN RAZVOJ RAČUNALNIŠKEGA PROGRAMA LOS-A0

Cilj je bil preskrbeti oz. ″opremiti″ sirsko Tehnično knjižnico z ustreznim matematičnim modelom in računalniškim programom za digitalno simuliranje termičnega sistema poslopij in drugih inženirskih sistemov vključenih v to omrežje.

Računalniški program LOS-A0 je bil prilagojen za različne delovne razmere (počitnice, čas začetka/prekinitve ogrevanja oz. hlajenja) in letne čase v Siriji.

Sedaj se lahko bolje osredotočimo na delovanje in metodo izračuna LOS-A0, ki je sistematično orodje za študiranje, načrtovanje in računanje različnih poslopij (toplotni sistemi).

Dinamična analiza prenosa toplote v stavbah je "vodena" z matematičnim modelom, ki upošteva enourni prirastek. Metodo toplotnega ravnotežja prostora uporabljamo za začetek kalkulacije neustaljenega prenosa toplote v zgradbah. Z uporabo te metode dobimo linearni sistem m+1 enačb za m poljubnih površin in temperatur zraka. Pri zunanjih površinah je prevajanje toplote skozi steno popisano z konvekcijo in sevanjem. Energijska bilanca za površino i ob času t:

$$q_{i,t} = \alpha_{ii}(\vartheta_{ia,t} - \vartheta_{ii,t}) + \sum_{k=1,k\neq i}^{m} g_{i,k}(\vartheta_{ik,t} - \vartheta_{ii,t}) + R_{si,t} \qquad (7)$$

Leva stran te enačbe pomeni prevodni toplotni tok. Desna stran (od leve proti desni) pomeni konvekcijo, sevanje ter notranje toplotne vire (sončno sevanje skozi okna, luči, oprema, stanovalci).

Prevod toplote skozi homogeno konstrukcijo (stena, strop, tla) določimo s toplotnimi odzivnimi faktorji (TRFs), ki so določljivi po Kusudovi oz. Stephensonovi metodi [9] in [10]. "Obnašanje" časovne temperaturne odvisnosti na zunanji in notranji strani je ponazorjeno kot:

- trikotna impulzna funkcija (Kusudov ali Stephensonov tip TRFs)
- skupina harmonskih (Stephensonov tip TRFs)

Prevod toplote skozi homogeno konstrukcijo i ob času t je izražen kot:

$$q_{i,t} = \sum_{j=0}^{n} X_{i,j}\vartheta_{ii,t-j} - \sum_{j=0}^{n} Y_{i,j}\vartheta_{oi,t-j} + SR_i q_{i,t-1} \qquad (8).$$

Enačbo (8) vstavimo v enačbo (7) in po ureditvi dobimo:

$$(X_{i,0} + \alpha_{ii} + \sum_{k=1,k\neq i}^{n} g_{i,k})\vartheta_{ii,t} - \sum_{k=1,k\neq i}^{n} g_{i,k}\vartheta_{ik,t} - \alpha_{ii}\vartheta_{ia,t} = -\sum_{j=1}^{n} X_{i,j}\vartheta_{ii,t-j} + \sum_{j=0}^{n} Y_{i,j}\vartheta_{0i,t-j} - SR_i q_{i,t-1} + R_{si,t} \qquad (9).$$

Sistemu m enačb (9) dodamo sledečo enačbo energijske bilance za notranji zrak:

3 MODIFICATION AND DEVELOPMENT OF THE LOS-A0 COMPUTER PROGRAM

The aim was to provide the Syrian Technical Library for Heat Transfer Sciences with the relevant mathematical model and computer program for digital simulation of the thermal system of a building, and other engineering systems included in this framework.

The LOS-A0 computer program was modified to make it adaptable for use according to the working conditions (holidays, and time of starting/ stopping of heating/or refrigeration) and weather seasons (months of winter and summer) in Syria.

Since the LOS-A0 computer program is a scientific tool for studying, planning and calculating various buildings (thermal systems), where unusual planning or operating conditions are requested to be taken into account, it is useful to focus on the principle used and the method of calculation.

In the LOS-A0 computer program, the dynamic analysis of heat transfer in buildings is conducted according to the adopted mathematical model by using a one-hour time increment. As a starting point for the calculation of non-stationary heat transfer in a building, the "Room Thermal Balance Method" was adopted. Using this method we obtain a linear system of m+1 equations for m unknown surfaces and air temperatures. At each boundary surface of the enclosure, the heat conducted through the surface is removed from it by a combination of convection and radiation. The energy balance for the surface i at time t would give:

The left side of this equation represents conducted heat flow rate. The right side (from left to right) represents convected, radiated and radiated from internal heat sources (solar energy coming through the windows, lights, equipment and occupants) heat flow rates, respectively.

The conducted heat flow rate $q_{i,t}$ through a system of homogeneous slabs i (composite wall, roof and floor) is defined by using the so-called thermal response factors (TRFs) method. TRFs are calculated by making use of either the Kusuda or Stephenson method [9] and [10]. Time-dependent temperature behavior on the outer and inner side, of the system, respectively, is specified as:

- Triangle unit-pulse functions (Kusuda-type and Stephenson type TRFs),
- Group of harmonics (Stephenson type-TRFs).

The conducted heat flow rate through a system of homogeneous slabs i at time t may be expressed in the form:

Substitution of equation (8) into equation (7) and convenient reorganization yields:

To the system of m equations (9) the following equation of energy balance for enclosure air is added:

$$\sum_{i=1}^{m} A_i \alpha_{ii} (\vartheta_{ii,t} - \vartheta_{ia,t}) - (q_{mf,t} + q_{mv,t}) c_p \vartheta_{ia,t} = -q_{mf,t} c_p \vartheta_{oa,t} - q_{mv,t} c_p \vartheta_{v,t} - R_{ci,t} \quad (10).$$

V zgornjih dveh enačbah (9) in (10) nimamo znane temperature površine $\vartheta_{ii,t}$, niti temperature zraka $\vartheta_{ia,t}$ ob času *t*. Tak sistem je podan v obliki matrike:

Equations (9) and (10) form a linear system of m+1 equations with m unknown surface temperatures $\vartheta_{ii,t}$ and air temperature $\vartheta_{ia,t}$ at time *t*. Such system can be expressed in the following matrix terms:

$$\begin{bmatrix} a_{1,1} & a_{1,2} & - & - & - & a_{1,m+1} \\ a_{2,1} & a_{2,2} & - & - & - & a_{2,m+1} \\ - & - & - & - & - & - \\ - & - & - & - & - & - \\ - & - & - & - & - & - \\ a_{m+1,1} & a_{m+1,2} & - & - & - & a_{m+1,m+1} \end{bmatrix} \begin{bmatrix} \vartheta_{1,t} \\ \vartheta_{2,t} \\ - \\ - \\ \vartheta_{m,t} \\ \vartheta_{a,t} \end{bmatrix} = \begin{bmatrix} b_1 \\ b_2 \\ - \\ - \\ - \\ b_{m+1} \end{bmatrix} \quad (11)$$

iz katere lahko določimo neznane temperature površin in zraka $[\vartheta_t]$. Ko je vektor temperature $[\vartheta_t]$ določen, je lahko toplotna obremenitev ϕ_t prostora izračunana z uporabo energijske ravnovesne enačbe (10) za notranji zrak:

from which the unknown surface and air temperatures $[\vartheta_t]$ can be defined. Since the vector of temperaturesis $[\vartheta_t]$ determined, the thermal load ϕ_t of the enclosure can be calculated by using the energy balance equation (10) for enclosure air:

$$\phi_t = \sum_{i=1}^{m} A_i \alpha_{ii} (\vartheta_{ii,t} - \vartheta_{ia,t}) + q_{mf,t} c_p (\vartheta_{oa,t} - \vartheta_{ia,t}) + q_{mv,t} c_p (\vartheta_{v,t} - \vartheta_{ia,t}) + R_{ci,t} \quad (12)$$

V enačbi (12) pomeni negativna vrednost ϕ_t ogrevalne obremenitve, pozitivna vrednost pa hladilne obremenitve pri času *t*.

Podatki za izračun toplote sončnega sevanja, virov toplote v klimatiziranem prostoru ter pri prezračevanju in infiltracijskem zraku so enaki tistim v [11].

Računalniški program je bil prilagojen za izračun poljubno določenega obdobja v letu z uporabo urnih vremenskih podatkov za vsak vnaprej določen parameter. V programu se metode in enačbe niso spreminjale. To je omogočala podatkovna baza RMY drugega modela, ki je bil urejen in razvit v prejšnji stopnji tega dela. Ta nova razvita verzija programa je bila imenovana CLIMA.

In equation (12), the negative ϕ_t represents heating load and positive ϕ_t represents cooling load at the time *t*.

Information on calculating heat gains from: solar radiation, heat sources within the conditioned space and ventilation and infiltration air are identical to those given in reference [11].

The computer program was re-organized to calculate for an optionally determined period within the year, using the hourly weather data for each of the predetermined physical parameters. Such re-organization was carried out keeping the methodology and equations for hour-by-hour calculations unchanged. It was provided with the RMY Database of the second pattern, which was reorganized and developed in the previous stage of this work. The newly developed version of this program was named CLIMA.

4 UPORABA "SPREMENJENEGA LOS-A0" IN "CLIMA" PROGRAMOV

Spremenjeni računalniški program LOS-A0 in rač.program CLIMA smo uporabili za izračun temperature zraka in toplotnih izgub v poslopjih. Obravnavani prostor je v drugem nadstropju štirinadstropnega poslopja. Prostori nad in pod njim so klimatizirani. Zunanje izmere tega prostora so 3 m × 8,5 m × 8,5 m, površina tal znaša 72,3 m^2. Vsaka zunanja stena ima enojno zastekljeno okno s površino 4,5 m^2.

Z upoštevanjem opisanih navodil za uporabo programa LOS-A0 [12], so bili vneseni podatki zapisani v ločen dokument ″FOR20.DAT″. Ti podatki so:

- značilnosti stavbe,

4 USE OF "THE MODIFIED LOS-A0" AND "CLIMA"COMPUTER PROGRAMS

The modified LOS-A0 and CLIMA computer programs were used to calculate the air temperature and heat loss in an enclosure within a building. The building consists of four floors, the studied enclosure is located on the second floor. The spaces above and under the enclosure are conditioned. The outer dimensions of the enclosure are 3m × 8.5m × 8.5m, with a ground plan area of 72.3m^2. Each outer wall has a single glazed window with an area of 4.5m^2.

Following the described instructions in the LOS-A0 user's guide [12], input data of the enclosure were recorded in the relevant separate file 'FOR20.DAT". The recorded input data are:

- characteristics of the building,

- lokacija, usmerjenost in osenčenost stavbe,
- načrt bivalnih prostorov,
- razsvetljava, število stanovalcev, notranja oprema ter sredstev in procesov, ki prispevajo k notranjim toplotnim virom. Upoštevali smo, da so se stanovalci zadrževali v prostoru od 6:00 do 22:00.

Informacije o metodah vnašanja podatkov dobimo v referenci [12]. Sestava stropa, sten in tal so bili podani glede na sistem plasti od znotraj navzven. Fizikalne lastnosti gradbenih materialov so bile prilagojene območju Damaska ([13] in [14]).

December je bil izbran kot reprezentativni mesec v zimskem obdobju, 21. dan v mesecu pa kot reprezentativen dan. Temperaturna porazdelitev v mesecu decembru je ekstremno nizka glede na temperaturno porazdelitev v novembru, januarju in februarju.

Rezultati izračunov so zapisani v dokumentu FOR21. DAT in nekateri glavni podatki so grafično prikazani na slikah 1 in 2. Tam vidimo temperaturo zraka in obnašanje toplotnega toka v prostoru za 21. december.

5 UGOTOVITVE IN SKLEP

Vremenski podatki za območje Damaska od leta 1970 do 1993, ki jih zahteva program LOS-A0, so bili natančno pregledani in obdelani. S temi merjenimi podatki je bila podatkovna baza RMY urejena in

- building location, orientation and external shading,
- indoor design conditions,
- proposed schedule of lighting, occupants, internal equipment, appliances and processes that would contribute to the internal thermal load. Occupation of the enclosure from 6:00 through to 22:00 hours was considered.

Information on the methodology for recording them is available in reference [12]. Compositions of the ceiling, walls and floor were described, taking into account that the systematization of layers starting from the inside towards the outside. The physical properties of building materials used in the Damascus zone were adopted ([13] in [14]).

December is adopted in the analysis as a representative month for the winter season and the 21st as its representative day. The temperature distribution in December is characteristic of an extremely cold month compared with the temperature distribution in November, January and February. Furthermore, the 21st of each month is representative of the conditions on average cloudless days.

The results of calculations were recorded in a separate file FOR21.DAT and some of the main output data are graphically presented in figures 1 and 2. These figures show the enclosure air temperature and heat flow behavior, respectively, for the 21st day of December.

5 DISCUSSION AND CONCLUSION

The weather data for the Damascus zone measured for the years 1970 through 1993, which are required in the existing computer programs LOS-A0, were scrutinized and reconditioned. Using these

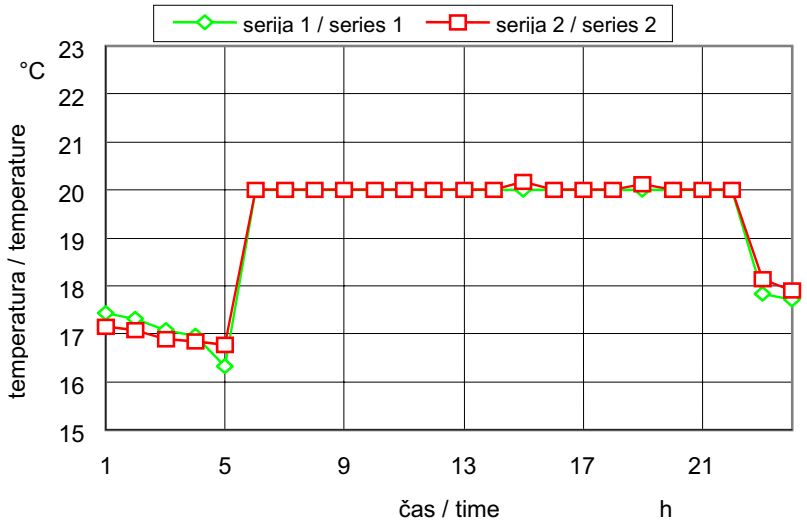

Sl. 1. *Obnašanje temperature zraka za 21. december (1 - z uporabo spremenjnenega računalniškega programa LOS-A0 - podatkovna baza RMY za mesečno povprečje urnih vremenskih podatkov, 2 - z uporabo računalniškega programa CLIMA - podatkovna baza RMY za urne vremenske podatke)*

Fig. 1. *Enclosure air temperature behavior for the 21st of December (1- using modified LOS-A0 computer program -RMY Database for monthly average of hourly weather data, 2- using CLIMA computer program - RMY Database for hourly weather data)*

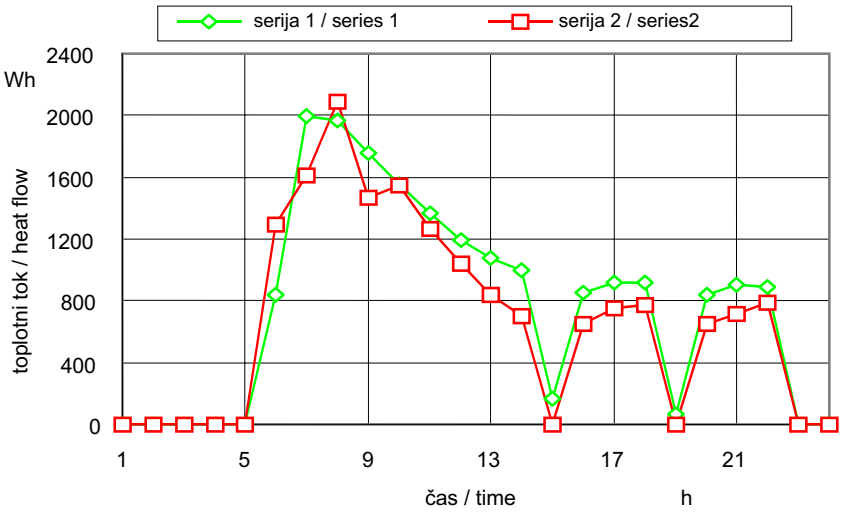

Sl. 2. *Obnašanje toplotnega toka za 21. december (1 - z uporabo spremenjenega računalniškega programa LOS-A0 - podatkovna baza RMY za mesečno povprečje urnih vremenskih podatkov, 2 - z uporabo računalniškega programa CLIMA - podatkovna baza RMY za urne vremenske podatke)*
Fig. 2. *Enclosure heat flow behavior for the 21st of December (1- Using the modified LOS-A0 computer program -RMY Database for monthly average of hourly weather data, 2- Using CLIMA computer program -RMY Database for hourly weather data)*

razvita glede na naslednje vzorce:
- urno mesečno povprečje,
- urno povprečje,
- dnevna količina sonca, merjena v urah.

Računalniški program LOS-A0 je bil pripravljen skupaj s podatkovno bazo prvega modela. Prilagojen je bil glede na delovne razmere in letne čase v Siriji.

Omenjeni program je bil dopolnjen za izračun poljubnega obdobja v letu in ta različica se imenuje CLIMA. Ta pa je bil pripravljen skupaj s podatkovno bazo drugega modela.

Spremenjena programa LOS-A0 in CLIMA sta bila uporabljena za energijske analize prostora. Natančne analize rezultatov, dobljenih z uporabo obeh programov, so pokazale, da so vrednosti za temperaturo zraka skladne (sl. 1). Vrednosti za toplotne izgube so se razlikovale (sl. 2). Največjo vrednost toplotnih izgub dobimo z uporabo povprečnih urnih podatkov o vremenu, najnižjo vrednost pa z izračunom urnih vremenskih podatkov. Ti odmiki se pojavljajo zaradi povprečnih urnih vremenskih podatkov za mesec december in tipičnih urnih vremenskih podatkov za 21. december. Dobljeni mesečni toplotni dobitki z uporabo spremenjenega LOS-A0 in CLIMA so 567,2 kWh in 279,2 kWh. Kakorkoli že, čas računanja z uporabo osebnega računalnika s procesorjem PENTIUM 166 sta bila 0,66 s in 3,35 s. Iz teh številk je razvidno, da je vrednost toplotnih obremenitev, izračunana po spremenjenem LOS-A0, precenjena. Ta precenjenost je posledica kumulativnih dnevnih razlik v izračunu toplotnih obremenitev skozi ves december. Bolj natančne rezultate dobimo z

measured data, an RMY Database was organized and developed according to the following patterns:
- monthly average of the hourly weather data,
- hourly weather data,
- daily sunshine hours.

The LOS-A0 computer program was provided with an RMY Database of the first pattern. It was also modified to be adapted for utilization according to working conditions and weather seasons in Syria.

The last mentioned program was re-organized, to be used in the calculation for an optionally determined period within the year, and a new version, CLIMA, was obtained. The CLIMA computer program was provided with an RMY Database of the second pattern.

Modified LOS-A0 and CLIMA computer programs were utilized in the energy analysis of an enclosure. Detailed analysis of the results calculated by the two programs revealed that the values obtained for air temperature behavior were in good agreement (Fig. 1). The values for heat loss behavior were, however, different (Fig. 2). The highest values of heat loss are obtained by using the monthly average of hourly weather data, and the lowest values are obtained by using the hourly weather data. Such deviations are due to the discrepancies between the monthly average of hourly weather data for the month of December and the typical hourly weather data for the 21st of December. Moreover, the obtained monthly heat load by using the modified LOS-A0 and CLIMA were 567.2 kWh and 279.2 kWh respectively. However, the computing times using a PC with a PENTIUM 166 processor were 0.66 seconds and 3.35 seconds respectively. From these figures it can be seen that the value of heat load calculated by the modified LOS-A0 is an overestimation. Such an overestimation is due to the

uporabo urnih vremenskih podatkov namesto uporabe mesečnega povprečja urnih vremenskih podatkov.

Toplotna zmožnost ter stroški ogrevanja in klimatizacije so sorazmerni s toplotnimi obremenitvami in zato je pomembno, da je podatkovna baza dostopna, saj omogoča natančen izračun, katerega posledica je zmanjšanje porabe energije. Računalniški program CLIMA priporočamo za dinamične analize prenosa toplote v stavbah, skupaj s podatkovno bazo RMY, v kateri so predstavljeni urni vremenski podatki določenega fizikalnega parametra.

cumulative daily discrepancies in the calculated heat load over all the days of December. More accurate results are obtained by the use of hourly weather data instead of using the monthly average of hourly weather data.

Since the thermal capacity and cost of heating and air-conditioning systems are proportional to the heat load and since an RMY Database is available it is important that accurate results are achieved to reduce energy consumption. Therefore, the use of the CLIMA computer program for the dynamic analysis of heat transfer in buildings, provided with an RMY Database in which the hourly weather data of predetermined physical parameters are represented, is suggested.

ZAHVALA

Avtor se zahvaljuje prof.dr. Ibrahim-u Othman-u, generalnemu direktorju, za izraženo zanimanje in vzpodbude ter prof.dr. Tawfik-u Kassam-u in dr. Mohamed-u Tlass-u za razprave in nasvete. Končno gre zahvala tudi Oddelku za meteorologijo za pridobitev uporabljenih urnih vremenskih podatkov za Damask.

ACKNOWLEDGMENT

The author would like to express his gratitude to Prof. Dr. Ibrahim Othman, the Director General, for his continued interest and encouragement and to Prof. Dr. Tawfik Kassam and Dr. Mohamed Tlass, for valuable discussions and suggestions. Finally, thanks are due to the Department of Meteorology, for providing the determined hourly weather data for the Damascus zone.

6 OZNAČBE
6 NOMENCLATURE

površina A	A	surface A
spremenljivka a; element matrike [a]	a	variable a; elements of matrix [a]
spremenljivka b; element matrike [b]	b	variable b; elements of matrix [b]
specifična toplota zraka	c_p	air specific heat
razlika	D	difference
kritična vrednost Kolmogorovovega testa	$D_n^{(\gamma)}$	critical values of the Kolmogrov goodness-of-fit test
funkcija standardne normalne kumulativne porazdelitve	$F(z)$	standard normal cumulative distribution function
funkcija normalne gostote verjetnosti	$f(x)$	normal probability density function
koeficient sevalnega prenosa toplote	g	radiation heat transfer coefficient
spremenljivka x ima kumulativno krivuljo frekvence F(z)	H_0	the variable x has cumulative frequency curve F(z)
spremenljivka x nima kumulativne krivulje frekvence F(z)	H_1	the variable x does not have cumulative frequency curve F(z)
j-ti element	J	j-th element
število površin prostora	m	number of surfaces in the enclosure
število TRF; število točk	n	number of TRF; number of points
verjetnost	P	probability
odklonilno področje; stopnja energije, ki jo sevajo notranji viri toplote (sončna energija, ki prihaja skozi okna, razsvetljava, oprema in ljudje v prostoru) in ki jo absorbira površina i v času t; stopnja energije, ki se prenese na okoliški zrak s prestopom z notranjih virov toplote (sončna energija, ki prihaja skozi okna, razsvetljava, oprema in ljudje v prostoru) v času t	R	rejection region; rate of heat radiated from the internal heat sources (solar energy coming through the windows, lights, equipment and occupants) and absorbed by surface i at time t; rate of heat convected into the enclosure air from the internal heat sources (solar energy coming through the windows, lights, equipment and occupants) at time t
specifični toplotni/masni tok	q	specific heat/mass flow
funkcija kumulativne porazdelitve frekvence	S	sample cumulative frequency distribution function

spremenjeni TRFs	X	modified TRFs
spremenljivka x	x	variable x
aritmetično povprečje vzorca	$\bar{x}$	arithmetic mean of the sample
spremenjeni TRFs	Y	modified TRFs
standardna normalna spremenljivka	z	standard normal variable
koeficient prestopa toplote	α	convection heat transfer coefficient
stopnja pomembnosti preskusa	γ	level of significance of the test
aritmetično povprečje/pričakovano povprečje	μ	arithmetic mean/expected mean
standardno odstopanje	σ	standard deviation
temperatura	ϑ	temperature
toplotna obremenitev	ϕ	thermal load
tip oblačnosti	CTYP	type of cloud
temperatura suhega termometra	DBT	air dry-bulb temperature
temperatura rosišča	DPT	air dew-point temperature
eksponent	exp	exponent
največja vrednost	max	maximum
mesec	MON	month
celotno sončno sevanje	MGO	global solar radiation
model normalne porazdelitve	NDM	normal distribution model
relativna vlažnost	RH	relative humidity
referenčno meteorološko leto	RMY	reference meteorological year
atmosferski tlak	SP	atmospheric pressure
splošni delež	SR	common relation
stopnja celotne oblačnosti	TC	degree of global cloudless
toplotni odzivni faktorji	TRFs	thermal response factors
temperatura vlažnega termometra	WBT	air wet-bulb temperature
smer vetra	WD	wind direction
hitrost vetra	WS	wind velocity

Indeksi:	**Subscripts:**	
prenešena toplota v okoliški zrak iz notranjih virov toplote v času t	ci,t	convected into the enclosure air from the internal heat sources at time t
i-ta površina	i	i-th surface
notranja površina i	ii	interior surface i
notranja površina i v času t	ii,t	interior surface i at time t
notranja površina i v času t-j	ii,t-j	interior surface i at time t-j
i-ta površina v času t	i,t	i-th surface at time t
i-ta površina v času t-1	i,t-1	i-th surface at time t-1
notranji zrak v času t	ia,t	inside air at time t
notranja površina k v času t	ik,t	interior surface k at time t
površina i glede na površino k	i,k	surface i in respect to surface k
spremenjen TRF j za površino i, elementi i=1,2……m+1 in j=1,2…….m+1	i,j	modified TRF j for the surface i, elements i=1,2……m+1 and j=1,2…….m+1
j-ti element	j	j-th
zunanja temperatura površine i v času t-j	oi,t-j	outside temperature of surface i at time t-j
zunanji zrak v času t	oa,t	outdoor air at time t
masni pretok zunanjega zraka, ki prehaja v okolico v času t	mf,t	mass flow of outdoor air infiltrating into the enclosure at time t
masni pretok ventilacijskega zraka v času t	mv,t	mass flow of ventilation air at time t
največja vrednost	max	maximum
n-ti element	n	n-th
ventilacijski zrak v času t	v,t	ventilation air at time t
toplota,ki jo sevajo notranji viri toplote in jo absorbira površina i v času t	si,t	radiated from the internal heat sources and absorbed by surface i at time t
čas	t	time

7 LITERATURA
7 REFERENCES

[1] Saman, H. (1995) Energy balance in the Syria Arab Republic. *Internal statistical report, Ministry of petroleum*, Syria.
[2] Skeiker, K. (1990) LOS-A0, The computer program for dynamic analysis of heat transfer in building, Faculty of mechanical engineering in Ljubljana, Slovenia.
[3] Martz, H.V. (1991) Bayesian reliability analysis. *Krieger publishing company, Malabar*, Florida.
[4] Preston, D.V. (1991) The art of experimental physics. *John Wiley and Sons,* New York.
[5] Green, J.R. (1979) Statistical treatment of experimental data, *Elsevier Scientific Publishing Company,* New York.
[6] Goon, A.M. (1981) Basic statistics. *The world press private limited*, Calcutta.
[7] Brookes, B.C. (1967) Introduction to statistical method, *Heinemann,* London.
[8] Miller, J.C. (1993) Statistics for analytical chemistry, 3rd edition, *Ellis Horwood limited*, New York.
[9] Kusuda,T. (1969) Thermal response factors for multi-layer structure of various heat conduction systems. *ASHRAE Transactions*, Vol. 75, Part I.
[10] Stephenson, D.G. and G.P. Mitalas (1971) Calculation of heat conduction transfer functions for multi-layer slabs. *ASHRAE Transaction*, Vol. 77, Part II.
[11] ASHRAE (1995) ASHRAE handbook- Fundamentals, SI Edition, *American society of heating refrigerating and air-conditioning engineers inc.,* Atlanta.
[12] Zupančič, J. (1985) LOS-A0 Computer program for the building heating and cooling load calculation (Adopted NBSLD Program). *Faculty of mechanical engineering*, Ljubljana.
[13] Eldridge, H.J. (1974) Properties of building materials. *MTP company limited*, Great Britain.
[14] Rateb, S. (1998) Properties of building materials. *Faculty of civil engineering,* Damascus, Syria.

Naslov avtorjev: Kamal Skeiker
Komisija za jedrsko energijo
Oddelek za znanstvene storitve
p.p. 6091
Damask, Sirija

Authors' Address: Kamal Skeiker
Atomic Energy Comission
Department of Scientific Services
P.O. Box 6091
Damascus, Syria

Prejeto: 29.9.1999
Received:

Sprejeto: 2.6.2000
Accepted:

© Strojniški vestnik 46(2000)6,359-369
ISSN 0039-2480
UDK 620.178.3:621.833:539.42:621.89
Izvirni znanstveni članek (1.01)

© Journal of Mechanical Engineering 46(2000)6,359-369
ISSN 0039-2480
UDC 620.178.3:621.833:539.42:621.89
Original scientific paper (1.01)

Numerično simuliranje površinske utrujenostne razpoke na zobeh zobnikov

Numerical Simulation of the Surface Fatigue Crack Growth on Gear Teeth Flanks

Gorazd Fajdiga - Jože Flašker - Srečko Glodež - Zoran Ren

V tem prispevku je predstavljen dvodimenzijski računski model za simuliranje širjenja površinsko začetne utrujenostne razpoke v stičnem področju dveh zobnih bokov zobnikov. Diskretiziran model zoba zobnika je obremenjen s pravokotno obremenitvijo (Hertzov stični tlak), strižno obremenitvijo (trenje med zobnimi boki zobnikov) in dodatno stično silo, ki je posledica elastohidrodinamičnih (EHD) pogojev mazanja. Za določitev širjenja utrujenostne razpoke od začetne do kritične dolžine, ko se delček materiala odlomi od površine in povzroči nastanek jamice, je uporabljen postopek J-integrala v okviru metode končnih elementov. Primerjava računskih in eksperimentalnih rezultatov kaže, da je predstavljeni model primeren za spremljanje širjenja površinske utrujenostne razpoke pri stični obremenitvi in ga kot takega lahko uporabimo pri napovedovanju pojava jamičenja na stično obremenjenih elementih, kakor so zobniki, ležaji, kolesa itn.

(Ključne besede: utrujanje, problemi stikov, jamičenje, mehanika loma, mazanje)

The paper describes a two-dimensional computational model for simulation of the surface-initiated fatigue-crack growth in the contact area of gear-teeth flanks. The discretised model of gear teeth is subjected to normal loading (Hertzian contact pressure), tangential loading (friction between gear-teeth flanks) and additional external contact forces that arise from the EHD-lubrication conditions. The J-integral method in the framework of the finite-element analysis is used for the simulation of the fatigue-crack propagation from the initial to the critical crack length, when the material's surface layer breaks away and a pit appears on the surface. The comparison of computational and experimental results shows that the proposed model reliably simulates the surface-fatigue crack growth under contact loading and can be used for computational predictions of surface pitting for various contacting mechanical elements like gears, bearings, wheels, etc.

(Keywords: fatigue, contact problems, pitting, fracture mechanics, lubrication)

0 UVOD

Najpogostejši utrujenostni poškodbi pri zobnikih, obremenjenih s ciklično stično obremenitvijo, sta jamičenje stičnih površin zobnega boka zobnika in zlom zoba v korenu ([1] in [2]). V tem prispevku je obravnavana le poškodba jamičenje, za popis katere je razvit računski model, ki omogoča izračun odpornosti glede na jamičenje oziroma izračun dobe trajanja zobnega boka zobnika do pojava prvih poškodb. Začetek procesa jamičenja se kaže v nastanku majhnih začetnih razpok na površini oziroma tik pod površino, ki se pod pogoji kotalno stičnega utrujanja materiala širijo do take dolžine, ko se pojavi nestabilno širjenje razpoke. Zaradi tega se delček materiala odlomi od površine in povzroči nastanek jamice [3].

Nastanek utrujenostnih razpok pomeni eno izmed najpomembnejših faz v procesu kotalno

0 INTRODUCTION

Two kinds of teeth damage can occur on gears under repeated loading due to material fatigue, the pitting of gear-teeth flanks and tooth breakage in the tooth root ([1] and [2]). In this paper only the pitting phenomenon is addressed and the developed numerical model is used for determination of pitting resistance, *i.e.* the service life of gear-teeth flanks. The process of surface pitting can be visualised as the formation of small, surface-breaking or subsurface initial cracks, which grow under repeated contact loading. Eventually, the crack becomes large enough for unstable growth to occur, which causes the material's surface layer to break away and a void occurs on the surface [3].

The initiation of fatigue cracks represents one of the most important stages in the pitting process. The position and mode of fatigue-crack initiation de-

stičnega utrujanja materiala. Lega in način začetka utrujenostne razpoke sta odvisna od mikrostrukture materiala, vrste obremenitve ter makro- in mikrogeometrije elementa [4]. Glede na različno kombinacijo kotalno-drsnih stičnih pogojev lahko pride do nastanka razpoke na površini ali pod njo (sl. 1). Razpoke, začete v globini med 0 in 2 mm, so opredeljene kot površinske razpoke. Začetne razpoke v globini med 2mm in 0,4 *b* (*b* je polovična dolžina Hertzove stične ploskve) opredelimo kot podpovršinske razpoke, v globini več ko 0,4 *b* pa kot razpoke v globljih plasteh, kjer robni pogoji na površini nimajo več bistvenega vpliva na širjenje razpoke [5].

pends on the microstructure of a material, the type of the applied stress and the micro- and macro-geometry of the specimen [4]. Depending on the different combinations of rolling and sliding contact conditions the crack initiation periods can be very different and a crack can be initiated either on or under the surface (Figure 1). The cracks initiated at a depth *H* ranging from 0 to 2 mm are classified as surface cracks. Cracks initiated at a depth of 2 mm to 0.4×*b* are called subsurface cracks, where *b* is the half-width of the Hertz contact zone. Cracks initiated at depths larger than 0.4×*b* correspond to the regimes of internal crack initiation, since the boundary effects are negligible [5].

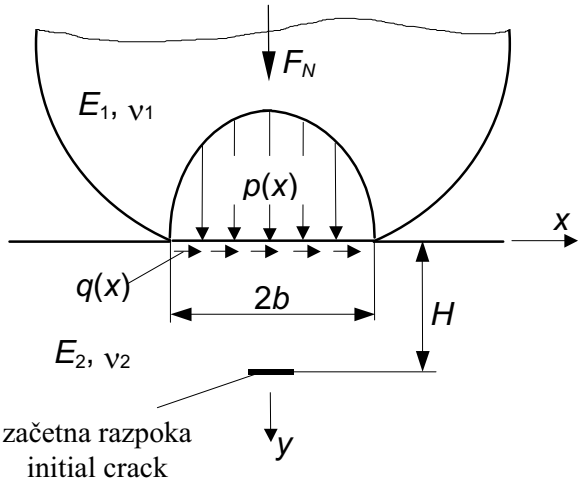

Sl. 1. *Nastanek utrujenostne razpoke pod pogoji stične obremenitve*
Fig. 1. *Modelling of fatigue crack initiation under contact loading*

Jamičenje kot posledica podpovršinskega nastanka razpok je opazno pri zobnikih z gladkimi stičnimi površinami in dobrim mazanjem. V tem primeru imajo velike strižne napetosti tik pod površino, ki nastanejo zaradi stične obremenitve, za posledico nastanek razpoke ([6] do [8]). Jamičenje zaradi nastalih razpok na površini pa je opaženo pri zobnikih s hrapavo površino in slabim mazanjem. Površinske razpoke se lahko pojavijo tudi zaradi mehanske in termične obdelave zobnika.

V tem prispevku je predpostavljena začetna razpoka na stični površini zaradi mehanske ali termične obdelave zobnika. Doba trajanja zobnega boka je tako enaka potrebnemu številu obremenitvenih obdobij, da se začetna razpoka razširi od začetne do kritične dolžine, ko se pojavijo tudi prve poškodbe na površini.

1 ŠIRJENJE UTRUJENOSTNIH RAZPOK PRI STIČNI OBREMENITVI

Zaradi majhnih dolžin razpok v stičnem področju zobnih bokov zobnikov je v splošnem treba pri širjenju razpoke uporabiti teorijo širjenja kratkih

Sub-surface pitting initiation is common in gears with smooth contact surfaces and good lubrication, where the large shearing sub-surface stresses, resulting from the contact loading, govern the crack initiation ([6] to [8]). Surface pitting initiation is observed in gears with rough surfaces and poor lubrication. Surface cracks may also appear as a consequence of the mechanical and thermal treatment of the material.

In this paper it is assumed that the fatigue crack is initiated on the surface as a consequence of mechanical and thermal treatment of the material. The service life of gear-teeth flanks is then estimated as the number of stress cycles required for the crack to propagate from some initial value to the critical crack length, when surface damage is expected to occur.

1 FATIGUE-CRACK GROWTH DUE TO CONTACT LOADING

The small crack lengths in the contact area of gear-teeth flanks imply that the short crack growth theory should be used for describing fatigue crack propagation.

razpok. V tem primeru ima pomembno vlogo mikrostruktura materiala, še posebej meje med kristalnimi zrni, ki bistveno vplivajo na proces širjenja razpoke ([9] in [10]). Iz predpostavke, da je hitrost širjenja razpoke da/dN sorazmerna plastičnemu pomiku vrha razpoke δ_{pl} izhaja:

The short fatigue crack growth is characterised by successive blocking of the crack's growth by the material's microstuctural grain boundaries, which implies a discontinuous character of the crack-growth process [9] and [10]. The crack growth rate da/dN is assumed to be proportional to the crack-tip plastic displacement δ_{pl}:

$$\frac{\mathrm{d}a}{\mathrm{d}N} = C_o \left(\delta_{pl}\right)^{m_o} \tag{1},$$

kjer sta C_o in m_o materialni konstanti, ki jih določimo eksperimentalno. Pri numeričnem preračunu je koristno izraziti plastični pomik vrha razpoke δ_{pl} s faktorjem intenzivnosti napetosti K. Enačba za povezavo med omenjenima parametroma ima po [9] obliko:

where C_o and m_o are material parameters that are determined experimentally. In view of the numerical simulation it is beneficial to express the crack-tip plastic displacement δ_{pl} in terms of the stress-intensity factor K. This relationship has been provided in the following form [9]:

$$\delta_{pl} = \frac{2(1-\nu)}{G\sqrt{\pi}} \cdot \frac{\sqrt{1-n^2}}{n} K\sqrt{a} \tag{2},$$

kjer sta: G - strižni modul, in ν - Poissonovo število. Parameter $n = a/c$ izraža relativno lego vrha razpoke glede na mejo kristalnega zrna (sl. 2). Z integriranjem enačbe (1) dobimo potrebno število obremenitvenih obdobij N_j za razširitev razpoke skozi posamezno kristalno zrno. Skupno število obremenitvenih obdobij za razširitev razpoke od začetne do kritične dolžine, ki dejansko pomeni dobo trajanja obravnavanega elementa, pa je definirano z enačbo:

where G is the shear modulus and ν is Poisson's ratio. The parameter $n = a/c$ describes the relative position of the crack tip with respect to the grain boundary, see Figure 2. The number of stress cycles N_j required for a crack to propagate through each crystal grain is then obtained with the integration of eqn (1). The corresponding total number of stress cycles required for pitting on gear teeth flanks to occur is then defined as:

$$N = \sum_{j=1}^{z} N_j \; ; \quad j = 1,\ 2,\ 3,\ \ldots,\ z \tag{3},$$

kjer je z število kristalnih zrn, skozi katera poteka razpoka. Izračunamo ga tako, da kritično dolžino razpoke a_c delimo s povprečnim premerom kristalnega zrna D ($z = a/D$) (sl. 2). Postopek je podrobno opisan v [3] in [6].

Predmet raziskave je bil določitev funkcijske odvisnosti faktorja intenzivnosti napetosti od dolžine razpoke, $K = f(a)$, ki je ključnega pomena za rešitev enačbe (2) in zaradi tega tudi enačbe (1). Če je funkcija $K = f(a)$

where z is the number of grains transversed by the crack - calculated by dividing the critical crack length a_c by the average grain diameter D, *i.e.* $z = a/D$, see Figure 2. This procedure is fully explained in [3] and [6].

The subject of this study was only the determination of $K = f(a)$, which is necessary for solving solution of eqn (2) and consequently eqn (1). If the function $K = f(a)$ is known, the service

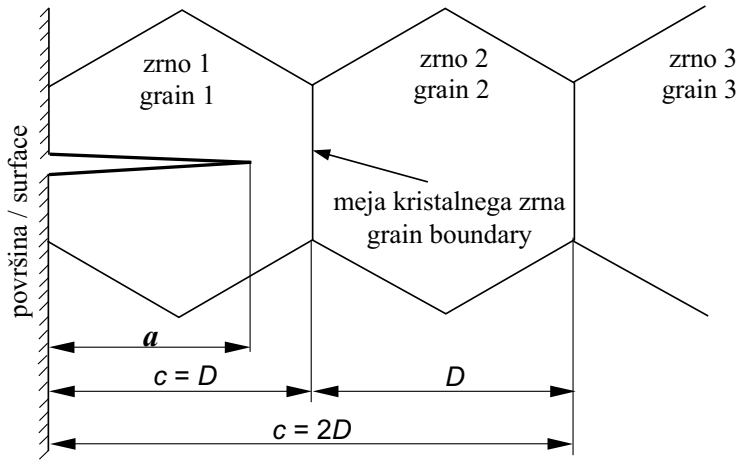

Sl. 2. *Začetna razpoka v prvem kristalnem zrnu*
Fig. 2. *Initial crack in the first crystal grain*

poznana, lahko ob poznavanju materialnih veličin C_0 in m_0 razmeroma preprosto določimo potrebno število obremenitvenih obdobij N do pojava jamičenja. Ta postopek je podrobno opisan v [3],[6]. Za določitev funkcije $K = f(a)$ je uporabljena metoda J-integrala v okviru metode končnih elementov (MKE - FEM).

2 METODA *J*-INTEGRALA

J-integral je definiran kot količina sproščene energije, potrebne za rast razpoke z enačbo [11]:

$$J = \int_S \left(W \cdot \mathrm{d}\, y - T \cdot \frac{\partial u}{\partial x} \right) \mathrm{d}\, s \qquad (4),$$

kjer so: W - deformacijska energija, T - vektor v smeri pravokotnica n na integracijsko krivuljo, u - pomik v smeri integracijske krivulje in S - integracijska pot okoli vrha razpoke (sl. 3). J-integral je neodvisen od izbrane integracijske poti okoli vrha razpoke, kar omogoča izračun integrala po integracijski poti, ki je poljubno oddaljena od vrha razpoke. Glavna prednost izračuna J-integrala je prav ta, da se ga lahko računa za pot, ki je dovolj oddaljena od področja vrha razpoke, s čimer se izognemo problemom singluarnosti v neposredni bližini konice razpoke. Zato za rešitev J-integrala ni potrebna drobna diskretizacija okoli vrha razpoke.

2 THE *J*-INTEGRAL METHOD

The J-integral is defined as the energy-release rate available for crack growth with the following equation [11]:

where W is the strain energy density, T is the vector of surface tractions, u is the displacement vector and S is the integration path around the crack tip (Figure 3). The J-integral is independent of the selected integration path around the crack tip, which enables the evaluation of the integral along an arbitrary path away from the crack-tip area. The main advantage of the J-integral calculation is that it can be calculated for a contour far from the crack-tip region, which is characterised by its steep stress and strain gradients. Hence there is no need for a very fine discretisation around the crack tip to arrive at the solution of the J-integral.

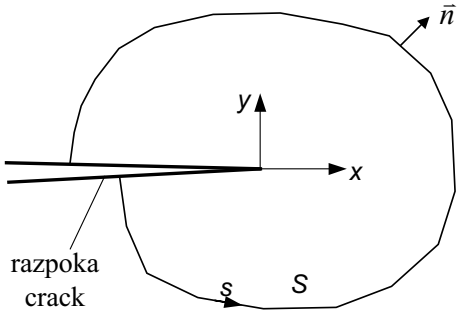

Sl. 3. *Integracijska pot za izračun J-integrala*
Fig. 3. *Close contour used in the evaluation of the J-Integral*

Iz numerično izračunane vrednosti J-integrala se faktor intenzivnosti napetosti K izračuna z uporabo enačbe [11]:

From the numerically determined J-integral value, the stress intensity factor K can be calculated from the following equation [11]:

$$K = \sqrt{J \cdot E'} \qquad (5),$$

kjer sta $E' = E$ za ravninsko napetostno stanje in $E' = E/(1-\nu^2)$ za ravninsko deformacijsko stanje (E - modul elastičnosti, ν - Poissonovo število).

Z uporabo metode J-integrala pri simuliranju širjenja utrujenostne razpoke je potrebno reševanje, kjer je pot širjenja razpoke izračunana koračno. V splošnem je znano, da se bo razpoka širila v smeri največje sprostitve potencialne energije, to pomeni v smeri največje vrednosti J-integrala oziroma faktorja intenzivnosti napetosti K. Torej mora biti J-integral in zato tudi faktor intenzivnosti napetosti K numerično

where $E' = E$ for the plane stress and $E' = E/(1-\nu^2)$ for the plane strain case, with E being the Young's modulus and ν the Poisson's ratio.

By applying the J-integral method for simulations of the fatigue-crack growth it is necessary to set up an incremental procedure, where the crack growth path is determined incrementally. It is generally accepted that the crack will always extend in the direction that corresponds to the maximum release of potential energy, i.e. the maximum value of the J-integral and consequently,the stress intensity factor K. This implies that the J-integral, and subsequently K, should be numerically calculated for the dif-

izračunan za različne podaljške razpoke. Predpostavljeni podaljški razpoke so enake dolžine a vendar v različnih smereh od vrha razpoke (sl. 4). Razpoka je podaljšana v smeri največjega J oziroma K, nato pa se ves proces zopet ponovi.

ferent virtual extensions of the crack around the crack tip. The virtual crack extensions are of the same length, but in different directions from the crack tip (Figure 4). The crack is incrementally extended in the direction of the maximum J or K value and the process is repeated.

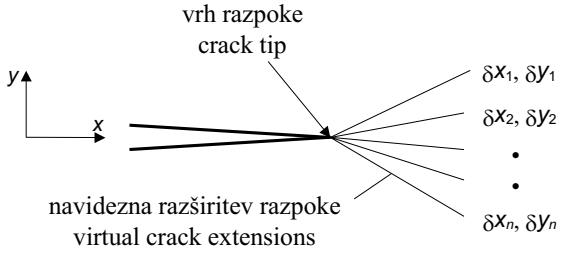

Sl. 4. *Predpostavljene navidezne razširive razpoke*
Fig. 4. *Virtual crack extensions of the crack tip*

3 VPLIVNI PARAMETRI NA ŠIRJENJE UTRUJENOSTNE RAZPOKE PRI ZOBNIKIH

V praksi je v splošnem najbolj obremenjeno mesto na zobnem boku notranja točka enojnega ubiranja pastorka B, kjer je tudi jamičenje zobnih bokov praviloma najbolj izrazito. To je tudi mesto, ki je upoštevano pri vseh numeričnih izračunih. Za obravnavano zobniško dvojico leži točka B na premeru d_{B1}, ubirni kot v tej točki pa je α_{B1} (sl. 5).

3 PARAMETERS INFLUENCING FATIGUE-CRACK GROWTH IN GEARS

The worst contact loading conditions appear when the gears' teeth are in contact at the inner point of a single teeth-pair engagement (point B), where the surface-breaking initial cracks are expected to develop first. This is also the case considered in all computations reported in this study. For the gear pair, the contact point B is located on diameter d_{B1}, with the associated pressure angle α_{B1} (Figure 5).

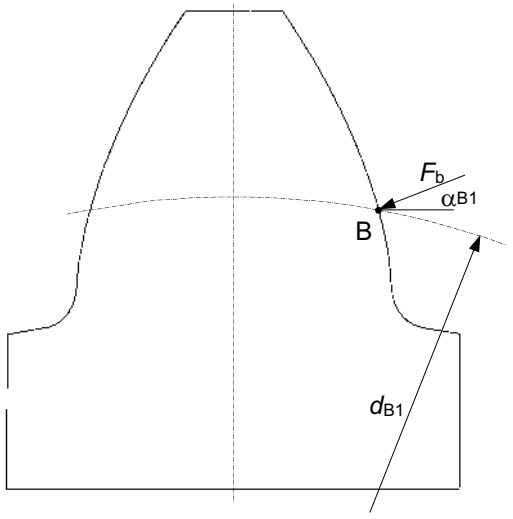

Sl. 5. *Model zoba pastorka s karakteristično ubirno točko B*
Fig. 5. *Pinion tooth model with associated contact point B*

Pri vseh preračunih je Hertzova pravokotna obremenitev $p(x)$, ki deluje v točki B, upoštevana kot pravokotna obremenitev zobnih bokov zobnikov. Poleg pravokotne Hertzove stične obremenitve $p(x)$, ki je odvisna od največjega bočnega tlaka σ_H in vpliva elastohidrodinamičnega mazanja (poglavje 3.1), je pri numeričnih izračunih upoštevan tudi vpliv trenja (sl. 6). Strižna obremenitev $q(x)$ je definirana kot:

In all computations the Hertzian normal-contact-loading distribution $p(x)$ acting at point B has been considered as the normal loading of the gear flanks. Apart from the normal contact loading $p(x)$, the distribution of which is dependent on the maximum contact pressure σ_H and elasto-hydro-dynamic (EHD)-lubrication conditions (see Section 3.1), the influence of friction has also been considered (Figure 6). The tangential loading distribution $q(x)$ was assumed to be equal to:

$$q(x) = \mu \cdot p(x) \tag{6},$$

kjer je μ koeficient trenja med zobnimi boki.

where μ is the coefficient of friction between the meshing gear flanks.

3.1 Vpliv mazanja EHD

Porazdelitev pravokotne obremenitve v stiku $p(x)$ v enačbi (6) upošteva tudi porazdelitev tlaka zaradi EHD mazanja (sl. 6). Ta porazdelitev je lahko določena eksperimentalno ali z uporabo ustreznih računalniških modelov ([12] in [13]).

3.1 Influence of the EHD lubrication

The normal-contact-loading distribution $p(x)$ in eqn. (6) also considers the EHD-pressure distribution, which is illustrated in Figure 6. This distribution can be determined experimentally or with use of relevant computational models ([12] and [13]).

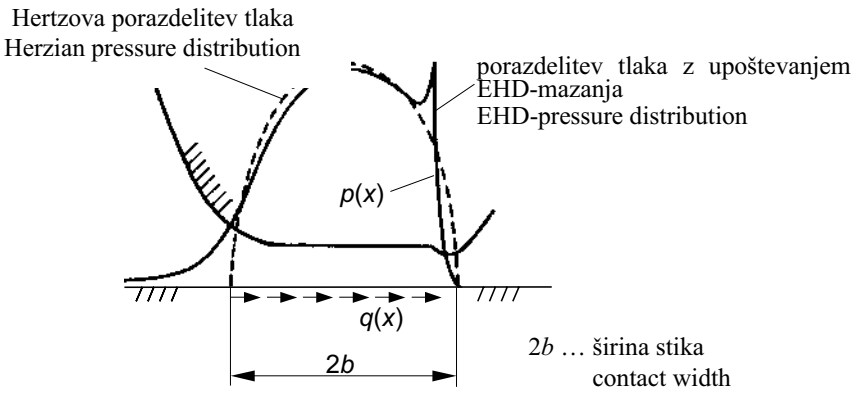

Sl. 6. *Porazdelitev obremenitve v stiku*
Fig. 6. *Contact loading distribution*

3.2 Vplivi procesa kotaljenja in maziva na širjenje razpoke

Za dejanski opis širjenja razpoke je treba upoštevati proces kotaljenja zobnih bokov okrog točke B, ki je tudi mesto, kjer je predpostavljena začetna razpoka. Za čim boljše simuliranje celotnega procesa kotaljenja bokov okrog točke B, je za vsako dolžino razpoke upoštevanih več obremenitvenih primerov, ki

3.2 The influence of moving contact and lubricant trapped into the crack

For a more realistic simulation of the fatigue-crack growth it is necessary to consider the moving gear teeth contact in the vicinity of point B, where the initial crack is assumed to appear. The moving contact can be simulated with different loading configurations as shown in Figure 7. In all configura-

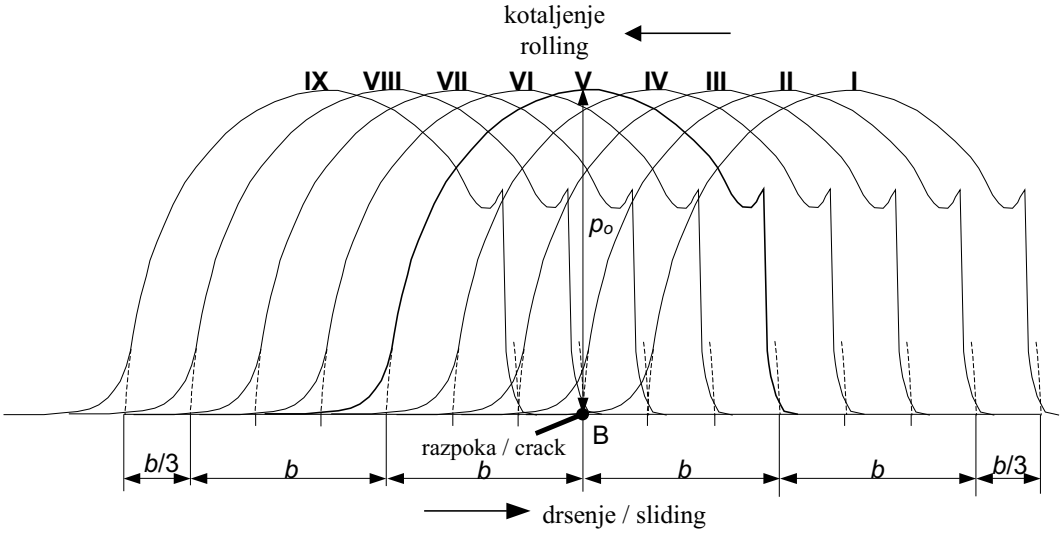

Sl. 7. *Obremenitveni primeri pri kotaljenju zobnih bokov okrog točke B*
Fig. 7. *Moving contact loading configurations in respect to point B*

so prikazani na sliki 7. Pri vseh obremenitvenih primerih sta pravokotna obremenitev $p(x)$ in strižna obremenitev $q(x)$ enaki po velikosti, vendar se pojavljata na različnih mestih glede na točko B.

Poleg poprej opisane pravokotne in strižne obremenitve zobnih bokov je pri simuliranju širjenja površinsko začete utrujenostne razpoke upoštevan tudi tlak v notranjosti razpoke, kot posledica mazanja zobnih bokov. Za opazovano razpoko v točki B ta tlak ni stalen, temveč je odvisen od trenutne lege tlačne elipse (sl. 8).

tions the normal $p(x)$ and tangential $q(x)$ contact loading distributions are of the same magnitude, however they are acting at different positions with respect to point B.

The simulation of the surface-initiated fatigue-crack propagation also needs to consider the influence of the lubricant pressure acting on the crack faces. The lubricant pressure is not constant and is dependent on the contact-loading position, *i.e.* the contact-pressure-distribution position with respect to point B, see Figure 8.

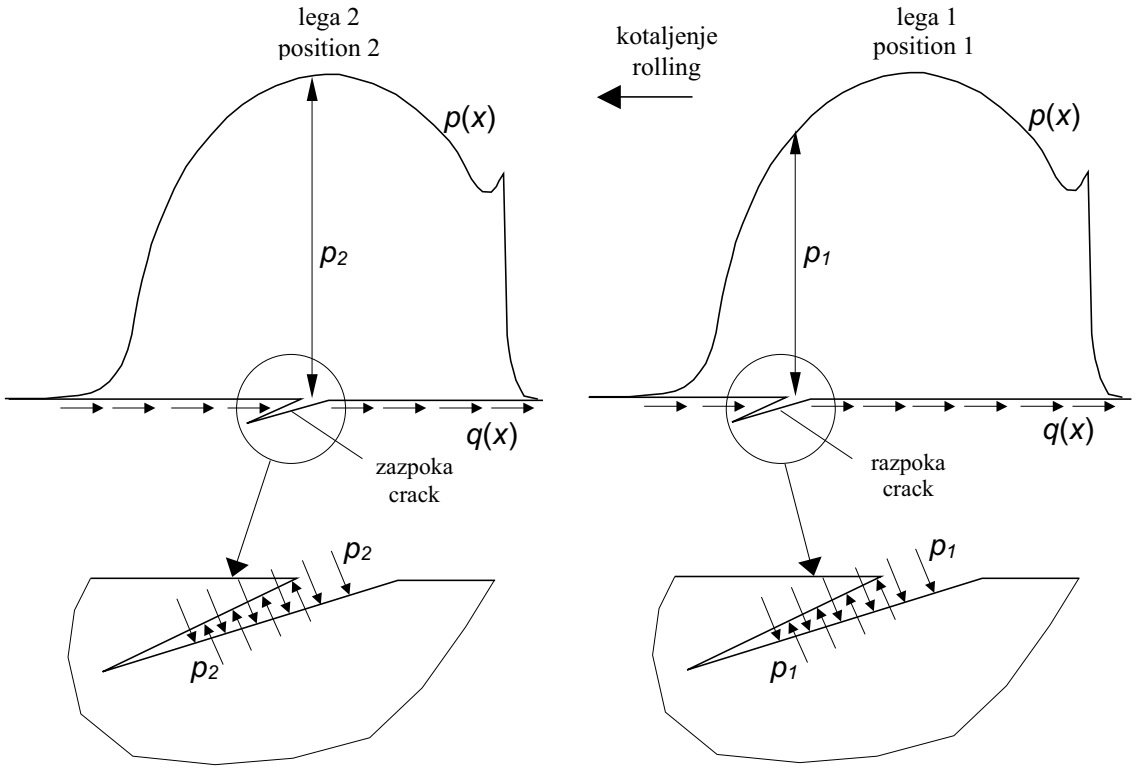

Sl. 8. *Obremenitev razpoke s tlakom olja*
Fig. 8. *Crack face loading with the lubricant pressure*

4 PRAKTIČEN PRIMER

Za analizo širjenja površinske utrujenostne razpoke je uporabljena zobniška dvojica s podatki ozobja, navedenimi v preglednici 1. Za obravnavano zobniško dvojico leži točka B na premeru d_{B1} = 84,708 mm, ubirni kot v tej točki pa je α_{B1} = 19,448° (sl. 5). Največji bočni tlak v točki B je p_o=1685 MPa in je izračunan z uporabo standarda DIN 3990 [1] z upoštevanjem spodnjih karakterističnih veličin:

- nominalni bočni tlak: σ_{H0} = 1525 MPa
- koeficient enojnega ubiranja: Z_B = 1,047
- koeficient obratovanja: K_A = 1,0
- dinamični koeficient: K_v = 1,06
- koeficient porazdelitve sile po širini zoba: $K_H\beta$ = 1,05
- koeficient porazdelitve sile na zobe: $K_H\alpha$ = 1,0

V predloženem delu je upoštevana vrednost za koeficient trenja μ = 0,04, kar je povprečna vrednost za zobniške dvojice z dobrim mazanjem [14].

4 PRACTICAL COMPUTATIONS

The real gear pair with the complete date set as given in Table 1 has been used for analyses of the surface-initiated fatigue-crack growth leading to pitting. For the treated gear pair the contact point B can be identified to be on diameter d_{B1} = 84.708 mm, with the associated pressure angle α_{B1} = 19.448° (Fig. 5). The maximum contact pressure p_o=1685 MPa has been determined according to the standard procedure DIN 3990 [1] taking into account the following assumptions:

- nominal contact pressure: σ_{H0} = 1525 MPa
- coefficient of single engagement: Z_B = 1,047
- application factor: K_A = 1,0
- dynamic factor: K_v = 1,06
- face load factor: $K_H\beta$ = 1,05
- transverse load factor: $K_H\alpha$ = 1,0

In the treated application the coefficient of friction μ = 0.04 has been used, which is the average value for well-lubricated gears [14].

Preglednica 1. *Osnovni podatki testne zobniške dvojice*
Table 1. *Data set of gear pair*

Pomen Parameter	Pastorek Pinion	Zobnik Gear
modul normal module	m_n = 5 mm	
število zob number of teeth	z_1 = 17	z_2 = 18
ubirni kot izhodnega profila pressure angle on pitch circle	α_n = 20°	
nagibni kot bočnic helical angle	β_o = 0°	
koeficient profilnih premikov coefficient of profile displacement	x_1 = 0.475	x_2 = 0.445
medosje centre distance	a = 91,5 mm	
širina zoba tooth width	b_1=b_2 = 16 mm	
premer razdelnega kroga pitch diameter	d_1 = 85 mm	d_2 = 90 mm

Porazdelitev EHD tlaka je izračunana s računalniškim programom ROSLCOR [12] in je prikazana na sliki 9. Upoštevano je olje ISO-VG-100 s kinematično viskoznostjo ν_{50} = 61 mm^2/s in gostoto ρ_{15} = 880 kg/m^3.

The EHD-pressure distribution has been determined with the computer program ROSLCOR [12] and is given in Figure 9. The lubricant oil used, ISO-VG-100, had a cinematic viscosity ν_{50} = 61 mm^2/s and a density ρ_{15} = 880 kg/m^3.

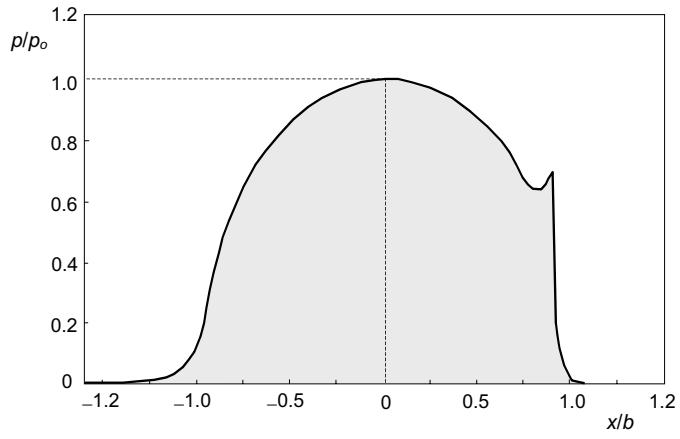

Sl. 9. *Porazdelitev EHD tlaka v kontaktnem področju*
Fig. 9. *EHD- pressure distribution in the contact area*

Pri vseh numeričnih preračunih je uporabljen model zoba pastorka na sliki 5, ter pravokotne in strižne obremenitve, opisane v poglavju 4. Slika 10 prikazuje mrežo končnih elementov za model zoba pastorka in konfiguracijo začetne razpoke na površini v notranji točki B enojnega ubiranja pastorka. Pri tem je predpostavljena dolžina začetne utrujenostne razpoke a_o=0,015 mm pod kotom α_o = 22°. Predpostavka o začetni razpoki izhaja iz rezultatov metalurških raziskav razpok na zobnikih [15].

Za numerično simuliranje širjenja razpoke in določitev faktorja intenzivnosti napetosti K (s tem tudi odvisnosti $K=f(a)$) je bil v tej študiji uporabljen programski paket MARC [16], ki bazira na metodi končnih elementov (MKE - FEM). Za simuliranje procesa

For all the numerical calculations the pinion-tooth model, shown in Figure 5, and the normal and tangential loading described in Section 4 have been used. Figure 10 shows the finite-element mesh of the pinion-tooth model and the configuration of the initial crack on the surface, located at point B. It was assumed that the initial length of the crack is equal to a_o=0.015 mm with the initial inclination angle α_o = 22°. This configuration of the initial crack corresponds to the metallographic investigations of cracks appearing on gears [15].

In this study the program package MARC [16], based on the FEM, has been used for computational simulation of crack growth and the associated determination of the function $K=f(a)$. For simu-

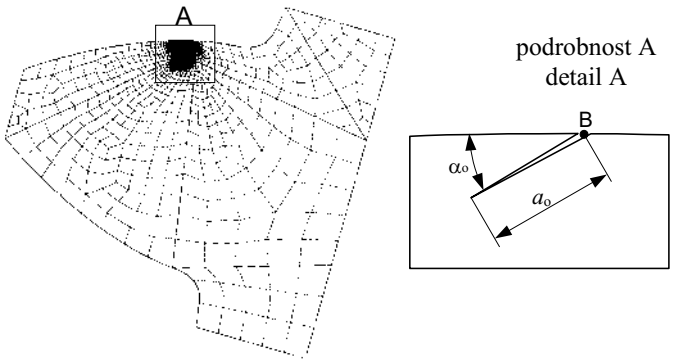

Sl. 10. *Numerični model in oblika začetne razpoke*
Fig. 10. *FE discretisation and configuration of the initial crack*

kotaljenja zobnih bokov je upoštevanih devet obremenitvenih primerov za vsako dolžino razpoke (sl. 7). V konici razpoke so določene različne navidezne razširitve razpoke (sl. 4) in za vsako od teh je izračunan faktor intenzivnosti napetosti. Razpoka se v naslednjem koraku podaljša v smeri največjega faktorja intenzivnosti napetosti, izbranega izmed vseh izračunanih vrednosti faktorjev intenzivnosti napetosti za različne navidezne razširitve razpoke in obremenitvene primere. Ta postopek je za prvi korak (začetna razpoka) prikazan na sliki 11. Vsi rezultati širjenja utrujenostne površinske razpoke pa so prikazani na sliki 12.

lations of the moving-gear-teeth contact, nine different loading configurations have been considered for each crack length (Fig. 7). Therefore, the stress intensity factor has been calculated for different virtual crack extensions (Fig. 4) of the crack tip and for each load case. The crack has then actually been extended in the direction of the maximum stress intensity factor K_{max} for all calculated load cases and virtual crack extensions. This procedure is for step 1 (initial crack), given in Figure 11. The complete results of the surface fatigue-crack growth are shown in Figure 12.

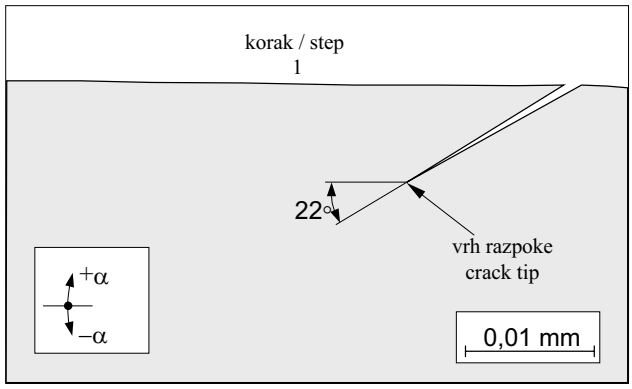

obrem. primer load case	I	II	III	IV	**V**	VI	VII	VIII	IX
J [MPa]	0,0003	0,005	0,115	0,323	**0,478**	0,434	0,373	0,044	0,001
K_{max} [MPa $\sqrt{mm}$]	8,2	33,6	161,4	270,4	**328,9**	313,5	290,6	99,8	15,0
smer K_{max} direction of K_{max} α °	20	18	8	0	**–8**	–12	–12	–20	–22
smer podaljška razpoke v naslednjem koraku: direction of the crack extension in the next step:	α = - 8°								

Sl. 11. *Numerični izračun J in K za začetno razpoko*
Fig. 11. *The numerical determination of J and K for the initial crack*

Po konfiguraciji razpoke na sliki 12 lahko sklepamo, da vodi začetna površinska razpoka dolžine 0,015 mm ob upoštevanih robnih pogojih do pojava zelo majhnih jamic na površini zobnih bokov, ki jih označimo kot mikrojamičenje.

On the basis of the results in Figure 12 it can be concluded that the initial surface crack of length 0.015 mm and the considered boundary conditions lead to the appearance of very small surface pits, which can be termed as micro-pitting on gear-teeth flanks.

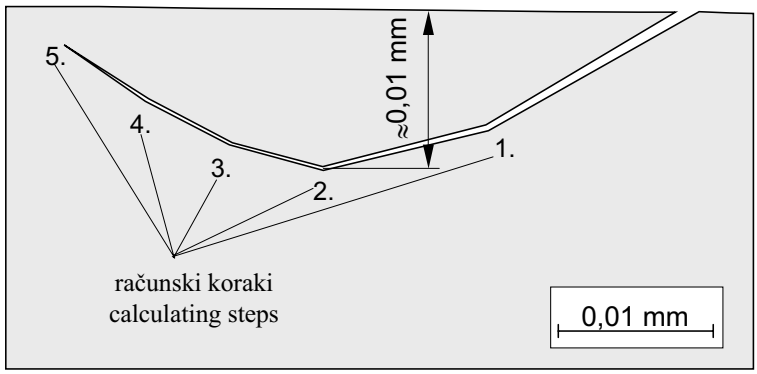

korak step	a mm	K MPa$\sqrt{\text{mm}}$	obrem. primer load case
1	0,015	329	V
2	0,025	374	VI
3	0,030	412	VI
4	0,035	500	VII
5	0,040	2132	VII

Sl. 12. *Potek širjenja površinsko inicirane razpoke*
Fig. 12. *Results of the surface initiated fatigue crack growth*

5 SKLEPI

V prispevku je predstavljen numerični model za analizo širjenja površinske utrujenostne razpoke na zobnih bokih zobnikov. Pri tem je predpostavljeno, da je zobni bok obremenjen s pravokotno obremenitvijo (največji bočni tlak) in strižno obremenitvijo (trenje) ter dodatno obremenitvijo zaradi EHD mazanja. Površinska razpoka je ob tem še dodatno obremenjena s tlakom olja, ki pritiska na obe površini razpoke in je odvisen od lege tlačne elipse glede na opazovano razpoko.

Simuliranje širjenja utrujenostne površinske razpoke je izvedeno na praktičnem primeru zobniške dvojice, ob uporabi metode *J*-integrala v okviru metode končnih elementov (MKE - FEM). Z uporabo modela izračunana odvisnost K= f(a) omogoča določitev dobe trajanja zobnika glede na jamičenje površine. Rezultati izvedenih numeričnih izračunov kažejo, da vodi zelo majhna začetna površinska razpoka do pojava mikrojamičenja zobnih bokov, kar se dobro ujema tudi z nekaterimi eksperimentalnimi raziskavami ([14] in [15]).

5 CONCLUSIONS

The paper presents a computational model for the simulation of surface-initiated fatigue-crack growth on gear-teeth flanks. The teeth flanks are subjected to the normal (normal contact pressure) and tangential (frictional forces) contact forces which also take into account the influence of EHD-lubrication conditions as well as the associated lubricant pressure acting on the crack faces.

The simulation of fatigue-crack propagation is performed on a practical application of gear contact with use of the *J*-integral method in the framework of the FEM. The consequent computational determination of the functional relationship K= f(a) enables an estimation of the gear service life in regard to the surface pitting. Computational results show that small initial surface cracks lead to micro-pitting of contacting gears, which corresponds well with the available experimental data ([14] and [15]).

6 LITERATURA
6 REFERENCES

[1] DIN 3990 (1987) Calculation of load capacity of cylindrical gears. *German standard*.
[2] Flašker, J., Glodež,S., S. Pehan (1995) Influence of contact area on service life of gears with crack in tooth root. *Com. Num. Methods Engng 11*.
[3] Glodež, S., Flašker, J., Z. Ren (1997) A new model for the numerical determination of pitting resistance of gear teeth flanks. *Fatigue Fract. Engng Mater. Struct. 20*.
[4] Zhou, R.S., Cheng, H.S., T. Mura (1989) Micropitting in rolling and sliding contact under mixed lubrication. *ASME Journal of Tribology 111*.

[5] Cheng, W., Cheng, H.S., Mura, T., L. M. Keer (1994) Micromechanics modelling of crack initiation under contact fatigue. *ASME J. Tribology 116.*
[6] Glodež, S., Winter, H., H.P. Stüwe (1997) A fracture mechanics model for the wear of gear flanks by pitting. *Wear 208.*
[7] Glodež, S., Z. Ren (1998) Modelling of crack growth under cyclic contact loading. *Theoretical and Applied Fracture Mechanics 30.*
[8] Glodež, S., Ren, Z., J. Flašker (1998) Simulation of surface pitting due to contact loading. *Int. j. numer. methods eng 43.*
[9] Navarro, A., E.R. Rios (1988) Short and long fatigue crack growth-a unified model. *Philosophical Magazine 57.*
[10] Sun, Z., Rios, E.R., K.J. Miller (1991) Modelling small fatigue cracks interacting with grain boundaries. *Fatigue Fract. Engng Mater 14.*
[11] Ewalds, H.L., R.J.H. Wanhill (1991) Fracture Mechanics. *Co-publication of Edward Arnold.*
[12] Oster, P, M. Simon (1988) Messung und Berechnung von Gleit-Wälzkontakten an Scheiben und Zahnrädern im Bereich der Elastohydrodynamik. *Antriebstechnik 27.*
[13] Fajdiga, G. (1998) Vpliv oljnega filma na bočni tlak zobniškega para. *Magistrsko delo*, Maribor.
[14] Winter, H., G. Knauer (1990) Einfluss von Schmierstoff und Betriebstemperatur auf die Grübchentragfähigkeit einsatzgehärteter Zahnräder. *Antriebstechnik 29.*
[15] Knauer, G. (1988) Zur Grübchentragfähigkeit einsatzgehärteter Zahnräder. *Ph.D. dissertation,* TU Munich.
[16] MARC, Users´ Manual, 1990

Naslov avtorjev: mag. Gorazd Fajdiga
prof.dr. Jože Flašker
doc.dr. Srečko Glodež
doc.dr. Zoran Ren
Fakulteta za strojništvo
Univerze v Mariboru
Smetanova 17
2000 Maribor

Authors' Address: Mag. Gorazd Fajdiga
Prof.Dr. Jože Flašker
Doc.Dr. Srečko Glodež
Doc.Dr. Zoran Ren
Faculty of Mechanical Engineering
University of Maribor
Smetanova 17
2000 Maribor, Slovenia

Prejeto: 29.2.2000
Received:

Sprejeto: 2.6.2000
Accepted:

© Strojniški vestnik 46(2000)6,370-382 © Journal of Mechanical Engineering 46(2000)6,370-382
ISSN 0039-2480 ISSN 0039-2480
UDK 621.311.25:621.039.536:621.039.58 UDC 621.311.25:621.039.536:621.039.58
Pregledni znanstveni članek (1.02) Review scientific paper (1.02)

Simuliranje odgovora zadrževalnega hrama jedrske elektrarne med veliko izlivno nezgodo

Simulation of Nuclear Power Plant Containment Response During a Large-Break Loss-of-Coolant Accident

Ivo Kljenak - Borut Mavko

S termohidravličnim računalniškim programom CONTAIN so bili simulirani pojavi v zadrževalnem hramu jedrske elektrarne med veliko izlivno nezgodo v dvozančnem tlačnovodnem reaktorju. Analizirani so bili tlačni in temperaturni odzivi ter porazdelitve hladiva in energije.

(Ključne besede: elektrarne jedrske, zadrževalni hram, nezgode izlivne, simuliranje)

Containment phenomena during a large-break loss-of-coolant accident in a two-loop pressurized-water reactor nuclear power plant were simulated with the CONTAIN thermal-hydraulic computer code. Pressure and temperature responses as well as coolant and energy distributions were analyzed.

(Keywords: nuclear power plant, containment, loss-of-coolant accident, simulations)

0 UVOD

Simuliranja nezgod v jedrskih elektrarnah s termohidravličnimi računalniškimi programi, ki omogočajo analizo različnih vidikov projektnih in resnih nezgod, lahko močno prispevajo k varnosti postrojenj. Čeprav vsebujejo rezultati določeno nezanesljivost, tovrstna simuliranja prispevajo tudi k boljšemu razumevanju medsebojnega vpliva fizikalnih pojavov, do katerih prihaja med nezgodami.

Računalniški program CONTAIN ([1] in [2]) je bil razvit v Sandia državnih laboratorijih (ZDA) s podporo Zvezne jedrske upravne komisije ZDA. CONTAIN omogoča celovito analizo pojavov v zadrževalnem hramu jedrske elektrarne. Eden izmed osnovnih načrtovanih ciljev CONTAIN-a je upravičeno napovedovanje prehodne funkcije zadrževalnega hrama (fizikalnih, kemičnih in radioloških pogojev) med resnimi in projektnimi nezgodami. Program CONTAIN med drugim vsebuje modele za termodinamiko vodne pare in zraka, pretoke med predelki, kondenzacijo in uparjanje na konstrukcijah in aerosolih, transport, aglomeriranje in usedanje aerosolov ter zgorevanje plinov. Prav tako vsebuje modele za pojave v reaktorski votlini, kakor sta interakcija med staljeno sredico in betonom ter uparjanje hladiva v bazenu. Prevod toplote v konstrukcijah, razpadanje in transport razcepkov, zaostala toplota zaradi radioaktivnih procesov ter

0 INTRODUCTION

Simulations of accidents in nuclear power plants (NPPs) with thermal-hydraulic computer codes, which were developed to analyze various aspects of design-basis and severe accidents, may significantly contribute to the safety of installations. Although results carry a certain amount of uncertainty, such simulations can contribute to a better understanding of the interaction between the physical phenomena which occur during accidents.

The CONTAIN computer code ([1] and [2]) was developed by Sandia National Laboratories, USA, with US Nuclear Regulatory Commission sponsorship. CONTAIN provides an integrated analysis of containment phenomena in NPPs. One of the major design objectives of CONTAIN is to provide reasonable predictions of the containment transient response (physical, chemical and radiological conditions) during the course of severe and design-basis accidents. The CONTAIN code includes atmospheric models for steam and air thermodynamics, intercompartment flows, condensation and evaporation on structures and aerosols, aerosol transport, agglomeration and deposition, and gas combustion. It also includes models for reactor cavity phenomena such as the interaction between concrete and the molten core as well as coolant-pool boiling. Heat conduction in structures, fission-product decay and transport,

termohidravlični in dekontaminacijski učinki varnostnih sistemov so prav tako modelirani.

Pri projektnem dogodku izlivne nezgode se snov (hladivo) in energija sproščata skozi zlom cevi iz reaktorskega hladilnega sistema v zadrževalni hram. Sproščanje poteka med izlivno fazo, ponovnim polnjenjem, poplavljanje sredice in popoplavno fazo. V tej raziskavi je bil program CONTAIN (verzija 1.2) uporabljen za simuliranje odziva zadrževalnega hrama med veliko izlivno nezgodo v hladni veji dvozančnega tlačnovodnega reaktorja vrste Westinghouse. Določeni so bili tlačni in temperaturni odziv ter porazdelitev kapljevitega in parnega hladiva med prvimi 3000 s prehodnega pojava. Prav tako so analizirane energijske bilance.

1 VHODNI MODEL ZADRŽEVALNEGA HRAMA JEDRSKE ELEKTRARNE

1.1 Celice zadrževalnega hrama

CONTAIN je ničrazsežni program, ki obravnava sistem zadrževalnega hrama kot mrežo medsebojno povezanih prostorov ali "celic". V vsaki celici so navzoče tekočine mirujoče in homogene. Vsaka celica lahko pomeni resnični notranji predelek ali skupino predelkov. V nekaterih primerih je primerno razdeliti predelek na več celic zaradi modeliranja pojavov, kakor so naravna konvekcija ali razslojevanje plinov. Celice so medsebojno povezane s pretokom snovi ali prevodom toplote preko vmesnih konstrukcij. CONTAIN je zasnovan za obravnavanje razmeroma majhnega števila celic.

radioactive-decay heating, and thermal-hydraulic and fission product decontamination effects of engineered safety features are also modeled.

In a design-basis event of a loss-of-coolant accident (LOCA), mass (coolant) and energy are released from the reactor coolant system (RCS) through the pipe break to the containment. These releases continue over blowdown, refill, reflood, and post-reflood phases. In this paper, the code CONTAIN (version 1.2) was used to simulate the containment response during a cold-leg large-break (LB) LOCA in a two-loop Westinghouse-type pressurized water reactor (PWR). Pressure and temperature responses, as well as coolant liquid and vapor distributions during the first 3000 s of the transient were calculated. Energy balances were also analyzed.

1 INPUT MODEL OF NUCLEAR POWER PLANT CONTAINMENT

1.1 Containment cells

CONTAIN is a lumped-parameter code, which treats a containment system as a network of interconnected control volumes or "cells". In each cell, fluids are stagnant and homogeneous. The cells represent an actual internal containment compartment or group of compartments. In some cases, a compartment may be partitioned into several cells to model phenomena such as natural convection or gas stratification. The cells communicate with each other by means of the mass flow of material or heat conduction through intermediate heat-transfer structures. CONTAIN is designed to use a relatively small number of cells.

Preglednica 1. *Prostornine in višine celic*
Table 1. *Cell volumes and heights*

Št. No.	Celica Cell	Prostornina Volume m^3	Višina Height m
1	glavni predelek - prva celica main compartment - first cell	19347	63,3
2	medprostor annulus	11122	60,7
3	okolica environment	10^{10}	1000
4	reaktorska votlina reactor cavity	112	13,2
5	predelek severnega uparjalnika north steam generator compartment	1135	23,1
6	predelek južnega uparjalnika south steam generator compartment	1243	26,2
7	predelek tlačnika pressurizer compartment	349	14,0
8	glavni predelek - druga celica main compartment - second cell	19347	63,3

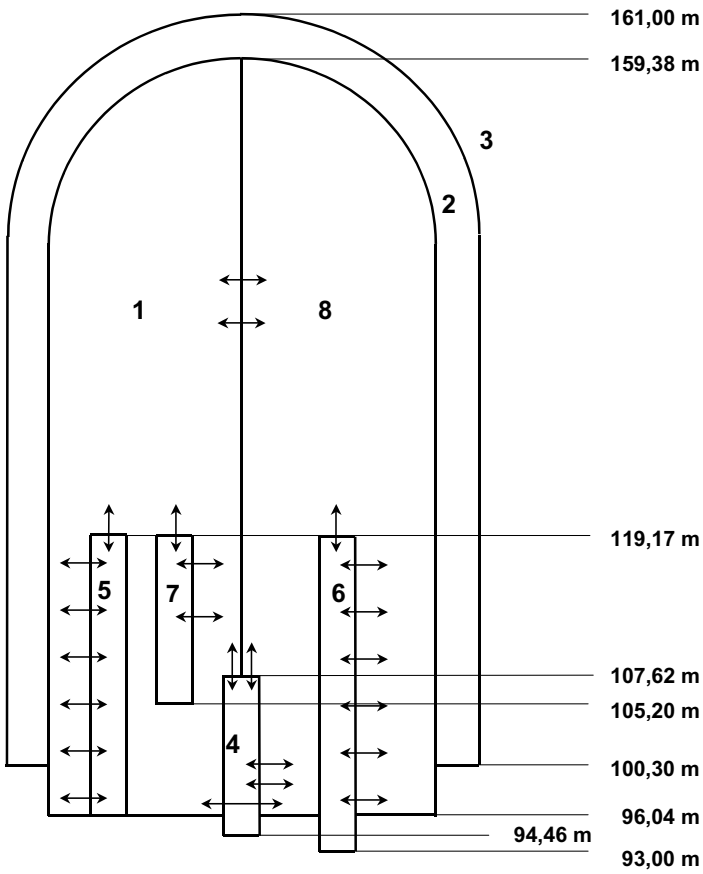

Sl. 1. *Shematični prikaz celic in tokovnih poti modela zadrževalnega hrama (višine se nanašajo samo na celice)*
Fig. 1. *Schematic of containment model cells and flow paths (elevations refer to cells only)*

V tem prispevku je bil uporabljen model zadrževalnega hrama, ki temelji na [3]. Razvoj modela se je začel že v prejšnjih delih ([4] in [5]). Zadrževalni hram je razdeljen takole (slika 1, preglednica 1):

- glavni predelek hrama, ki vključuje kupolo (2 celici),
- kolobarjasti medprostor med jekleno stavbo in zaščitno betonsko stavbo (1 celica),
- reaktorska votlina (1 celica),
- predelka severnega in južnega uparjalnika (1 celica za vsak predelek),
- predelek tlačnika (1 celica).

Okolica je bila prav tako upoštevana kot dodatna celica za modeliranje "izgube" toplote iz zadrževalnega hrama.

Opisana geometrijska razdelitev, čeprav dokaj preprosta, je zadostna za namene sedanje analize. Kakor vidimo iz primera vhodnega modela za jedrsko elektrarno Surry (ZDA) [2], so pri uporabi programa CONTAIN velike razlike med prostorninami posameznih celic običajne.

1.2 Tokovne poti med celicami zadrževalnega hrama

Obravnava tokov med celicami je značilna za ničrazsežni program. Pretok med celicami poteka prek povezav, imenovanih "tokovne poti", ki določajo

In this paper, a containment model based on the model described in [3] was used. The development of the model was started in the course of earlier work ([4] and [5]). The containment is subdivided as follows (fig. 1, table 1):

- containment main compartment, including the dome region (2 cells),
- annulus between containment steel vessel and containment concrete-shield building (1 cell),
- reactor cavity (1 cell),
- north and south steam-generator compartments (1 cell for each compartment),
- pressurizer compartment (1 cell).

The environment was also taken into account as an additional cell to model heat "loss" from the containment.

The presented geometrical configuration, although relatively simple, is sufficient for the purposes of the present analysis. As can be seen from the example input model for the Surry nuclear power plant, USA [2], large differences between the volumes of different cells are common when using the CONTAIN code.

1.2 Flow paths between containment cells

The treatment of intercell flow is typical of a control-volume code. Flow is assumed to occur between cells through junctions, called "flow paths",

izmenjavo snovi in energije med celicami. Tokovne poti ne opravljajo naloge zadrževanja mase: snov, ki se pretaka po tokovni poti, se hipoma prenese v ciljno celico.

Izračun masnega toka skozi tokovno pot temelji na enačbi:

$$\frac{dW}{dt} = \left(\Delta P - C_{FC} \frac{|W|W}{\rho A^2} \right) \frac{A}{L} \quad (1),$$

kjer pomenijo: W - masni tok, t - čas, ΔP- tlačno razliko med povezanima celicama, C_{FC} - koeficient izgub, ρ - gostoto tekočine, A - prerez tokovne poti in L - vztrajnostno dolžino tokovne poti.

Tokovne poti v vhodnem modelu so shematično prikazane na sliki 1. Njihove karakteristike so podane v preglednici 2. Vrednost koeficienta izgub C_{FC} je pri vseh tokovnih poteh enaka 1,0 (glej obravnavo v [6]).

1.3 Toplotne konstrukcije v celicah hrama

Ponori toplote v zadrževalnem hramu lahko prek procesov prenosa toplote in snovi zbirajo precejšnji delež toplotne energije, dovedene v zadrževalni hram med nezgodo, in tako omejujejo obremenitve hrama (tlak in temperaturo ozračja). V CONTAIN-u obstajata dve vrsti ponorov: toplotne

that determine the exchange of mass and energy between the cells. The flow paths are not repositories: the material flowing into a flow path is placed immediately in the downstream cell.

The calculation of the mass flow rate through a flow path is based on the following equation:

where W is the mass flow rate, t is the time, ΔP is the pressure difference between connected cells, C_{FC} is the flow-loss coefficient, ρ is the fluid density, A is the flow-path cross-sectional area and L is the flow-path inertial length.

Flow paths in the input model are shown schematically in fig. 1. Their characteristics are tabulated in table 2. The flow-loss coefficient C_{FC} is equal to 1.0 for all flow paths (see discussion in [6]).

1.3 Heat structures in containment cells

Through heat and mass transfer processes, containment heat sinks can absorb a considerable fraction of the thermal energy introduced into the containment during an accident and thus provide a mitigating effect with respect to the containment loads (atmosphere pressure and temperature). In CON-

Preglednica 2. *Tokovne poti med celicami*
Table 2. *Flow paths between cells*

Št. No.	Od celice From cell	do celice to cell	A m^2	A/L m
1	4	1	0,31	0,0415
2	8	4	0,31	0,0415
3	4	8	1,75	0,270
4	4	8	0,25	0,026
5	1	8	100	1,0
6	8	1	100	1,0
7	1	8	2,0	1,0
8	7	1	1,70	1,266
9	7	1	9,0	6,667
10	1	7	9,0	3,333
11	5	1	6,17	0,068
12	5	1	0,91	0,023
13	5	1	2,36	0,061
14	5	1	0,91	0,021
15	5	1	2,35	0,078
16	5	1	2,25	0,061
17	5	1	14,66	0,800
18	6	8	5,64	0,060
19	6	8	0,91	0,023
20	6	8	2,42	0,066
21	6	8	0,91	0,022
22	6	8	2,35	0,078
23	6	8	2,12	0,066
24	6	8	15,27	0,800

konstrukcije ter plasti spodnjih delov celic (v primeru obravnavanega simuliranja so to bazeni kapljevine in betonska tla). Zaradi njihove pomembnosti je modelirana vrsta procesov prenosa toplote in snovi, to so: naravni in prisilni konvektivni prenos toplote, prenos toplote in snovi pri kondenzaciji, prenos toplote pri uparjanju in prevod toplote.

Pri izračunu konvektivnega prenosa toplote z ozračja celic na toplotne konstrukcije je bilo Nusseltovo število določeno iz naslednje povezave:

TAIN, these sinks are of two main types: heat structures and lower cell layers (liquid pools and concrete floors in the present simulation). Because of their importance, a variety of heat and mass transfer processes are modeled, such as natural and forced convection heat transfer, condensation mass and heat transfer, boiling heat transfer and heat conduction.

When calculating convective heat transfer from the cell atmosphere to heat structures, the Nusselt number was determined from the following correlation:

$$Nu = 0{,}037\, Re^{0,8}\, Pr^{0,33} \qquad (2),$$

kjer so: *Nu* - Nusseltovo število, *Re* - Reynoldsovo število in *Pr* - Prandtlovo število. Reynoldsovo število je v programu CONTAIN določeno iz ustreznih povprečij hitrosti tokov v tokovnih poteh, priključenih na obravnavano celico.

V vhodnem modelu so bile upoštevane naslednje toplotne konstrukcije [3]: valj in kupola jeklene stavbe hrama, valj in kupola zunanje betonske zaščitne stavbe hrama, žerjav, cevovodi, električna in različna oprema, sistemi za gretje, prezračevanje in klimatizacijo, platforme, podloge, kanal za menjavo goriva in notranji beton.

Čeprav lahko resnične toplotne konstrukcije zavzamejo dokaj zapletene oblike, se v programu CONTAIN modelirajo kot krogle, valji ali ravne plošče, ki so lahko navpično ali vodoravno usmerjeni. Poleg tega elementi iz zgoraj naštetih kategorij niso bili modelirani posamično, temveč so bili zbrani v "reprezentativne" konstrukcije. Zaradi poenostavitev namreč, ki so opazne pri modeliranju tokov in termodinamičnih procesov v ozračju hrama, podrobno modeliranje toplotnih konstrukcij ne bi nujno izboljšalo zanesljivosti rezultatov simuliranja.

Toplotne konstrukcije so bile porazdeljene med vsemi celicami modela zadrževalnega hrama. Karakteristike toplotnih konstrukcij (material, geometrijska oblika, debelina) temeljijo na podatkih iz [3].

where *Nu* is the Nusselt number, *Re* is the Reynolds number and *Pr* is the Prandtl number. In the CONTAIN code, the Reynolds number is calculated from appropriate averages of flow velocities in the flow paths connected to the considered cell.

The following heat structures were taken into account in the input model [3]: containment vessel cylinder and dome, shield building cylinder and dome, polar crane, piping, electrical and miscellaneous equipment, HVAC (heating, ventilation and air-conditioning) systems, platforms, embedments, refueling canal and interior concrete.

Although actual heat structures may assume complex shapes, they are modeled in CONTAIN as either spheres, cylinders or slabs, which may assume either vertical or horizontal orientation. In addition, elements from the above-listed categories were not modeled individually, but were grouped into "representative" structures. Due to the inherent simplifications used in the modeling of flows and atmosphere thermodynamics, a detailed modeling of heat structures would not necessarily improve the reliability of the simulation results.

Heat structures were distributed among all the cells of the containment model. The characteristics of heat structures (material, geometry, thickness) are based on data from [3].

1.4 Varnostni sistemi

CONTAIN omogoča tudi modeliranje varnostnih sistemov zadrževalnega hrama: ventilatorskih hladilnikov in prh. Štirje ventilatorski hladilniki in dva sistema prh so bili vključeni v vhodni model (v celicah 1 in 8). V obravnavanem scenariju smo predpisali, da se prhe zadrževalnega hrama sprožijo, ko tlak v hramu doseže 2,06 bar, medtem ko ventilatorski hladilniki delujejo od nastanka zloma.

Pri modeliranju prenosa toplote in snovi med kapljicami iz prh in ozračjem celic je bila uporabljena naslednja povezava za Nusseltovo število:

1.4 Engineered safety features

CONTAIN also allows the modeling of containment engineered safety features: fan coolers and containment sprays. Four fan coolers and two spray systems were included in the input model (in cells 1 and 8). In the present simulation, it was prescribed that containment sprays are initiated when the containment pressure reaches 2.06 bar, whereas fan coolers are assumed to be active from the time when the break occurred.

When modeling heat and mass transfer between spray droplets and cell atmosphere, the following correlation was used for the Nusselt number:

$$Nu = 2{,}0 + 0{,}60\, Re^{1/2}\, Pr^{1/3} \qquad (3),$$

medtem ko je bilo Sherwoodovo število določeno iz naslednje povezave:

whereas the Sherwood number was calculated from the following correlation:

$$Sh = 2{,}0 + 0{,}60\ Re^{1/2}\ Sc^{1/3} \quad (4),$$

kjer sta *Sh* Sherwoodovo število in *Sc* Schmidtovo število.

where *Sh* is the Sherwood number and *Sc* is the Schmidt number.

2 ZAČETNI IN ROBNI POGOJI

2 INITIAL AND BOUNDARY CONDITIONS

2.1 Začetni pogoji

Predpisani začetni tlak v zadrževalnem hramu je bil enak 1,10 bar. Začetna izbrana temperatura atmosfere hrama in toplotnih struktur je bila 322 K, razen pri reaktorski posodi, uparjalnikih in tlačniku, pri katerih je bila začetna temperatura površine enaka 342 K. Zlom se začne pri t = 10 s.

2.1 Initial conditions

The initial pressure in the containment was prescribed to be 1.10 bar. The initial temperature of the containment atmosphere and heat structures was set equal to 322 K, except for the reactor pressure vessel, steam generators and pressurizer, whose initial surface temperature was set equal to 342 K. The break occurs at time t = 10 s.

2.2 Robni pogoji - vir hladiva iz reaktorskega hladilnega sistema

Velika izlivna nezgoda (prvih 1000 s) je bila simulirana ločeno od simuliranja s CONTAIN-om s termohidravličnim računalniškim programom RELAP5/MOD2 [7]. Pri tej nezgodi pride do dvostranskega zloma na hladni veji med reaktorsko posodo in črpalko reaktorskega hladiva. Velikost zloma je enaka 40% celotnega prereza hladne veje. Razpoložljivi so dva sistema za visokotlačno in en sistem za nizkotlačno varnostno vbrizgavanje ter dva zbiralnika.

Masna toka in specifični entalpiji hladiva (vode) z obeh strani zloma so bili vključeni kot viri v vhodni model za CONTAIN (v celico 6). Nedavno so bili razviti programi, ki omogočajo sklapljanje simuliranih procesov v reaktorskem hladilnem sistemu in v zadrževalnem hramu ([8] in [9]). Pri sedanjem delu, vpliv tlaka zadrževalnega hrama na tok skozi zlom iz reaktorskega hladilnega sistema ni bil upoštevan.

Pri veliki izlivni nezgodi se med popoplavno fazo v reaktorskem hladilnem sistemu vzpostavi masno ravnovesje med tokom skozi zlom in vbrizgavanjem sistema za zasilno hlajenje sredice [10]. Za oba vira hladiva (z obeh strani zloma) je bil masni tok skozi zlom med t = 1000 s in t = 3000 s izbran enak povprečni vrednosti med t = 500 s in t = 1000 s. Energijsko ravnovesje v reaktorskem hladilnem sistemu se vzpostavi med vbrizgavanjem hladne kapljevine iz sistema za zasilno hlajenje sredice, dovajanjem toplote iz sredice in odvajanjem tople tekočine skozi zlom. Ker je kapljevina iz sistema za zasilno hlajenje podhlajena in so hitrosti v hladni veji majhne, lahko predpostavimo, da para iz sredice kondenzira v hladni veji ter skozi zlom odteka kapljevina [10].

Rezultati simuliranja s programom RELAP5/MOD2 kažejo, da se tlak v primarnem

2.2 Boundary conditions – coolant source from reactor coolant system

A LB LOCA (first 1000 s) was simulated separately from the CONTAIN simulation with the RELAP5/MOD2 thermal-hydraulic computer code [7]. A double-ended cold-leg guillotine break occurs between the reactor vessel and the reactor coolant pump. The break size is equal to 40% of the full cold-leg cross-section. Two high-pressure safety injection systems, one low-pressure safety injection system and two accumulators are available.

Coolant (water) break mass flow rates and specific enthalpies from both ends of the break were included as sources in the CONTAIN input model (in cell 6). Recently, codes which enable coupling of simulated processes in the RCS and containment have been developed ([8] and [9]). In the present paper, the influence of containment backpressure on break flow from the RCS was not taken into account.

During the post-reflood period of a LB LOCA, an RCS mass balance exists with the break and emergency core-cooling system (ECCS) injection flow rates balanced [10]. For both coolant sources (from both ends of the break), the break mass flow rate between t = 1000 s and t = 3000 s was set equal to the average value between t = 500 s and t = 1000 s. A RCS energy balance is achieved by the injection of cold ECCS liquid, core heat addition, and removal of warm fluid at the break. Since the ECCS liquid is subcooled and the cold-leg velocities are small, we may assume that steam from the core is condensed within the cold leg and liquid flows out of the break [10].

According to the results of the RELAP5/MOD2 simulation, the pressure in the primary system

sistemu ustali na popoplavno vrednost 3,4 bar, ki je dosežena približno pri t = 750 s. Za oba vira je bila vrednost specifične entalpije hladiva pri t = 1000 s izbrana enaka povprečni vrednosti med t = 800 s in t = 1000 s, in entalpiji nasičene kapljevine pri 3,4 bar med t = 1500 s in t = 3000 s. Vrednosti med t = 1000 s in t = 1500 s so bile določene z linearno interpolacijo.

Slika 2 prikazuje skupno maso hladiva, dovedeno iz reaktorskega hladilnega sistema s tokom skozi zlom, medtem ko slika 3 prikazuje pripadajočo skupno dovedeno entalpijo (entalpija nasičene kapljevine je definirana kot 0 J pri temperaturi 273,15 K).

settles to a post-reflood value of about 3.4 bar, which is reached at t = 750 s approximately. For both sources, the value of the coolant specific enthalpy at t = 1000 s was set equal to the average value between t = 800 s and t = 1000 s, and to the liquid saturation enthalpy at 3.4 bar between t = 1500 s and t = 3000 s. Values between t = 1000 s and t = 1500 s were calculated by linear interpolation.

Figure 2 shows the cumulative coolant mass input from the RCS trough break flow, whereas figure 3 shows the corresponding cumulative enthalpy input (the liquid saturation enthalpy is defined as 0 J at 273.15 K).

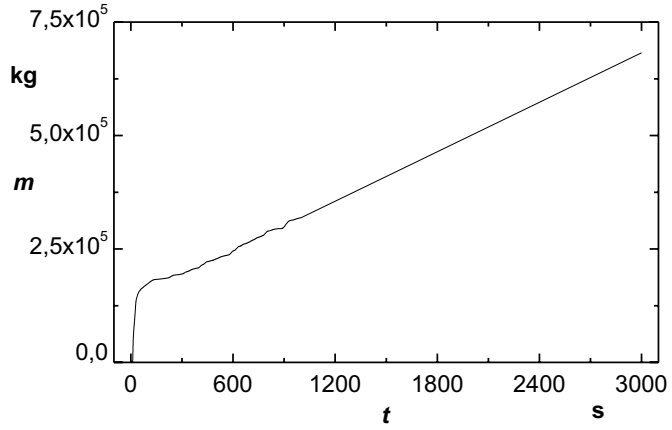

Sl. 2. *Skupna masa hladiva, dovedena s tokom skozi zlom (t - čas, m - masa)*
Fig. 2. *Cumulative coolant mass input through break flow (t - time, m - mass)*

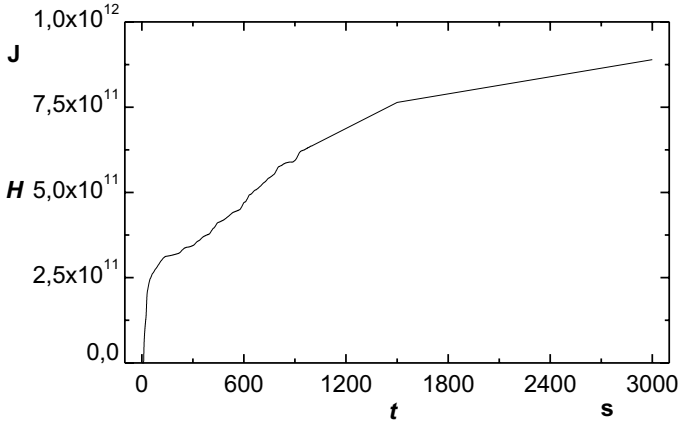

Sl. 3. *Skupna entalpija hladiva, dovedena s tokom skozi zlom (t - čas, H - entalpija)*
Fig. 3. *Cumulative coolant enthalpy input through break flow (t - time, H - enthalpy)*

3 REZULTATI IN RAZPRAVA

Razprava v tem poglavju se nanaša na notranjost jeklene stavbe zadrževanega hrama (brez upoštevanja kolobarjastega medprostora), razen če je navedeno drugače.

3.1 Tlak v ozračju zadrževalnega hrama

Slika 4 prikazuje tlak v ozračju celic zadrževalnega hrama (razlike v tlaku med različnimi celicami so zanemarljive). Takoj po nastanku zloma

3 RESULTS AND DISCUSSION

Unless stated otherwise, the discussion in this section refers to the interior of the containment steel vessel, thus excluding the annulus.

3.1 Pressure in containment atmosphere

Figure 4 shows the pressure of the atmosphere in the containment cells (pressure differences between different cells are negligible).

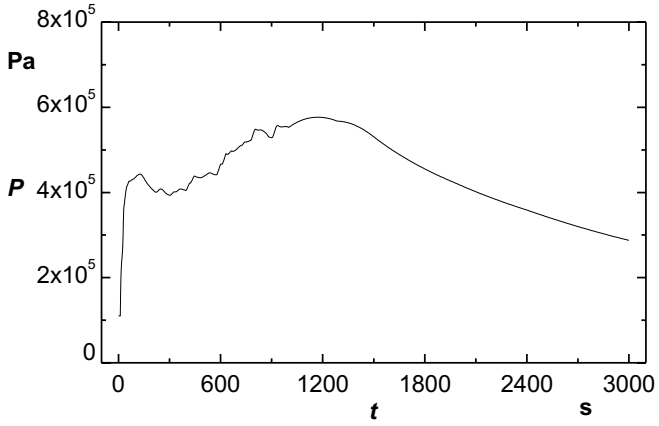

Sl. 4. *Tlak v ozračju celic zadrževalnega hrama (t - čas, P - tlak)*
Fig. 4. *Pressure in containment cells' atmosphere (t - time, P - pressure)*

se tlak skoraj hipoma dvigne, kar je posledica naglega dotoka mase in energije hladiva (sl. 2, 3). Po rahlem znižanju se tlak ponovno zviša. Nihanja tlaka so posledica nihanj pretoka skozi zlom in specifične entalpije. Tlak doseže največjo vrednost 5,8 bar približno v času 1200 s, ko se začne počasi zniževati.

3.2 Temperatura ozračja zadrževalnega hrama

Slika 5 prikazuje temperaturo ozračja v glavnem predelku zadrževalnega hrama (celici 1 in 8), v predelku južnega uparjalnika (celica 6) in v medprostoru (celica 2). Do najvišje temperature (z največjo vrednostjo 430 K) prihaja v celici 6, kjer je postavljen vir hladiva (tok skozi zlom iz reaktorskega hladilnega sistema). Temperatura v glavnem predelku kaže podoben vzorec obnašanja kakor tlak. Temperatura je nekoliko višja v celici 8, ki je povezana s celico 6 prek tokovnih poti. Do zvišanja temperature v medprostoru (celica 2) pride zgolj zaradi prevoda toplote skozi jekleno steno zadrževalnega hrama.

Immediately after the occurrence of the break, the pressure rises sharply, which is due to the sudden inflow of coolant mass and energy (see figs. 2 and 3). After a slight drop, the pressure continues to rise. Pressure oscillations are due to oscillations of break mass flow and specific enthalpy. The pressure reaches a maximum of 5.8 bar at about 1200 s, after which it starts slowly to decrease.

3.2 Temperature in containment atmosphere

Figure 5 shows the atmosphere temperature in the containment main compartment (cells 1 and 8), south steam generator compartment (cell 6) and annulus (cell 2). The highest temperature (with a maximum value of 430 K) occurs in cell 6, where the coolant source (break flow from RCS) is located. The temperature in the main compartment exhibits a similar pattern of behavior to the pressure. The temperature is slightly higher in cell 8, which is connected to cell 6 through flow paths. The temperature rise in the annulus (cell 2) is caused solely by heat transfer through the containment vessel's steel wall.

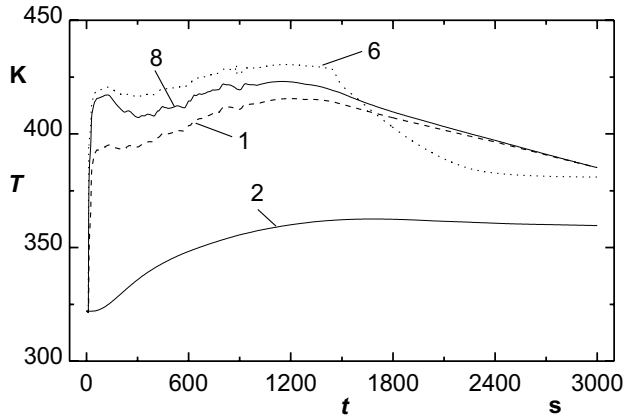

Sl. 5. *Temperatura ozračja v nekaterih celicah zadrževalnega hrama (t - čas, T – temperatura); številke označujejo celice*
Fig. 5. *Atmosphere temperature in some containment cells (t - time, T - temperature); numbers indicate cells*

3.3 Porazdelitev hladiva v zadrževalnem hramu

Hladivo v zadrževalnem hramu izvira predvsem iz dveh virov: toka skozi zlom in prh zadrževalnega hrama. Tok skozi zlom iz reaktorskega hladilnega sistema nastaja iz hladiva, navzočega pred zlomom, in hladiva, vbrizganega prek sistema za zasilno hlajenje sredice. Hladivo iz zbiralnika vode za menjavo goriva je razpoložljivo za sistem za zasilno hlajenje sredice med celotnim simulirnim prehodnim pojavom. Prhe zadrževalnega hrama črpajo hladivo iz zbiralnika vode za menjavo goriva vse do časa 1285 s, ko preidejo na obtočni način in črpajo hladivo iz zbiralnika, ki se nahaja na dnu celice 6.

Kakor lahko vidimo na sliki 6, je masa hladiva, ki je dovedena s tokom skozi zlom v časovnem obdobju od 0 s do 3000 s, približno štirikrat večja od neto dovedene mase prek prh (iz zbiralnika vode za menjavo goriva).

Slika 7 prikazuje porazdelitev hladiva v zadrževalnem hramu. Večina hladiva je v obliki kapljevine v bazenih na dnu celic. Pomemben delež je navzoč v ozračju v obliki pare in razpršene kapljevine, medtem ko je delež, ki se nahaja kot plast kondenzata na toplotnih konstrukcijah, za red velikosti manjši. Vendar lahko pomembnost kondenzacije pare na konstrukcijah opazimo na sliki

3.3 Coolant distribution in containment

Coolant in the containment originates mainly from two sources: break flow and containment sprays. Break flow from the RCS results from coolant present before the break and coolant injected by the ECCS. Coolant from the refueling water storage tank (RWST) is available for the ECCS throughout the simulated transient. Containment sprays draw coolant from the RWST until t = 1285 s when they switch to recirculation mode and draw coolant from the sump, which is located at the bottom of cell 6.

As can be seen in figure 6, the mass of the coolant input through the break flow in the time interval from 0 s to 3000 s is about four times higher than the net mass of coolant input through sprays (from RWST).

Figure 7 shows the coolant distribution in the containment. Most of the coolant is located as liquid in the pools on the cell floors. A significant fraction is present in the atmosphere as vapor and dispersed liquid, whereas the fraction located as condensate film on heat structures is an order of magnitude smaller. However, the importance of vapor condensation on structures can be seen in figure 8,

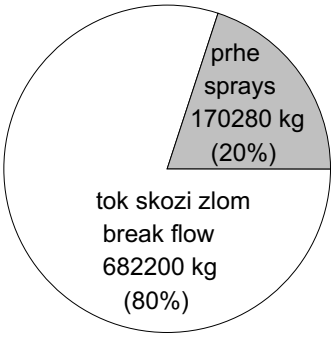

Sl. 6. *Vir hladiva, prisotnega v zadrževalnem hramu v času t = 3000 s*
Fig. 6. *Origin of coolant present in the containment at t = 3000 s*

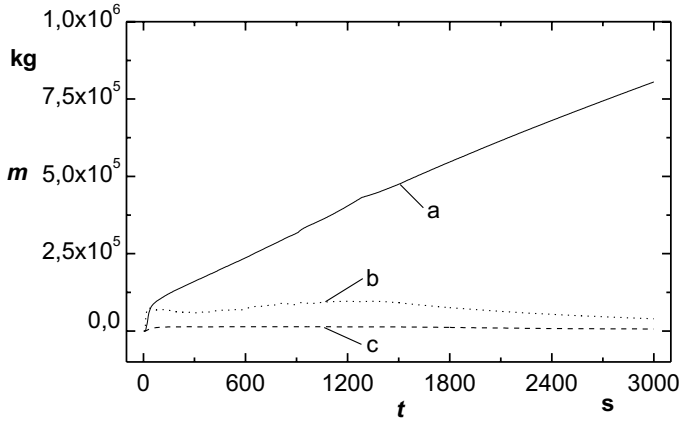

Sl. 7. *Masa hladiva v zadrževalnem hramu (t - čas, m - masa); a - bazeni kapljevine na dnu celic, b - para in kapljevina v ozračju celic, c - kondenzat na toplotnih strukturah*
Fig. 7. *Coolant mass in containment (t - time, m - mass); a - liquid pools on cell floors, b - vapor and liquid in cells' atmosphere, c - condensate on heat structures*

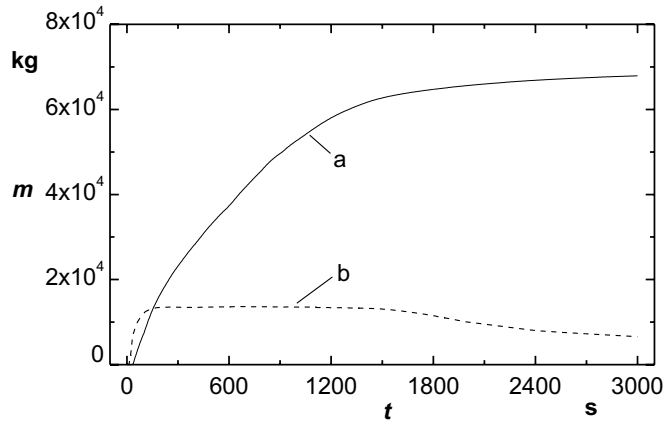

Sl. 8. *Kondenzat hladiva v zadrževalnem hramu (t - čas, m - masa); a - skupna masa kondenzata, ki je odtekel s toplotnih konstrukcij, b - preostali kondenzat na toplotnih konstrukcijah*
Fig. 8. *Coolant condensate in containment (t - time, m - mass); a - cumulative runoff condensate from heat structures, b - remaining condensate on heat structures*

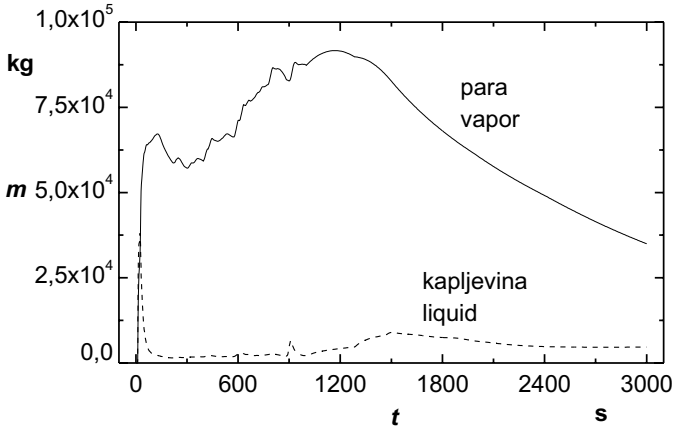

Sl. 9. *Masa hladiva v ozračju celic zadrževalnega hrama (t - čas, m - masa)*
Fig. 9. *Coolant mass in containment cells' atmosphere (t - time, m - mass)*

8, ki kaže, da znatna količina kondenzata odteka v bazene kapljevine.

Slika 9 prikazuje porazdelitev hladiva v ozračju zadrževalnega hrama. Večina hladiva je v obliki pare. Večji del kapljevine, ki priteče v ozračje hrama z velikim masnim tokom mešanice kapljevine in pare skozi zlom med prvimi 20 s nezgode, se zelo hitro usede v bazene na dnu celic.

3.4 Porazdelitev energije v zadrževalnem hramu

V času med 0 s in 3000 s je bila večina entalpije dovedena s tokom skozi zlom in le manjši delež z delovanjem prh zadrževalnega hrama (sl. 10). Glavni cilj omejitvenih ukrepov je odvajanje notranje energije iz ozračja zadrževalnega hrama ter iz celotnega hrama. Večina notranje energije je bila odvedena iz hrama z delovanjem ventilatorskih hladilnikov in le majhen del s prevodom toplote skozi jekleno steno hrama (sl. 11).

Slika 12 prikazuje porazdelitev notranje energije v zadrževalnem hramu v času t = 3000 s. Večji del energije je v toplotnih konstrukcijah in v

which shows that a considerable amount of condensate runs off into liquid pools.

Figure 9 shows the coolant distribution in the containment atmosphere. Most of the coolant is present as vapor. Most of the liquid, which flows into the containment atmosphere with the high liquid-vapor-mixture flow rate during the first 20 s of the accident, drops very quickly into pools on the cell floors.

3.4 Energy distribution in containment

Most of the enthalpy from 0 s to 3000 s was introduced via the break flow and only a small fraction by the action of containment sprays (fig. 10). The main purpose of mitigating actions is to remove internal energy, first from the containment atmosphere, and then from the entire containment. Most of the internal energy was removed from the containment by the action of fan coolers and only a small part by heat conduction through the containment vessel's steel wall (fig. 11).

Figure 12 shows the internal energy distribution in the containment at time t = 3000 s. Most of the energy is contained in the heat structures and the

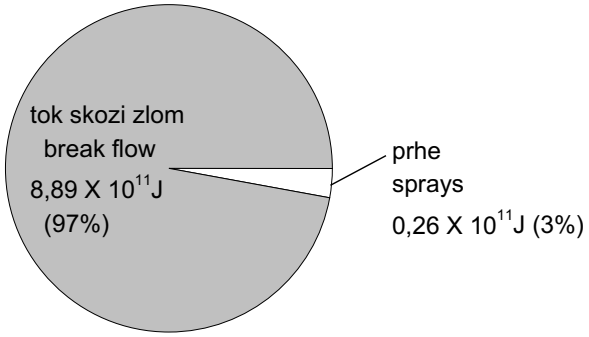

Sl. 10. *Dovedena entalpija v zadrževalni hram od t = 0 s do t = 3000 s*
Fig. 10. *Enthalpy input in containment from t = 0 s to t = 3000 s*

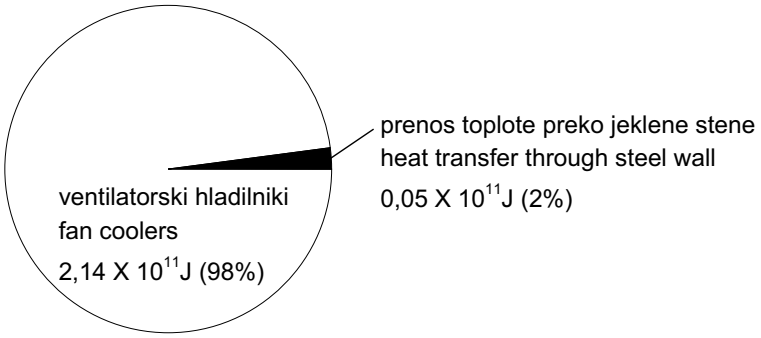

Sl. 11. *Odvedena notranja energija iz zadrževalnega hrama od t = 0 s do t = 3000 s*
Fig. 11. *Internal energy output from the containment from t = 0 s to t = 3000 s*

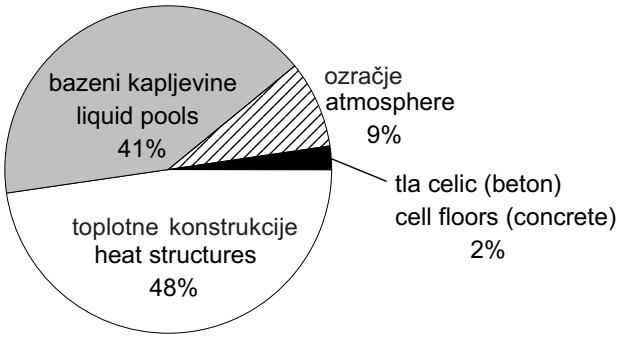

Sl. 12. *Porazdelitev notranje energije v zadrževalnem hramu v času t = 3000 s*
Fig. 12. *Internal energy distribution in the containment at t = 3000 s*

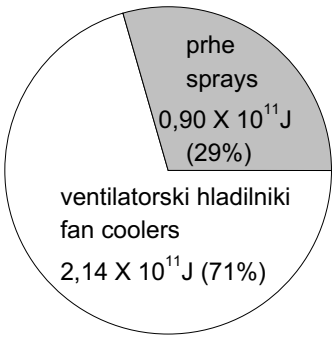

Sl. 13. *Notranja energija, odvedena iz ozračja zadrževalnega hrama s prhami in ventilatorskimi hladilniki od t = 0 s do t = 3000 s*
Fig. 13. *Internal energy removed from containment atmosphere by sprays and fan coolers from t = 0 s to t = 3000 s*

bazenih kapljevine na dnu celic, medtem ko je precej manjši delež v ozračju hrama in betonskih tleh celic. Toplotne konstrukcije in bazeni kapljevine tako prek procesov prenosa toplote in snovi absorbirajo znaten delež dovedene toplotne energije ter na ta način omejujejo obremenitve hrama.

Slika 13 ponuja primerjavo med učinki varnostnih sistemov pri odvajanju notranje energije iz ozračja zadrževalnega hrama. V obdobju med 0 s in 3000 s je bilo več ko dvakrat več energije odvedene z ventilatorskimi hladilniki kakor s prhami zadrževalnega hrama.

4 SKLEPI

S termohidravličnim računalniškim programom CONTAIN so bili simulirani pojavi v zadrževalnem hramu dvozančnega tlačnovodnega reaktorja med prvimi 3000 s velike izlivne nezgode. Rezultati kažejo naslednje:

1. Tlak v ozračju zadrževalnega hrama doseže največjo vrednost 5,8 bar 1200 s po nastanku zloma.
2. Temperatura ozračja zadrževalnega hrama doseže ustrezno največjo vrednost 430 K.
3. Po začetnem izpustu iz reaktorskega hladilnega sistema je večina hladiva v zadrževalnem hramu v bazenih kapljevine, večina hladiva v ozračju pa je navzoča v obliki pare.
4. Toplotne konstrukcije in bazeni kapljevine učinkujejo omejitveno na obremenitve zadrževalnega hrama, ker na koncu simulirnega prehodnega pojava vsebujejo skoraj 90 odstotkov notranje energije.

liquid pools at cell floors, whereas a much smaller fraction is contained in the containment atmosphere and the concrete cell floors. Thus, through heat- and mass-transfer processes, heat structures and liquid pools absorb a considerable fraction of the thermal energy introduced into the containment and provide a mitigating effect with respect to containment loads.

Figure 13 provides a comparison between the effects of engineered safety features in removing the internal energy from the containment atmosphere. In the interval from 0 s to 3000 s, more than twice as much energy was removed by fan coolers than by containment sprays.

4 CONCLUSIONS

Phenomena in the containment of a two-loop pressurized water reactor during the first 3000 s of a large-break loss-of-coolant accident were simulated with the CONTAIN thermal-hydraulic computer code. The results show the following:

1. The pressure in the containment atmosphere attains a maximum value of 5.8 bar 1200 s after the occurrence of the break.
2. The temperature of the containment atmosphere attains a corresponding maximum value of 430 K.
3. After the initial release from the reactor coolant system, most of the coolant in the containment is located in liquid pools and most of the coolant in the containment atmosphere is present as vapor.
4. Heat structures and liquid pools provide a mitigating effect with respect to containment loads as they contain almost 90% of the internal energy at the end of the simulated transient.

5 LITERATURA
5 REFERENCES

[1] Murata, K.K., Carroll, D.E., Washington, K.E., Gelbard, F., Valdez, G.D., Williams, D.C., K.D. Bergeron (1989) User's Manual for CONTAIN 1.1: A computer code for severe nuclear reactor accident containment analysis, NUREG/CR-5026, SAND87-2309, with additions C110O/C110P through C110AF, Sandia National Laboratories, Albuquerque, USA.

[2] Murata, K.K., Williams, D.C., Tills, J., Griffith, R.O., Gido, R.G., Tadios, E.L., Davis, F.J., Martinez, G.M., K.E. Washington (1997) Code Manual for CONTAIN 2.0: A computer code for nuclear reactor containment analysis, SAND97/-1735, NUREG/CR-65, Sandia National Laboratories, Albuquerque, USA.

[3] Westinghouse Energy Systems (1995) Krško nuclear power plant updated safety analysis report.

[4] Kljenak, I. (1998) Low-pressure severe accident scenario simulation with the CONTAIN code, *Transactions of the American Nuclear Society*, 79, 381-382, LaGrange Park, Illinois, USA.

[5] Kljenak I., Parzer I., I. Tiselj (1998) Containment phenomena during a severe accident with reactor vessel failure at low pressure in a two-loop pressurized water reactor, *Proceedings of the 5th Regional Meeting* "*Nuclear energy in Central Europe '98",* Nuclear Society of Slovenia, Ljubljana, Slovenia.

[6] Stamps, D.W. (1998) Analyses of the thermal hydraulics in the NUPEC 1/4-scale model containment experiments, *Nuclear Science and Engineering*, 128, 243-269.

[7] Mavko, B., Stritar, A., A. Prošek (1993) Application of code scaling, applicability and uncertainty methodology to large-break LOCA analysis of two-loop PWR, *Nuclear Engineering and Design*, 143, 95-109.

[8] Smith, K.A., Baratta, A.J., G.E. Robinson (1995) Coupled RELAP5 and CONTAIN accident analysis using PVM, *Nuclear Safety*, 36, 1, 94-108.

[9] Kwon, Y.M., Song, J.H., S.K. Lee (1997) Realistic LB-LOCA containment analysis using a merged version

of RELAP5/CONTEMPT4, *Proceedings, The Fifth International Topical Meeting on Nuclear Thermal Hydraulics, Operations and Safety (NUTHOS-5),* Beijing, China.

[10] Fletcher, C.D., R.A. Callow (1989) Long-term recovery of pressurized water reactors following a large break loss-of-coolant accident, *Nuclear Engineering and Design*, 110, 313-328.

Naslov avtorjev: dr. Ivo Kljenak
prof.dr. Borut Mavko
Institut Jožef Stefan
Odsek za reaktorsko tehniko
Jamova 39
1000 Ljubljana

Authors' Address: Dr. Ivo Kljenak
Prof.Dr. Borut Mavko
Jožef Stefan Institute
Reactor Engineering Division
Jamova 39
1000 Ljubljana, Slovenia

Prejeto:
Received: 1.3.2000

Sprejeto:
Accepted: 2.6.2000

© Strojniški vestnik 46(2000)6, 383-390
ISSN 0039-2480
UDK 658.512.2:378.147
Predhodna objava (1.03)

© Journal of Mechanical Engineering 46(2000)6, 383-390
ISSN 0039-2480
UDC 658.512.2:378.147
Preliminary paper (1.03)

Inteligentni računalniški sistem za pomoč pri poučevanju konstruiranja

An Intelligent Computer System for Supporting Design Education

Marina Novak - Bojan Dolšak

Odločitve, sprejete v procesu konstruiranja, odločilno vplivajo na konkurenčnost izdelka na trgu. Zato sta zelo pomembni kakovost in uspešnost poučevanja konstruiranja na univerzitetnem študiju. V članku je predstavljen potek poučevanja konstruiranja, ki temelji na praktičnem skupinskem delu pri izdelavi projektne naloge. Opisane so težave, s katerimi se pri tem, predvsem zaradi svoje neizkušenosti, srečujejo študenti, in možnosti uporabe metod umetne inteligence za pomoč pri premagovanju teh težav. Podrobneje je opisan inteligentni računalniški sistem, ki naj študentom pomaga oceniti rezultate analize po metodi končnih elementov, jih pravilno razlagati in predstaviti kritična mesta v konstrukciji. Nadalje naj sistem študentom predlaga tudi ustrezne korake za izboljšanje konstrukcije. Za pravilno razumevanje rezultatov numerične analize in izbiro ustreznih konstrukcijskih ukrepov je treba veliko izkušenj in znanja. Obojega študentom primanjkuje, zato je uporaba metod umetne inteligence v tem primeru upravičena in lahko bistveno pripomore k učinkovitejšemu reševanju problemov.

(Ključne besede: konstruiranje, sistemi inteligentni, analize numerične, procesi učenja)

Decisions made in the design process have a significant influence on the competitiveness of a future product in the market. Therefore, the quality and success of design education at the university level is very important. This paper presents the process of design education, based on practical team work on project elaboration with an emphasis on the problems that appear, mostly due to the inexperience of students. The possibilities of applying artificial intelligence to solve these problems more efficiently are also discussed. An intelligent computer system to assist the students in evaluating the results of a finite-element analysis, correctly interpreting them and presenting the critical places in the structure, is described in detail. Moreover, the system should also suggest to the students the appropriate redesign actions to optimise the structure. To be able to properly understand the results of the numerical analysis and consequently choose the appropriate redesign steps, considerable knowledge and experience are required, which students tend not to possess. Thus, the use of artificial intelligence in this particular area makes sense and could help to overcome many problems more efficiently.

(Keywords: design, intelligent systems, numerical analysis, educational processes)

0 UVOD

Konstruiranje pomeni zapleteno in obsežno nalogo, ki ima v času moderne tehnologije zelo pomembno vlogo, saj lahko dandanes le najboljše rešitve prevladajo na tržišču. Glede na to je zelo pomembno, kako so osnovna načela konstruiranja predstavljena študentom in v kolikšni meri študenti spoznajo proces konstruiranja in njegovo obsežnost. Študij procesa konstruiranja na Fakulteti za strojništvo Univerze v Mariboru že nekaj časa poteka na temelju praktične izdelave projekta v majhnih skupinah. Med poukom strojništva študenti pridobijo različna znanja, ki jih morajo uporabiti pri predmetu

0 INTRODUCTION

Design is a very complex and wide-ranging task that has a very important role in modern high technology, where only the best solutions will succeed in the market. It is therefore very important how the fundamental principles of design are presented to students and to what extent the students become aware of the design process and its complexity. For some time the teaching of design at the Faculty of Mechanical Engineering at the University of Maribor has been based mainly on practical team work. Through the mechanical engineering educational process the students obtain a variety of knowledge that

"metode konstruiranja". Namen predmeta o konstruiranju ni le naučiti študente, kako izvesti proces konstruiranja, temveč tudi ugotoviti, ali so, in v kolikšni meri, študenti zmožni rešiti resnični problem iz prakse. Poleg tega želimo pri študentih spodbuditi tudi lastnosti, kakor so iznajdljivost, domiselnost, ustvarjalnost in samozavest. Celoten proces konstruiranja skušamo simulirati z izdelavo projekta v majhnih skupinah. Asistent vodi študente tako, da s sistematičnim delom in z lastnimi zmožnostmi izdelajo izbrani projekt.

Med projektnimi vajami študenti pridobijo znanje o novih metodah in orodjih konstruiranja, ki povečujejo ustvarjalnost in produktivnost ter lahko pomagajo izboljševati kakovost novih izdelkov. Študenti navadno končajo projekt zelo uspešno in so s potekom vaj zelo zadovoljni. Običajno smo nad njihovim znanjem in rezultati presenečeni, saj so zelo ustvarjalni in iznajdljivi. Vendar pa nimajo praktičnih izkušenj, kar je še posebej očitno predvsem v drugi polovici procesa konstruiranja, ko morajo pregledati in oceniti izbrani osnutek konstrukcije. Uporaba metod umetne inteligence v obliki inteligentnega svetovalnega računalniškega sistema bi lahko bila v tem primeru zelo koristna. Prispevek podaja kratek pregled procesa (poučevanja) konstruiranja in nekaj zamisli za uporabo metod umetne inteligence v tem procesu.

1 PROCES (POUKA) KONSTRUIRANJA IN PROJEKT

Projekt se prične z definicijo problema. V našem primeru pouka konstruiranja skupina šestih ali sedmih študentov skupaj z asistentom definira zanimiv problem – projekt, ki še ni bil rešen. Njihova osnovna naloga je najti optimalno tehnično rešitev za novi izdelek [1]. Vloga asistenta je voditi študente skozi sistematični proces in simulirati proces konstruiranja, kakor se ta odvija v praksi. Proces konstruiranja sledi osnovnim zamislim Pahla in Beitza [2], ki izhajajo iz tradicionalnega konstruiranja. Za proces konstruiranja je značilno napredovanje po korakih. Obstajajo štirje osnovni koraki oz. faze procesa konstruiranja: razjasnitev/specifikacija naloge, konstruiranje osnutka, snovanje konstrukcije in razdelava podrobnosti.

Prva faza, specifikacija naloge, ima zelo velik vpliv na zahtevnost novega izdelka in njegovo ekonomsko uspešnost. Študenti, otroci novega časa, imajo običajno različne potrebe, želje ali zahteve in tako veliko zamisli za projekte, še posebej ker niso omejeni s sedanjimi rešitvami.

Iskanje čim več variantnih rešitev problema je glavni cilj naslednje faze – konstruiranja osnutka. Z uporabo novih metod konstruiranja, ki so primerne za skupinsko delo, in v sproščenem, svobodomiselnem ozračju študenti običajno razvijejo veliko število idejnih rešitev problema. Ustvarjalnost in

should be used in a subject named "design principles". The purpose of the design course is not only to teach students how to under take design, but also to ascertain if the students are capable of solving a real-life problem. Moreover, the aim is also to stimulate the students' inventiveness, creativeness and self-confidence. The whole design process is simulated with the practical team work on project elaboration. The teacher should guide the students to use their own abilities to elaborate the project through systematic work.

Through project-based exercises the students acquire modern design methods and tools, which increase creativity and productivity, and can help to improve the quality of new products. The project elaboration for the students is usually very successful and the students are very satisfied with the course of exercises. They usually present knowledge and results, which are unexpected, as they are very creative and innovative. On the other hand, they have lack of experience, which is especially obvious in the second part of the design process, when the students should examine and verify their proposed design solution. The use of artificial-intelligence methods in the form of an intelligent advisory computer system can be very helpful in this case. A short review of the design (education) process and some ideas for applying artificial-intelligence methods within this process are presented in this paper.

1 PROJECT–BASED DESIGN (EDUCATION) PROCESS

A project begins with a problem definition. In our example of design education a small group of six or seven students together with an assistant lecturer define an interesting problem – the project, which has not been solved yet. Their main goal is to find the best possible technical solution for the new product [1]. The lecturer's role is to guide the students through the systematic process and simulate a real-life design process. The design process follows the main ideas of Phal and Beitz [2], based on traditional design. The design progresses in a step-by-step manner. There are four main steps or phases: clarification/specification of the task, conceptual design, embodiment design and detail design.

The first phase, specification of the task, has a great influence on the pretentiousness of the new product and its economic success. The students have a lot of project ideas, and are not handicapped with experience of existing solutions.

Looking for as many solution variants as possible is the main goal in the next phase of the problem – conceptual design. With an open mind and modern design methods, suitable for the group work, the students usually generate a very wide range of solution ideas. The students' inventiveness and

domiselnost študentov sta najbolj zaželeni dejavnosti v fazi konstruiranja osnutka. Rezultat objektivne ocene vseh idejnih rešitev je "optimalna" tehnična rešitev, ki je izhodišče za naslednjo fazo.

V fazi snovanja konstrukcije študenti določijo obliko in načrt novega izdelka. Mimo tega morajo študenti tudi preveriti izbrano različico izdelka. Študenti korakoma razvijajo tehnično rešitev izdelka. V številnih korakih, na podlagi analize in sinteze, vedno znova spreminjajo in dopolnjujejo trenutno verzijo izdelka.

Končni videz konstrukcije je osnova za izdelavo načrtov in druge dokumentacije za proizvodnjo, ki jo študenti izdelajo v zadnji fazi – razdelavi podrobnosti. Predstavljen postopek konstruiranja je prikazan na sliki 1.

creativity are the most welcome activities in the conceptual design phase. The "optimal" solution variant of the design is selected by an objective evaluation.

In the next phase - embodiment design, the students determine the design layout and the form of the new product. In addition, they should also verify the selected variant of the design. Step by step, the students develop a technical product. During many corrective steps, using analysis and synthesis, they constantly alternate and complement each preliminary layout.

The final design is a basis for all drawings and other production documents that are made in the last, detailed, design phase. The presented design process is shown in Figure 1.

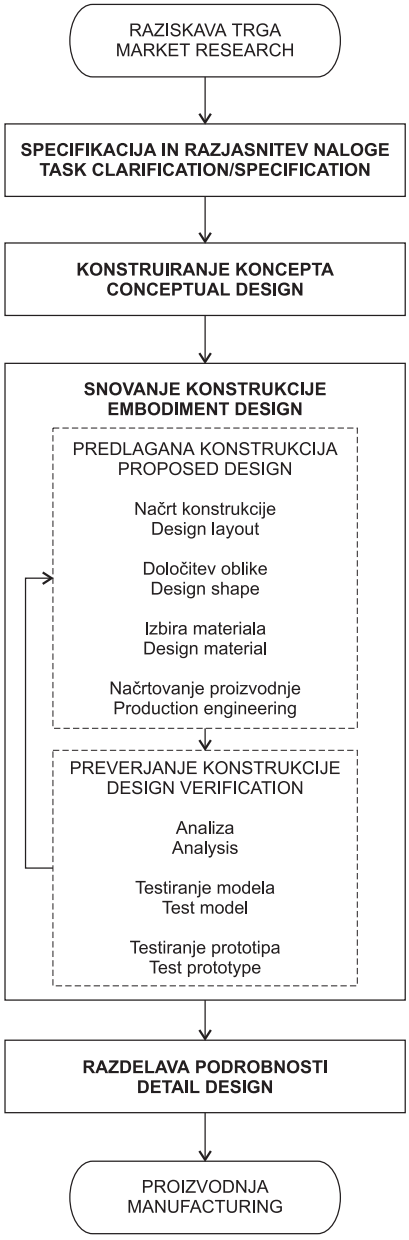

Sl. 1. *Glavne faze postopka konstruiranja*
Fig. 1. *The main phases in the design process*

Postopek spreminjanja, izboljšanja konstrukcije v fazi snovanja terja od študentov veliko znanja o mehaniki, sestavah in tehnologiji materialov. Pomanjkanje izkušenj je zelo pogosto. Kljub temu pa so študenti zmožni razviti kar dobre konstrukcije. Širok ustvarjalni duh, brez zadržkov, ki jih imajo običajno bolj izkušeni konstrukterji, omogoča študentom, da razvijejo konstrukcije zanimivih oblik in izvedb. Izbira ustreznega materiala je zanje že nekoliko težja naloga.

Prvi večji uspeh za študente pomeni predlagana izvedba novega izdelka. Ali je predlagana konstrukcija preveč, ali premalo dimenzionirana, pa žal študenti zaradi pomanjkanja izkušenj ne vedo. Če je konstrukcija predimenzionirana, je lahko pretežka ali predraga. V primeru premalo dimenzionirane konstrukcije pa obstaja verjetnost porušitve pri uporabi. Zato morajo študenti predlagano konstrukcijo preveriti.

Dandanes od študentov pričakujemo, da uporabljajo moderna orodja, to so sistemi za računalniško podprto konstruiranje (RPK - CAD). Modeliranje predlagane konstrukcije je običajno zelo učinkovito. Obstoječi geometrijski oblikovalniki so uporabniško zelo prijazni. Študenti z navdušenjem uporabljajo pripomočke, kakor so: premikanje, rotiranje, senčenje, sestavljanje itn. Razmere v konstrukciji med njeno uporabo lahko simuliramo in preverjamo z uporabo analize po metodi končnih elementov (MKE), ki je običajno del sistema RPK. MKE je najbolj pogosto uporabljena numerična metoda za analize napetosti in deformacij v fizikalnih sestavah. V bistvu te analize omogočajo študentom, da bolje razumejo obnašanje konstrukcije in jim dajejo smernice za optimizacijo konstrukcije. Vendar študenti običajno ne poznajo osnovnih načel MKE. Poleg tega so neizkušeni. Zaradi tega morajo rešiti številne probleme preden definirajo končno izvedbo konstrukcije. Najprej imajo študenti težave s pripravo mreže končnih elementov, ki predstavlja idealiziran model dejanske konstrukcije. Naslednji problem predstavlja ustrezna razlaga rezultatov analize. In nazadnje, študenti ne vedo, kateri ukrepi in spremembe konstrukcije so nujni in bodo zadovoljili dane zahteve.

Večino teh problemov bi lahko bolje obvladovali z uporabo inteligentnega svetovalnega sistema za podporo pri ključnih odločitvah pri procesu analize konstrukcije [3]. Prvi modul predlaganega sistema, ekspertni sistem za pomoč pri gradnji mreže končnih elementov, je že bil razvit v našem laboratoriju ([4] in [5]). Šolsko verzijo tega sistema poskusno uporabljamo na naši fakulteti, predvsem v pedagoške namene. Danes nekateri programski paketi MKE že vsebujejo bolj ali manj inteligentne module, ki vodijo neizkušenega uporabnika skozi proces analize. Ob podpori visoke tehnologije računalniške grafike večina paketov

The improving process, or redesign, in the embodiment design phase, demands from the students a lot of knowledge about the principles of mechanics, structures and materials technology. A lack of experiences is very common, however, they are able to define quite good designs. With a lot of imagination and not so many restrictions as the more experienced designers usually have, they create interesting design shapes and forms. But the definition of a proper material is a more difficult task for them.

The proposed design of the new product is the first big success for the students. However, as they are inexperienced, they do not know whether their proposed design is over- or under-sized. In the case of the design being over-sized it can be too heavy or too expensive. On the other hand, an under-sized structure can break during use. Therefore, it is necessary for the students to verify the proposed design.

Nowadays, it is expected that the students will use modern tools like Computer Aided Design (CAD) systems. Modelling of the proposed design is mostly very efficient. The existing geometric modellers are very user friendly. The students use facilities like moving, rotating, shading, assembly, etc. with enthusiasm. Simulation and verification of the conditions within the structure during its exploitation can be performed with the Finite Element Method (FEM), which usually forms part of the CAD system. FEM is the most frequently used numerical method to analyse stresses and deformations in physical structures. Indeed, the analysis can provide the students with a greater understanding of how a structure behaves and give them guidelines for the optimisation of the design. However, the students do not understand very well, the basic principles of FEM; they are also inexperienced. Consequently, they should solve a lot of problems on the way to the adequate design definition. First of all, they do not have experiences in how to prepare the appropriate finite-element mesh model – the idealised real design. The next problem is the adequate interpretation of the analysis' results. And finally, the students do not know what actions and which changes to the design are necessary to satisfy the given criteria.

Most of these problems can be overcome with the use of an intelligent advisory system for overall support to the key decisions within the analysis process [3]. The first module of the proposed system, an expert system for intelligent finite-element mesh design has already been developed in our laboratory ([4] and [5]). The academic version of it is already in experimental use at our faculty, mostly for educational purposes. At the present time, some of the FEM packages already have more-or-less intelligent modules for guiding inexperienced users through the analysis process. Supported by high computer graphics technology they also offer a very good

omogoča tudi zelo dober grafični prikaz. Kljub temu pa to ni dovolj učinkovito. Študenti potrebujejo tudi navodila, ki izhajajo iz izkušenj. Namen našega raziskovalnega dela v prihodnje je odkriti znanje, ki izhaja iz izkušenj in ga vključiti v inteligentni računalniški sistem.

2 OPTIMIZACIJA OBLIKE KONSTRUKCIJE

Grafični prikaz rezultatov numerične analize ponazarja porazdelitev, obliko in velikost deformacij in napetosti v konstrukciji. Na podlagi takšne predstavitve, mora konstrukter/študent ugotoviti, ali konstrukcija izpolnjuje zahteve, oziroma kateri so tisti konstrukcijski koraki, s katerimi je mogoče konstrukcijo izboljšati. To je zelo zahteven in pomemben del procesa konstruiranja. Izbira drugačnega materiala je običajno najlaže izvedljiva sprememba, ki pa žal ni vedno uspešna. Izbira boljšega (dražjega) materiala je velikokrat tudi ekonomsko neupravičena. Zaradi pomanjkanja praktičnih izkušenj študenti običajno uporabljajo teoretično znanje in iščejo pomoč pri izkušenih konstrukterjih – ekspertih. Slika 2 prikazuje primer predlagane konstrukcijske rešitve in možnosti za njeno optimizacijo.

Odveč je poudarjati, da je običajno mogočih več različnih konstrukcijskih korakov za izboljšanje konstrukcije. Izbira koraka je odvisna od zahtev, možnosti in tudi želja. Računalniški sistem, ki bi vseboval znanje o spreminjanju konstrukcij in bi lahko svetoval ter razlagal ustrezne konstrukcijske spremembe, bi bil v veliko pomoč. Zato obstaja velika utemeljitev za razvoj in vključitev takšnega inteligentnega sistema v izobraževalni proces.

3 INTELIGENTNI SISTEM ZA OPTIMIZACIJO KONSTRUKCIJ

V tehnični praksi je izvedba optimalne konstrukcije v prvem poskusu zelo redka. Konstruiranje je ponavljajoč se proces. Število potrebnih ponovitev je odvisno predvsem od kakovosti začetnega predloga konstrukcije in ustreznosti kasnejših konstrukcijskih sprememb. Kakovost in pravilnost izbrane spremembe konstrukcije sta odvisni od znanja in izkušenj. Razvoj inteligentnega sistema za pomoč pri poučevanju konstruiranja načrtuje zapis znanja in izkušenj, potrebnih za kakovostno spreminjanje konstrukcij, v obliki, ki jo lahko uporablja računalniški sistem.

Nedvomno bo razvoj predlaganega inteligentnega sistema pomenil zapleteno in zahtevno raziskovalno nalogo. Najprej je treba definirati vhodne podatke. Poleg danih kriterijev, zahtev in vseh osnovnih parametrov o samem problemu: geometrijske oblike, obremenitev in robnih pogojev, bodo vhodni podatki vsebovali tudi rezultate analize

graphical presentation. Nevertheless, this is not enough for the students, who also need instructions, which come from experience. The aim of our future research is to discover the knowledge in the form of experience and include it in the intelligent computer system.

2 OPTIMISING PROCESS – REDESIGN

Graphical representation of numerical analysis' results represents a distribution, the form and size of displacements and stresses within the structure. With that kind of representation the designer/student should confirm that the structure meets the requirements or choose the appropriate design steps to improve the initial design. This is a very difficult and important part of the design process. Selecting a different material is usually the easiest way to change the structure, but this is not always successful. Moreover, selecting a better (more expensive) material is often economically unjustified. Due to a lack of practical experience students mostly use theoretical knowledge and look for help from experienced designers – experts. Figure 2 presents an example of the proposed initial design and possibilities for optimisation – redesign.

Usually, several different redesign steps are possible for improving the design. The choice of redesign action depends on the requirements, possibilities and also on wishes. A computer system with encoded redesign knowledge, that could advise and explain the appropriate redesign actions, would be very helpful. For this reason, there exists a great motivation to develop such an intelligent redesign system and include it in the education process.

3 INTELLIGENT REDESIGN SYSTEM

An optimal design achieved at the first attempt is very rare in engineering. Design is an iterative process. The number of iterations/cycles needed mostly depends on the quality of the initial design and adequacy of the redesign actions. The quality and correctness of a selected redesign action are dependent on knowledge and experience. The development of an intelligent system for supporting design education anticipates the encoding of the knowledge and experiences required for quality redesign in a form that could be used by a computer system.

Undoubtedly, the development of the proposed intelligent system will be a complex and exacting research task. First of all, we should define the input data. Beside given criteria, demands and all basic parameters about the problem in terms of geometry, loads and boundary conditions, the input data will include the results of the FEM analysis. The investigation of the analysis' results should be per-

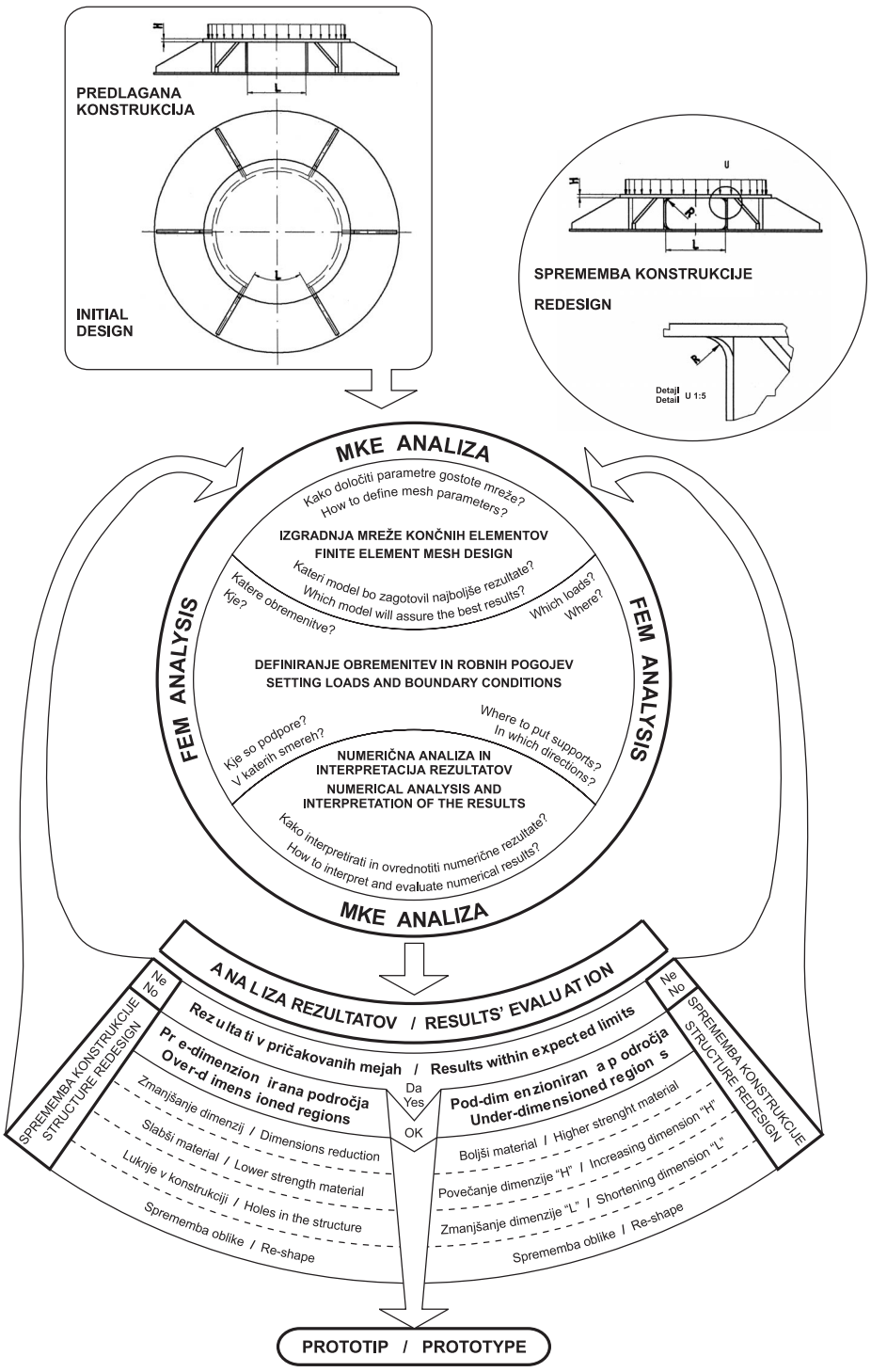

Sl. 2. *Predlagana konstrukcija in ustrezni nadaljnji konstrukcijski koraki*
Fig. 2. *Initial design and appropriate further design actions*

MKE. Prav obravnava rezultatov analize mora biti izvedena skrbno in temeljito, saj lahko le pravilna razlaga rezultatov zagotovi ustrezno izbiro potrebnih sprememb konstrukcije. Pojavi se tudi vprašanje, kako ločiti in prenesti najpomembnejše rezultate (kritična mesta) iz zapletene in obsežne datoteke v inteligentni sistem in kakšno obliko zapisa uporabiti. Preučiti moramo vse teoretično in praktično znanje

formed fully and carefully. Only a correct interpretation of the results can ensure the accurate selection of redesign actions. Another question is how to separate and transfer the important part of the numerical results (critical places) from a complex and extensive file to the intelligent system and which form should be used. We should also study all theoretical and practical knowledge about redesign. An examina-

o spreminjanju konstrukcij. Zelo uporabna bo raziskava sedanjih poročil o izvedenih konstrukcijskih spremembah. V tem primeru bi lahko uporabili avtomatično učenje kot zelo uporabno metodo za gradnjo baze znanja. Veliko praktičnega znanja lahko pridobimo tudi z intervjuji ekspertov. Intervjuji in proučevanje poročil o konstrukcijskih spremembah so odvisni od sodelovanja različnih strokovnjakov in lahko trajajo precej časa. Sledilo bo oblikovanje pravil, ki bodo predstavljala 'osvojeno' znanje in izkušnje. Največjo nevarnost v načrtu razvoja sistema pomeni obsežnost procesa konstruiranja, saj bi kaj lahko zašli s poti. Glede na vse to bi bilo dobro, da se vsaj na začetku omejimo na temeljni in tipični konstrukcijski proces, kakor je to primer tudi pri poučevanju. Razširitev sedanjega sistema na širše področje uporabe ne bi smelo delati težav.

Slika 3 prikazuje osnovno arhitekturo predlaganega inteligentnega, ekspertnega sistema za pomoč pri poučevanju konstruiranja.

tion of the existing old redesign elaborates will be very useful. In this case, we could use machine learning as a very useful method for building a knowledge base. A lot of practical knowledge can be acquired by interviewing experts. Interviewing and investigating the old redesign elaborates is conditional on the co-operation of several experts and can be time-consuming. After that, we should find out the rules for the presentation of the knowledge and experiences acquired. The complexity of the design process is the weakest part in the system development plan, as we could easily lose the way. Considering this, we should, at least at the start, limit our research to the elementary and typical design process, which is also the case at the beginning of the educational process. It should not be a problem to extend the existing system to a wider area of application.

Figure 3 shows the basic architecture of the proposed intelligent knowledge-based system for supporting design education.

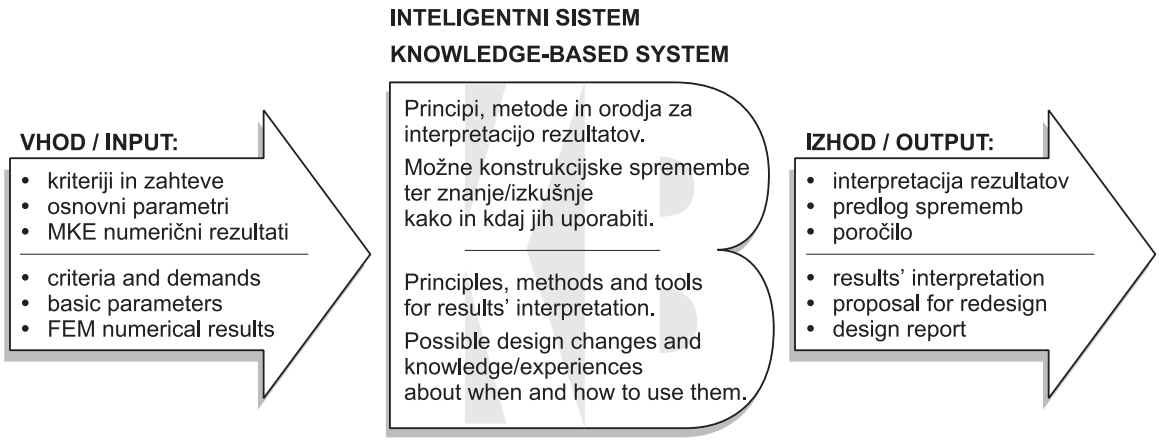

Sl. 3. *Inteligentni sistem za optimizacijo konstrukcij*
Fig. 3. *Intelligent redesign system*

4 SKLEP

Ideja o inteligentnem računalniškem sistemu za optimizacijo konstrukcij je rezultat izkušenj, pridobljenih med poučevanjem procesa konstruiranja in predhodnega razvoja inteligentnega sistema za gradnjo mreže končnih elementov. Namen našega raziskovalnega dela v prihodnje je razviti sistem, ki bo lahko uporabniku/študentu v pomoč pri ocenitvi rezultatov analize po MKE, njihovi razlagi in predstavitvi kritičnih mest v konstrukciji. Na koncu mora sistem študentom predlagati tudi ustrezne korake za izboljšanje konstrukcije. Pri tem je treba upoštevati premalo pa tudi preveč dimenzionirana področja konstrukcije.

Trenutno proučujemo rezultate analiz MKE ter vpliv določenih sprememb konstrukcij. Hkrati poskušamo najti ustrezne primere osnovnih začetnih konstrukcij. Menimo, da bo predstavljeni inteligentni sistem zelo uporaben pri študiju procesa

4 CONCLUSION

The idea of an intelligent redesign computer system is the result of experiences acquired through the design education process and the previous development of intelligent systems for finite-element mesh design. The aim of our future research work is to develop a system, which will be able to help the user/student to evaluate the results of FEM analysis, correctly interpret them and present the critical places in the structure. At the end, the system should also suggest to the students the appropriate redesign actions to optimise the structure. The system should consider under-dimensioned as well as over-dimensioned places in the structure.

At present, we have examined results of the FEM analyses and the influence of some redesign actions. We have also tried to find convenient examples of elementary initial design. We believe the intelligent system application will be very useful in

konstruiranja. Lastnost ekspertnih sistemov, ki so z odgovori na vprašanja: 'Kako?' in 'Zakaj?' zmožni pojasnjevati delovanje mehanizma sklepanja, je še posebej dobrodošla, saj lahko študentom omogoči pridobivanje novih znanj. Še več, uporaba predlaganega sistema bi bila gotovo dobrodošla tudi pri konstruiranju v praksi.

the design-education process. The ability of the knowledge-based systems that explain the inference process by answering the questions "How" and "Why" could be especially welcome, as it can enable the students to acquire some new knowledge. Moreover, the use of the proposed system would certainly be welcome in the practical design process too.

5 LITERATURA
5 REFERENCES

[1] Novak, M., B. Dolšak (1998) Project-based design learning, *Proceedings of the International Workshop PDE Pedagogics in Design Education*, Pilsen, Czech Republic, 7 strani.

[2] Pahl, G., W. Beitz (1996) Engineering Design – A systematic approach, *Springer Verlag*.

[3] Dolšak, B., Novak, M., A. Jezernik. (1997) Expert systems in design, *Proceedings of the Third International Conference: Design to Manufacture in Modern Industry (Edited by Jezernik, A. & Dolšak, B.)*, Portorož, Slovenia, Faculty of Mechanical Engineering, Maribor.

[4] Dolšak, B., A. Jezernik (1998) A Rule-Based Expert System for Finite Element Mesh Design, *Proceedings of the 5th International Design Conference - DESIGN'98 (Edited by Marjanović, D.)* – Dubrovnik.

[5] Dolšak, B., Bratko, I., A. Jezernik (1998) Application of Machine Learning in Finite Element Computation, *Machine Learning, Data Mining and Knowledge Discovery: Methods and Applications (Edited by R.R. Michalski, I. Bratko and M. Kubat), John Wiley & Sons*.

Naslov avtorjev: mag. Marina Novak
doc.dr. Bojan Dolšak
Fakulteta za strojništvo
Univerze v Mariboru
Smetanova 17
2000 Maribor

Authors' Address: Mag. Marina Novak
Doc.Dr. Bojan Dolšak
Faculty of Mechanical Engineering
University of Maribor
Smetanova 17
2000 Maribor, Slovenia

Prejeto: 10.1.2000
Received:

Sprejeto: 2.6.2000
Accepted:

Strokovna literatura
Professional Literature

Nove knjige

Springer for Science, AM Ijmuiden

Astashev, V.K., Babitsk, V.I., Kolovsky, M.Z.: Dynamics and Control of Machines, 233 str. 169 DEM;

Alfutov, N.A.: Stability of Elastic Structure, 337 str., 169 DEM;

Kovaleva, A.: Optimal Control of Mechanical Oscillations, 264 str., 129 DEM;

Guz, A.N.: Fundamentals of the Three-Dimensional Theory of Stability of Deformable Bodies, 557 str., 279 DEM;

Babitsky, JV.I.: Theory of Vibro-Impact Systems and Applications, 318 str, 169 DEM;

Kolovsky, M.Z.: Nonlinear Dynamics of Active and passive Systems of Vibration Protection, 426 str., 189 DEM;

Morozov, N., Petrov, Y.: Dynamics of Fracture, 98 str., 89 DEM;

Berthelot, J.-M.: Composite Materials, 645 str., 298 DEM;

Fischer-Cripps, A.C.: Introduction to Contact Mechanics, 225 str., 159 DEM;

Basar, Y., Weichert, D.: Nonlinear continuum mechanics of solids, 198 str., 98 DEM;

Awrejcewicz, J., Andrianov, I.V., Manevitch, L.I.: Asymptotic Approaches in Nonlinear Dynamics, 310 str., 128 DEM;

Findeisen, D.: System Dynamics and Mechanical Vibrations, ca. 400 str., 179 DEM;

Haupt, P.: Continuum Mechanics and Theory of Materials, 583 str., 139 DEM;

Kapitaniak, T.: Chaos for Engineers, 2nd edition, 142 str., 59 DEM;

Mylvaganam, K.S.: Ultrasonic Gas Flowmeters, ca. 200 str., 128 DEM;

Arcoumanis, C.: Flow and Combustion in Automotive Engines, ca. 350 str., ca. 168 DEM;

Schmid, P., Henningson, D.S.: Stability and Transition in Shear flows, ca. 575 str., 159 DEM;

Schlichting, H., Gersten, K.: Boundary-Layer Theory, 799 str., 179 DEM;

John Wiley & Sons Limited, Chichester

Steinberg, D.: Vibration Analysis for Electronic Equipment (3rd Edition). Ca. 400 str., 71,50 GBP.

Fletcher, R.: Practical Metohods of Optimization (2nd Edition). Ca. 450 str., 34,95 GBP.

Michalski, L., Eckersdorf, K., Kucharski, J., McGHEE, J.: Temperature Measurement (2nd Edition). Ca. 478 str., 100,00 GBP.

Cross, N.: Engineering Design Methods; Strategies for Product Design (3rd Edition). Ca. 230 str., 24,95 GBP.

Figliola, R. and Beasley, D.: Theory and Design for Mechanical Measurements (3rd Edition). Ca. 600 str., 32,50 GBP.

Iz revij

IZ DOMAČIH REVIJ

EGES, Energetika, gospodarstvo in ekologija skupaj, Ljubljana

2000, 2

Odzračevanje in odplinjevanje sistemov za ogrevanje

Jovanovič, S.: Enocevni sistem toplovodnega ogrevanja, 2. del, Primer iz prakse

Kac, B.: Kondenzacijski kotli

Čretnik, J.: Sistemi za izvajanje trajnih meritev emisije

Les, Ljubljana

2000, 5

Papotnik, A.: Projektna naloga za tehniko in tehnologijo

2000, 6

Zbašnik-Senegačnik, M.: Kriteriji za vrednotenje montažnih hiš

Zupančič Strojan, T.: Kriteriji za analiziranje, vrednotenje in načrtovanje montažne gradnje

Obzornik za matematiko in fiziko, Ljubljana

2000, 2

Založnik, A.: O valčkih, prvič

2000, 3

Vidav, I.: Sprehod po matematiki: Od delitve dediščine do avtomorfnih funkcij

Jeromen, A., Trontelj, Z.: Termoakustični hladilnik in hladilnik s pulzno cevjo

Organizacija, Maribor, Kranj

2000, 5

Jereb, E.: Rajkovič, V.: Izbira delavcev za teledelo s pomočjo ekspertnega sistema

Sporočila Urada za standardizacijo in meroslovje, Ljubljana
2000, 4
Tasič, T.: Programska oprema v zakonskem meroslovju
Zalar, B.: Standardi za ravnanje z okoljem

2000, 5
Zalar, B.: Pomen standardov za embalažo pri varovanju okolja

Vakuumist, Ljubljana
2000, 4
Kek, D., Pejovnik, S.: Vpliv faznih mej na električne lastnosti keramičnih gorivnih celic
Povh, B.: Vakuumska molekularna destilacija (3. del)
Čekada, M.: Primerjava metod merjenja debeline tankih plasti

Varilna tehnika, Ljubljana
2000, 1
Kramar, J., Jezeršek, M.: Uporabnost elastoplastične analize pri proučevanju varjenih spojev

IZ TUJIH REVIJ

CDA
Condizionamento dell'aria Riscaldamento Refrigerazione, Milano
2000, 4
Alfano, G., D'Ambrosio, F.R., Riccio, G.: Misure di temperatura equivalente
Sherman, M.: Indoor air quality per edifici residenziali

2000, 5
Beccali, M., Cellura, M., Giaconia, c., Lo Brano, V., Orioli, A.: Il software TH.EL.D.A., La trasmissione del calore in regime vario nelle pareti multistrato

HLH
Heizung Lüftung/Klima Haustechnik, Düsseldorf
2000, 5
Hartmann, M.: Entwicklungsstand der thermostatischen Einzelraumregelung
Hanning, H., Brennwertgeräte für herkömmliche Schornsteine

MEMOIRS, Kobe
Fukusumi, T., Fujiwara, S.: geometrical nonlinear Analysis of Hyperbolic-Paraboloid Structure with Pin Joints
Sakagami, K., Morimoto, M.: Effect of vibration on the acoustic properties of porous absorbent layers

Travail & Sécurité, Paris
2000, No 593
Un nouveau chapeau pour les bouteilles de gaz

Ocene knjig

P. Kairies: Direktmarketing für technische Produkte und Dienstleistungen

Zal.: Expert Verlag, GmbH, Renningen-Malmsheim 1999.
Obseg: format 15 x 21 cm, 149 strani, 41 slik in 13 preglednic.
Cena je 48 DEM.

Knjiga pokaže, kako je mogoče z uvedbo novih metod neposrednega trženja doseči dobre rezultate prodaje izdelkov.

Prvo poglavje govori o pomenu neposrednega trženja izdelkov in pogojih za njegovo uvedbo. Sledi poglavje o skupinsko usmerjenih dejavnostih neposrednega trženja in segmentiranju ciljev podjetja. Posebna pozornost je dana načinu zbiranja informacij o lastnih izdelkih in kupcih izdelkov ter načinu gradnje baze podatkov. Podrobno so opisane metode komuniciranja podjetja s kupci (osebni razgovori, preskok zaprek, dialog, argumenti). Zadnje poglavje govori o korakih načrtovanja in izvedbe dejavnosti neposrednega trženja.

Knjiga je namenjena vodjem gospodarske propagande, vodjem trženja in prodaje ter študentom proizvodnega strojništva.

M. Starbek

W. Dreger: Management der Kundenzufriedenheit

Zal.: Expert Verlag, GmbH, Renningen-Malmsheim 1999.
Obseg: format 15 x 21 cm, 312 strani, 112 slik.
Cena je 79 DEM.

Uvodno poglavje obravnava problematiko zadovoljstva kupcev in daje pregled nalog, ki jih je treba rešiti, da dosežemo zadovoljstvo kupcev. Podrobno je opisan postopek obravnave pritožb in reklamacij kupcev in način njihovega reševanja.

Posebno poglavje je namenjeno novim načinom organiziranja podjetij s poudarkom na oblikovanju profitnih centrov ob upoštevanju pravil vitke organizacije. Na zadovoljstvo kupcev ima velik

vpliv osebje podjetja in zato eno od poglavij govori o kvalifikaciji, motivaciji in vodenju osebja podjetja.

Zadnje poglavje obravnava problematiko primerjave opazovanega podjetja s konkurenco, in to glede na zadovoljstvo kupcev. Podrobno je opisan postopek, kako postati najboljši.

Knjiga je namenjena vodjem oddelkov podjetja in študentom univerzitetnega študija proizvodnega strojništva.

M. Kos

G.H. Schlick: Projektmanagement – Gruppen-prozesse - Teamarbeit

Zal.: Expert Verlag, GmbH, Renningen-Malmsheim 1999.
Obseg: format 15 x 21 cm, 417 strani.
Cena je 74 DEM.

Uvodno poglavje govori o razumevanju in oblikovanju procesov ter problematiki oblikovanja in vodenja delovnih skupin oziroma projektnih skupin. Posebno poglavje je namenjeno opisu metod načrtovanja in vodenja projektov (definicija in opis projekta, organizacija in finansiranje projekta, nadzor in konec projekta). V knjigi je izpostavljeno poglavje o projektni kulturi. Podrobno so opisani elementi projektne kulture in njihova povezava v celoto.

Knjiga se konča s poglavjem, ki daje pregled o možnem izobraževanju na univerzah, visokih šolah in podjetjih na temo: Skupinsko delo in načrtovanje ter vodenje projektov.

Knjiga je namenjena vodjem projektov, pa tudi udeležencem projektnih skupin.

M. Starbek

K.Etschberger (Hrsg.): Controller-Area-Network

Zal.: Carl Hanser Verlag, München, Wien, 2. predelana in dopolnjena izdaja 2000.
Obseg: format 17 × 24 cm, 437 strani.
Cena je 98 DM.

Glavna tema knjige izdajatelja in s prispevki še šestih sodelavcev je omrežje CAN (Controller-Area-Network), ki si ga je sredi 80. let zamislilo podjetje Bosch, predvsem za uporabo pri električnih in elektronskih sistemih v motornih vozilih. Vsebina je podrobneje zajeta v podnaslovu: osnove, protokoli, komponente in uporaba.

Omrežje CAN s serijskim prenosom informacij po skupnih prenosnih vodih poenostavi in poceni žične povezave med podsistemi in same podsisteme. Zaradi široke uporabe pri vozilih so komponente omrežij CAN lahko široko dostopne, zato najdemo dandanes omrežja CAN tudi pri upravljanju poslopij, procesov, pri avtomatizaciji, na ladjah in drugod. Uporaba omrežij CAN je primerna za objekte z dimenzijami od delov metra do npr. 1000 m. Seveda je zmogljivost omrežja odvisna od največje razdalje v sistemu in od števila povezanih podsistemov, ki med seboj komunicirajo.

V uvodnem delu so zaradi primerjave lastnosti omrežja CAN z drugimi obdelane tudi preostale vrste omrežij, omenjen je sam model komuniciranja OSI, topologije omrežij in protokoli. Sledi podrobnejša obdelava omrežja CAN, zgradba telegrama (preprostega in razširjenega), določanje vrste in prednosti sporočil oz. telegramov in zaščita pred napakami pri prenosu in pri okvarah komponent omrežja. Obdelane so prenosne linije in priključitve nanjo, to je spodnja dva nivoja 7-nivojskega modela OSI, kasneje tudi najvišji nivo, CAL (CAN Application Layer).

Za gradnjo omrežij poleg prenosnih linij potrebujemo tudi druge komponente, ki poenostavijo sestavo, pošiljanje, sprejemanje in preverjanje telegramov. Za gradnjo omrežij CAN so na voljo specializirane komponente, ki v povezavi z mikroprocesorji poenostavijo gradnjo omrežij, obstajajo pa tudi mikrokontrolerji, ki imajo za uporabo v omrežjih CAN že dodane ustrezne obrobne enote. V knjigi sta obe vrsti komponent podrobno obdelani.

Omrežje za delovanje potrebuje ustrezno programsko opremo. V delu je več skic in diagramov, ki ponazarjajo delovanje programov. Knjigi je dodana tudi zgoščenka, z dodatno literaturo, opisom orodij, gonilniki, demonstracijskimi programi in drugim.

Omrežja, od medmrežja pa vse navzdol do povezav IIC, brezžična, z optičnimi ali kovinskimi vodniki, so v današnjem času zelo aktualna tema. Knjiga je zato dobrodošel pripomoček vsem, ki se že ali se imajo namen ukvarjati z omrežji CAN, bodisi v vozilih, avtomatizaciji procesov ali drugje.

A. Hussu

Osebne vesti
Personal Events

Doktorati, magisteriji, diplome

DOKTORATI

Na Fakulteti za strojništvo Univerze v Ljubljani sta z uspehom zagovarjala svoji doktorski disertaciji in sicer:

dne 16. maja 2000: mag. **Bojan Podgornik**, doktorsko disertacijo z naslovom: "Vpliv kemotermične priprave podlage na tribološke lastnosti trdih prevlek pri drsenju" in

dne 30. maja 2000: mag. **Marija Kisin**, doktorsko disertacijo z naslovom: "Vpliv strukture materialov na energijske kvante in entropijo pri odrezavanju".

Na Fakulteti za strojništvo Univerze v Mariboru je dne *15. maja 2000* mag. **Aleš Lesnika**, z uspehom zagovarjal svojo doktorsko disertacijio z naslovom: "Optimiranje naključno vzbujanih nelinearnih dinamičnih sistemov".

S tem so navedeni kandidati dosegli akademsko stopnjo doktorja tehničnih znanosti.

MAGISTERIJI

Na Fakulteti za strojništvo Univerze v Ljubljani sta z uspehom zagovarjala svoji magistrski deli, in sicer:

dne 22. maja 2000: **Sebastijan Marinič**, magistrsko delo z naslovom: "Optimiranje merilnega modula visokotokovnega števca";

dne 31. maja 2000: **Darko Korošec,** magistrsko delo z naslovom: "Lomnomehanska analiza reaktorske posode tlačnovodne jedrske elektrarane".

Na Fakulteti za stroništvo Univerze v Mariboru sta z uspehom zagovarjala svoji magistrski deli, in sicer:

dne 4. maja 2000: **Boštjan Hari**, magistrsko delo z naslovom: "Prostorska numerična simulacija turbulentnega zgorevanja";

dne 8. maja 2000: **Vasilije Vasić**, magistrsko delo z naslovom: "Analiza energijskih tokov v trigeneracijskih postrojih".

S tem so navedeni kandidati dosegli akademsko stopnjo magistra tehničnih znanosti.

DIPLOMIRALI SO

Na Fakulteti za strojništvo Univerze v Ljubljani so pridobili naziv univerzitetni diplomirani inženir strojništva:

dne 24. maja 2000: Domen KOMAC, Martin PANČUR, Janez PATERNOSTER, Matjaž PTIČAR, Iza UKMAR, Urban ŽARGI;

dne 29. maja 2000: Miha AMBROŽ, Uroš KRULJC, Domen OTONIČAR.

Na Fakulteti za strojništvo Univerze v Mariboru so pridobili naziv univerzitetni diplomirani inženir strojništva:

dne 25. maja 2000: Miha KOVAČIČ, Dominik KRAMPL, Borut SUHADOLNIK;

dne 31. maja 2000: Peter KLAJNŠEK, Gregor TEPEŽ, Goran VUČKOVIĆ.

*

Na Fakulteti za strojništvo Univerze v Ljubljani so pridobili naziv diplomirani inženir strojništva:

dne 12. maja 2000: Jože BOGOLIN, Aleksandar DJOROVIĆ, Jernej Jurij LEVIČAR, Dušan MALI, Aleksander PIPAN, Iztok TRAFELA, Matjaž VALENČIČ.

Na Fakulteti za strojništvo Univerze v Mariboru so pridobili naziv diplomirani inženir strojništva:

dne 25. maja 2000: Alen STEPIŠNIK;

dne 31. maja 2000: Matjaž ES, Sebastjan KOTNIK.

*

Na Fakulteti za strojništvo Univerze v Mariboru so pridobili naziv inženir strojništva:

dne 25. maja 2000: Igor KOSAR, Boštjan KOVAČEC, Simon KRAŠNA, Marijan MARUŠIČ, Anton OZEBEK;

dne 31. maja 2000: Peter BEVC.

Navodila avtorjem
Instructions for Authors

Članki morajo vsebovati:
- naslov, povzetek, besedilo članka in podnaslove slik v slovenskem in angleškem jeziku,
- dvojezične preglednice in slike (diagrami, risbe ali fotografije),
- seznam literature in
- podatke o avtorjih.

Strojniški vestnik izhaja od leta 1992 v dveh jezikih, tj. v slovenščini in angleščini, zato je obvezen prevod v angleščino. Obe besedili morata biti strokovno in jezikovno med seboj usklajeni. Članki naj bodo kratki in naj obsegajo približno 8 tipkanih strani. Izjemoma so strokovni članki, na željo avtorja, lahko tudi samo v slovenščini, vsebovati pa morajo angleški povzetek.

Vsebina članka

Članek naj bo napisan v naslednji obliki:
- Naslov, ki primerno opisuje vsebino članka.
- Povzetek, ki naj bo skrajšana oblika članka in naj ne presega 250 besed. Povzetek mora vsebovati osnove, jedro in cilje raziskave, uporabljeno metodologijo dela,povzetek rezulatov in osnovne sklepe.
- Uvod, v katerem naj bo pregled novejšega stanja in zadostne informacije za razumevanje ter pregled rezultatov dela, predstavljenih v članku.
- Teorija.
- Eksperimentalni del, ki naj vsebuje podatke o postavitvi preskusa in metode, uporabljene pri pridobitvi rezultatov.
- Rezultati, ki naj bodo jasno prikazani, po potrebi v obliki slik in preglednic.
- Razprava, v kateri naj bodo prikazane povezave in posplošitve, uporabljene za pridobitev rezultatov. Prikazana naj bo tudi pomembnost rezultatov in primerjava s poprej objavljenimi deli. (Zaradi narave posameznih raziskav so lahko rezultati in razprava, za jasnost in preprostejše bralčevo razumevanje, združeni v eno poglavje.)
- Sklepi, v katerih naj bo prikazan en ali več sklepov, ki izhajajo iz rezultatov in razprave.
- Literatura, ki mora biti v besedilu oštevilčena zaporedno in označena z oglatimi oklepaji [1] ter na koncu članka zbrana v seznamu literature. Vse opombe naj bodo označene z uporabo dvignjene številke[1].

Oblika članka

Besedilo naj bo pisano na listih formata A4, z dvojnim presledkom med vrstami in s 3 cm širokim robom, da je dovolj prostora za popravke lektorjev. Najbolje je, da pripravite besedilo v urejevalnilku Microsoft Word. Če uporabljate kakšen drug urejevalnik besedil, prosimo, da besedilo konvertirate v navadno ASCII (tekstovno) obliko. Hkrati dostavite odtis članka na papirju, vključno z vsemi slikami in preglednicami ter identično kopijo v elektronski obliki.

Prosimo, da ne uporabljate urejevalnika LaTeX, saj program, s katerim pripravljamo Strojniški vestnik, ne uporablja njegovega formata. V urejevalniku LaTeX oblikujte grafe, preglednice in enačbe in jih stiskajte na kakovostnem laserskem tiskalniku, da jih bomo lahko presneli.

Enačbe naj bodo v besedilu postavljene v ločene vrstice in na desnem robu označene s tekočo številko v okroglih oklepajih

Enote in okrajšave

V besedilu, preglednicah in slikah uporabljajte le standardne označbe in okrajšave SI. Simbole fizikalnih veličin v besedilu pišite poševno (kurzivno), (npr. *v, T, n* itn.). Simbole enot, ki sestojijo iz črk, pa pokončno (npr. ms^{-1}, K, min, mm itn.).

Papers submitted for publication should comprise:
- Title, Abstract, Main Body of Text and Figure Captions in Slovene and English,
- Bilingual Tables and Figures (graphs, drawings or photographs),
- List of references and
- Information about the authors.

Since 1992, the Journal of Mechanical Engineering has been published bilingually, in Slovenian and English. The two texts must be compatible both in terms of technical content and language. Papers should be as short as possible and should on average comprise 8 typed pages. In exceptional cases, at the request of the authors, speciality papers may be written only in Slovene, but must include an English abstract.

The format of the paper

The paper should be written in the following format:
- A Title, which adequately describes the content of the paper.
- An Abstract, which should be viewed as a miniversion of the paper and should not exceed 250 words. The Abstract should state the principal objectives and the scope of the investigation, the methodology employed, summarize the results and state the principal conclusions.
- An Introduction, which should provide a review of recent literature and sufficient background information to allow the results of the paper to be understood and evaluated.
- A Theory
- An Experimental section, which should provide details of the experimental set-up and the methods used for obtaining the results.
- A Results section, which should clearly and concisely present the data using figures and tables where appropriate.
- A Discussion section, which should describe the relationships and generalisations shown by the results and discuss the significance of the results making comparisons with previously published work. (Because of the nature of some studies it may be appropriate to combine the Results and Discussion sections into a single section to improve the clarity and make it easier for the reader.)
- Conclusions, which should present one or more conclusions that have been drawn from the results and subsequent discussion.
- References, which must be numbered consecutively in the text using square brackets [1] and collected together in a reference list at the end of the paper. Any footnotes should be indicated by the use of a superscript[1].

The layout of the text

Texts should be written in A4 format, with double spacing and margins of 3 cm to provide editors with space to write in their corrections. Microsoft Word for Windows is the preferred format for submission. If you use another word processor, please convert to normal ASCII (text) format. One hard copy, including all figures, tables and illustrations and an identical electronic version of the manuscript must be submitted simultaneously.

Please do not use a LaTeX text editor, since this is not compatible with the publishing procedure of the Journal of Mechanical Engineering. Graphs, tables and equations in LaTeX may be supplied in good quality hard-copy format, so that they can be copied for inclusion in the Journal.

Equations should be on a separate line in the main body of the text and marked on the right-hand side of the page with numbers in round brackets.

Units and abbreviations

Only standard SI symbols and abbreviations should be used in the text, tables and figures. Symbols for physical quantities in the text should be written in Italics (e.g. *v, T, n,* etc.). Symbols for units that consist of letters should be in plain text (e.g. ms^{-1}, K, min, mm, etc.).

Vse okrajšave naj bodo, ko se prvič pojavijo, napisane v celoti, npr. časovno spremenljiva geometrija (ČSG).

Slike

Slike morajo biti zaporedno oštevilčene in označene, v besedilu in podnaslovu, kot sl. 1, sl. 2 itn. Posnete naj bodo v kateremkoli od razširjenih formatov, npr. BMP, JPG, GIF. Za pripravo diagramov in risb priporočamo CDR format (CorelDraw), saj so slike v njem vektorske in jih lahko pri končni obdelavi preprosto povečujemo ali pomanjšujemo.

Pri označevanju osi v diagramih, kadar je le mogoče, uporabite označbe veličin (npr. *t, v, m* itn.), da ni potrebno dvojezično označevanje. V diagramih z več krivuljami, mora biti vsaka krivulja označena. Pomen oznake mora biti pojasnjen v podnapisu slike.

Vse označbe na slikah morajo biti dvojezične.

Za vse slike po fotografskih posnetkih je treba priložiti izvirne fotografije ali kakovostno narejen posnetek. V izjemnih primerih so lahko slike tudi barvne.

Preglednice

Preglednice morajo biti zaporedno oštevilčene in označene, v besedilu in podnaslovu, kot preglednica 1, preglednica 2 itn. V preglednicah ne uporabljajte izpisanih imen veličin, ampak samo ustrezne simbole, da se izognemo dvojezični podvojitvi imen. K fizikalnim veličinam, npr. *t* (pisano poševno), pripišite enote (pisano pokončno) v novo vrsto brez oklepajev.

Vsi podnaslovi preglednic morajo biti dvojezični.

Seznam literature

Vsa literatura mora biti navedena v seznamu na koncu članka v prikazani obliki po vrsti za revije, zbornike in knjige:

[1] Tarng, Y.S., Y.S. Wang (1994) A new adaptive controler for constant turning force. *Int J Adv Manuf Technol* 9(1994) London, pp. 211-216.

[2] Čuš, F., J. Balič (1996) Rationale Gestaltung der organisatorischen Abläufe im Werkzeugwesen. *Proceedings of International Conference on Computer Integration Manufacturing,* Zakopane, 14.-17. maj 1996.

[3] Oertli, P.C. (1977) Praktische Wirtschaftskybernetik. *Carl Hanser Verlag,* München.

Podatki o avtorjih

Članku priložite tudi podatke o avtorjih: imena, nazive, popolne poštne naslove, številke telefona in faksa ter naslove elektronske pošte.

Sprejem člankov in avtorske pravice

Uredništvo Strojniškega vestnika si pridržuje pravico do odločanja o sprejemu članka za objavo, strokovno oceno recenzentov in morebitnem predlogu za krajšanje ali izpopolnitev ter terminološke in jezikovne korekture.

Avtor mora predložiti pisno izjavo, da je besedilo njegovo izvirno delo in ni bilo v dani obliki še nikjer objavljeno. Z objavo preidejo avtorske pravice na Strojniški vestnik. Pri morebitnih kasnejših objavah mora biti SV naveden kot vir.

Rokopisi člankov ostanejo v arhivu SV.

Vsa nadaljnja pojasnila daje:

Uredništvo
STROJNIŠKEGA VESTNIKA
p.p. 197/IV
1001 Ljubljana
Telefon: (061) 1771-428
Telefaks: (061) 218-567
E-mail: strojniski.vestnik@fs.uni-lj.si

All abbreviations should be spelt out in full on first appearance, e.g., variable time geometry (VTG).

Figures

Figures must be cited in consecutive numerical order in the text and referred to in both the text and the caption as Fig. 1, Fig. 2, etc. Figures may be saved in any common format, e.g. BMP, GIF, JPG. However, the use of CDR format (CorelDraw) is recommended for graphs and line drawings, since vector images can be easily reduced or enlarged during final processing of the paper.

When labelling axes, physical quantities, e.g. *t, v, m,* etc. should be used whenever possible to minimise the need to label the axes in two languages. Multi-curve graphs should have individual curves marked with a symbol, the meaning of the symbol should be explained in the figure caption.

All figure captions must be bilingual.

Good quality black-and-white photographs or scanned images should be supplied for illustrations. In certain circumstances, colour figures may be considered.

Tables

Tables must be cited in consecutive numerical order in the text and referred to in both the text and the caption as Table 1, Table 2, etc. The use of names for quantities in tables should be avoided if possible: corresponding symbols are preferred to minimise the need to use both Slovenian and English names. In addition to the physical quantity, e.g. *t* (in Italics), units (normal text), should be added in new line without brackets.

All table captions must be bilingual.

The list of references

References should be collected at the end of the paper in the following styles for journals, proceedings and books, respectively:

[1] Tarng, Y.S., Y.S. Wang (1994) A new adaptive controler for constant turning force. *Int J Adv Manuf Technol* 9(1994) London, pp. 211-216.

[2] Čuš, F., J. Balič (1996) Rationale Gestaltung der organisatorischen Abläufe im Werkzeugwesen. *Proceedings of International Conference on Computer Integration Manufacturing,* Zakopane, 14.-17. maj 1996.

[3] Oertli, P.C. (1977) Praktische Wirtschaftskybernetik. *Carl Hanser Verlag,* München.

Author information

The following information about the authors should be enclosed with the paper: names, complete postal addresses, telephone and fax numbers and E-mail addresses.

Acceptance of papers and copyright

The Editorial Committee of the Journal of Mechanical Engineering reserves the right to decide whether a paper is acceptable for publication, obtain professional reviews for submitted papers, and if necessary, require changes to the content, length or language.

Authors must also enclose a written statement that the paper is original unpublished work, and not under consideration for publication elsewhere. On publication, copyright for the paper shall pass to the Journal of Mechanical Engineering. The JME must be stated as a source in all later publications.

Papers will be kept in the archives of the JME.

You can obtain further information from:

Editorial Board of the
JOURNAL OF MECHANICAL ENGINEERING
P.O.Box 197/IV
1001 Ljubljana, Slovenia
Telephone: +386 (0)61 1771-428
Fax: +386 (0)61 218-567
E-mail: strojniski.vestnik@fs.uni-lj.si